1989

Thermal hydraulic analysis of a packed bed reactor fuel element.

Tuddenham, Read Stapley

Monterey, California. Naval Postgraduate School

Thermal Hydraulic Analysis of a Packed Bed Reactor Fuel Element

by

READ STAPLEY TUDDENHAM

B. S., Chemical Engineering, Cornell University
(1972)

SUBMITTED TO THE DEPARTMENT OF
NUCLEAR ENGINEERING
IN PARTIAL FULFILLMENT OF THE REQUIREMENTS
FOR THE DEGREES OF

NUCLEAR ENGINEER

and

MASTER OF SCIENCE IN NUCLEAR ENGINEERING

at the

MASSACHUSETTS INSTITUTE OF TECHNOLOGY

May 1989

THERMAL HYDRAULIC ANALYSIS OF A PACKED BED REACTOR FUEL ELEMENT

by

READ STAPLEY TUDDENHAM

Submitted to the Department of Nuclear Engineering
on May 25, 1989 in partial fulfillment of the
requirements for the degrees of Nuclear Engineer and
Master of Science in Nuclear Engineering.

ABSTRACT

A model of the behavior of a packed bed nuclear reactor fuel element is developed. It is capable of predicting the temperature, pressure and velocity fields as a function of position throughout the fuel element in both transient and steady state conditions. It is the starting point for the design of a real time analysis module for a reactor power controller.

The fuel element consists of a packed bed of fuel particles between two concentrically mounted retention elements. It is cooled by hydrogen flowing radially inward through the bed.

The model is based on the fundamental principles of mass, momentum and energy conservation. The balances are applied to a two dimensional array of control volumes, using the lumped parameter approach, to generate sets of simultaneous linear semi-implicit finite difference equations. The Pressure Implicit with Splitting of Operators (PISO) algorithm is then used to advance the model variables in time. An energy balance derived from a single node model of a fuel particle is performed on the solid phase.

The model code is applied to a series of steady state and transient problems, varying the peak power density from 0 to 2.1 GW/m^3. The model predicts significant axial flow in the fuel particle bed. If the proper flow distribution is obtained along the inlet retention element, it is not maintained in the particle bed. This redistribution leads to a 300 K temperature variation along the outlet plenum at high power. The magnitude of the redistribution is a function of power level. A design change in the shape of the inlet frit may give a more uniform temperature distribution at the full power condition. The model also predicts significant effects from conduction and radiation in the solid phase.

Thesis Supervisor: J. E. Meyer
Title: Professor of Nuclear Engineering

Acknowlegements

I would like to extend my thanks to all those who helped in so many ways with this thesis. In particular, Professor J.E. Meyer whose skilfull guidance, patience and attention to basic principles ensured there was never a shortage of ideas. The Reactor Controls Group, including Professor A. F. Henry, Professor D. D. Lanning, Dr. J. A. Bernard, S. H. Lau, B. Aviles and K. Kwok, provided indespensible assistance and inspiration on this and many other projects.

Thank you to my fellow Naval Officers for their help and friendship and to the United States Navy for the funding and opportunity to pursue an advanced degree.

Lastly, and most importantly, thank you to my family whose understanding, sacrifice and moral support made this endeavor possible.

Table of Contents

Table of Figures

Table of Tables

CHAPTER 1

INTRODUCTION

1.1 PROBLEM STATEMENT

MIT, in conjunction with the Sandia National Laboratory, is developing an automated control system for a space based reactor. The proposed reactor consists of several annular packed bed fuel elements cooled by hydrogen flowing radially inward through the fuel particles. The hydrogen enters from distribution channels in the surrounding moderator block, Fig. 2.1. The control system under consideration uses a model based algorithm which relies on an accurate representation of the reactor in calculating the control signals. Because the design is unique for the application, well established thermal-hydraulic models may not be directly applicable. The objective of this investigation is to develop a thermal hydraulic model of a reactor fuel element which can, in turn, be expanded to include the entire reactor system and be incorporated in the controller.

The thermal hydraulic model serves two purposes in this type of reactor control. One, it is used to describe the heat transfer processes and provide the information to prevent temperatures from exceeding design limits. Two, it provides the temperature and pressure data required to quantify the reactivity feedback associated with the hydrogen coolant. It should be capable of predicting coolant flow distribution, temperature, pressure and density during steady state and rapid transient operations.

1.2 METHOD

To be an effective part of the controller, the model should function in real time in a stable and robust manner. These requirements place competing constraints on its form. It must contain sufficient detail to give an accurate representation of the fluid flow and heat transfer processes, but yet be simple enough that its outputs are available when required by the controller. Thus, constructing the model is a stagewise process. First, one must determine what aspects of the fuel element should be included to give an accurate picture. Then, given the minimum requirements, the model must be tailored to meet the time constraint. The work described here addresses the first of these tasks.

A detailed reference model is constructed and used to evaluate the sensitivity of the model predictions to various simplifications. One example is radiative heat transfer in the solid phase. The results of the reference case and a simpler version without the effect can be compared to determine if this mode of heat transfer contributes significantly to the behavior of the fuel element and if it must be modeled explicitly.

The building of the reference model is the major emphasis of this work. Future development can then take the results and perform the simplifications required for a real time, predictive, model.

1.3 ISSUES

The specific issues investigated can be summarized in two categories, hydraulic and heat transfer.

Hydraulic issues include:

a. Flow distribution: Does the model accurately reflect the flow distribution of hydrogen?

b. Pressure losses: What are the major sources of pressure loss and how can they be modeled?

c. Coolant flow: Can coolant flow in the particle bed be considered one dimensional or are two dimensions required?

d. Hydrogen compressibility: Must the model explicitly represent the coolant as a compressible gas or are pressure changes small enough that incompressible models are adequate?

Heat transfer issues include:

a. Interphase heat transfer: Can heat transfer between the gas and solid phase be modeled as purely convective? How should the heat transfer coefficient be calculated? Is radiative heat transfer important?

b. Intraphase heat transfer: Is there significant conduction and radiation between particles in the solid phase? How should transfer within the fuel particle be simulated?

c. Discretization: Is a fine node analysis required or can fuel element behavior be represented with a few or single node model?

The chapters that follow describe the details of the packed bed reactor and then discuss the development of the mathematical representations of the fuel element. These are then combined in a computer code to form the reference case used to evaluate the questions above.

CHAPTER 2

BACKGROUND AND APPROACH

2.1 OBJECTIVE

Before one can abstract a thermal-hydraulic system to a series of predictive mathematical relations, the design and operation of the actual system must be clearly understood. The objective of this chapter is to present the physical details of the packed bed reactor and the fuel particles within it.

Space based reactor designs have been evolving since the ROVER program of the 1960s and its subsidiary NERVA project. After a lull in the 1970s and early 1980s, United States interest in the area has been rejuvenated. Major portions of the ongoing studies are being conducted at the Brookhaven and Sandia national laboratories. The Brookhaven work (L-1, H-1) analyzes and discusses reactor system designs, capabilities and design philosophy. Sandia's investigators have constructed prototype fuel elements and tested them in the Annular Core Research Reactor (ACRR). The former provide the best understanding from a system perspective while the Sandia project gives a detailed dimensioned design suitable for modeling.

2.2 THE REACTOR SYSTEM

2.2.1 Design Philosophy

Space based reactor systems are by necessity constrained to be lightweight and compact. This translates to a design favoring high power density, low material density and large

heat transfer surface per unit volume. For example, systems launched by the space shuttle are limited to a cylinder 4 m in diameter and 17 m long with a maximum mass of 29,500 kg. (H-1). Particle bed nuclear reactors are ideal for this application, because of their small size and their ability to deliver twice the specific impulse of a chemical rocket (H-1) in open cycle applications.

Proposed systems have included both open and closed cycles (L-1). Open cycle systems have the advantage of low weight and simplicity, since there is no need for recovery and reuse of the coolant. However, reactor life is then determined by the amount of coolant tankage. Typically these systems are considered for pulsed operation or propulsion designs. Closed systems have been proposed for continuous electrical power generation. Helium and hydrogen are the usual coolants. Hydrogen is generally preferred for the higher power pulsed operation systems. The pulsed open cycle variant is of principal interest in this investigation.

2.2.2 Pulsed Reactor Design

Open system pulsed operation designs are discussed in references P-1, L-1 and B-1. The basic cycle includes compressing liquid hydrogen, providing two stages of heating and directing the high temperature coolant to the power conversion unit.

The core consists of fuel elements mounted in a moderator block which is in turn surrounded by a series of control drums and a reflector chamber. The entire assembly is encapsulated in an aluminum pressure vessel (P-1). The core is a right cylinder .79 m in diameter and 1.03 m long (P-1). Other designs place the reflector outside the pressure vessel (H-1). The moderator block (Fig. 2.1) can be ZrH_2, BeH_2 or LiH. Either a single drilled piece, or an

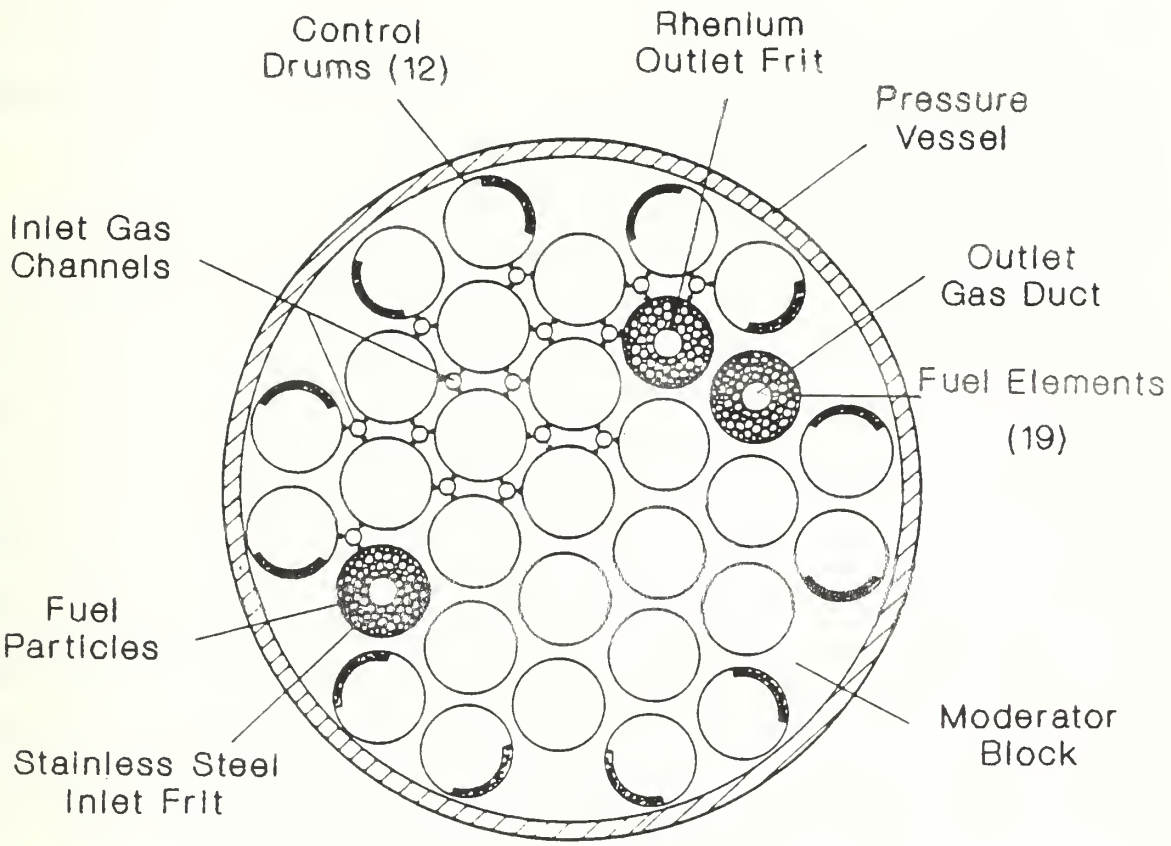

Figure 2.1

Reactor Cross-Section

Adapted from (P-1)

assembly of smaller modular blocks, the moderator is channeled to create a coolant flow path and sites for the fuel elements. Nineteen elements are arranged in a hexagonal array around a central cell (Depending on one's perspective this may be considered a triangular arrangement). Control drums are used in lieu of control rods for compactness and simplicity of operation. A portion of each drum surface is coated with a strong neutron absorber. Rotating the absorber away from the fuel assemblies is the equivalent of withdrawing a control rod.

The fuel elements, Fig. 2.2, are composed of two concentrically mounted cylindrical retention pieces, referred to as frits. The frits are porous enough to allow coolant flow but strong enough to function as retainers for the fuel particles in the annular space between them. The space between the outer frit and the moderator block forms an inlet plenum for the coolant. Similarly, the region inside the inner frit forms an outlet plenum from which the hot exit gasses are extracted and directed to the energy conversion device, most likely a turbine, or are exhasted for propulsion. The outer cold frit is fabricated by sintering micron sized stainless steel particles. However, because of the high exhaust temperatures (approximately 2,000 K) the inner, hot frit poses a material selection problem. Drilled rhenium is used in the currently favored design.

The fuel particles are similar to the coated fuel particles used in high temperature gas reactors (HTGR). Each consists of a central kernel of fuel coated with two pyrographite layers and zirconium carbide. But unlike the HTGR the 500 micron particles are used directly in a packed bed configuration not combined with graphite structure to form a ball or block.

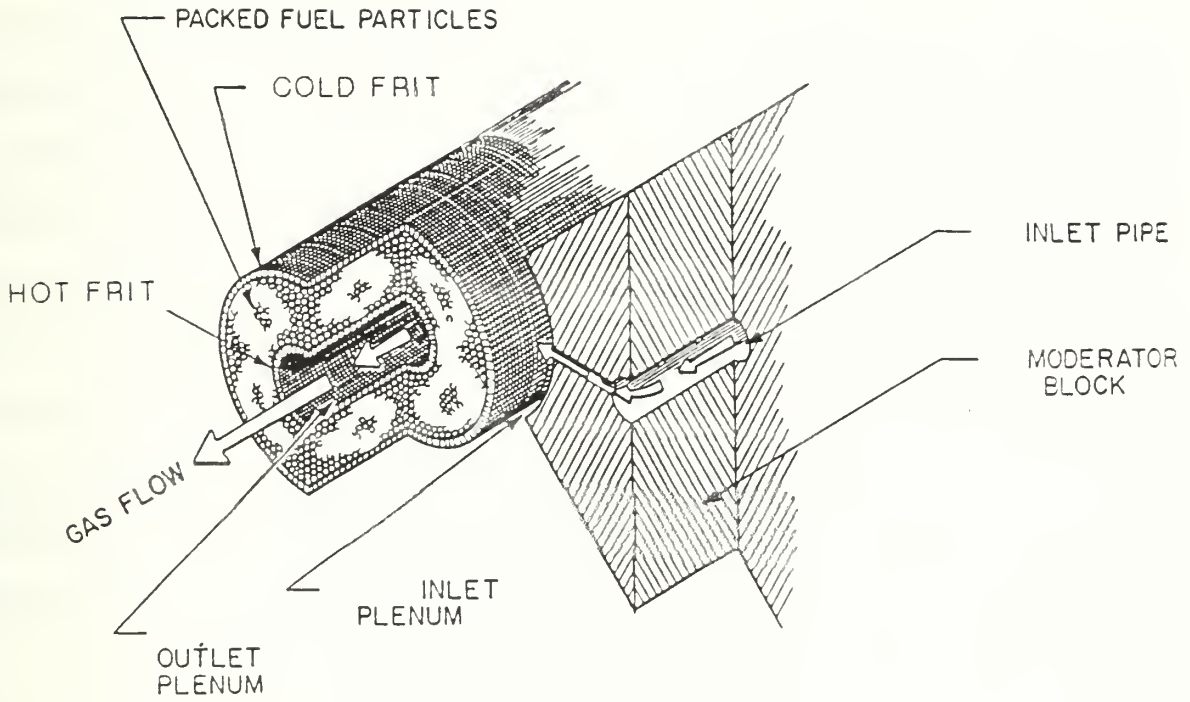

Figure 2.2

Packed Bed Fuel Element

(From L-1)

2.2.3 Hydraulics and Heat Transfer

Liquid hydrogen is stored in a separate container. When power operation is initiated, the hydrogen passes from the tank to a turbo pump where it is compressed to a supercritical fluid with a pressure as high as 6 MPa. It is discharged to the reactor reflector, the first heating stage. From the reflector, the coolant passes into the reactor core. Once in the core, the hydrogen flows axially through coolant passages located between the fuel elements and the moderator block. These channels are slotted lengthwise to create a gas flow path to the inlet plenum throughout the entire length of the fuel element. Each coolant channel feeds three fuel elements and six channels feed each fuel element as shown in Fig. 2.1. The inlet plenum provides communication for the coolant over the entire surface of the cold frit. Pressure losses in the core to this point can be considerable, since the flow has made three 90 degree direction changes in the core by the time it gets to the cold frit. At this point the hydrogen flows radially inward through the packed bed of fuel and hot frit. Collected in the outlet plenum, the hot gas is exhausted to the turbine.

Two alternatives exist for powering the turbopump (S-1,S-2 and S-3), a bleed system and a topping system. The bleed system takes a small portion of the reflector outlet gas, expands it through a turbine and exhausts it to the surroundings. The topping system expands all of the reflector gasses through a turbine and discharges them to the reactor core. The larger volume is used to reduce the pressure drop.

One of the design imperatives of any reactor is to match coolant flow and power distribution. This matching for a packed bed reactor provides a nearly constant temperature throughout the length of the outlet plenum. Zoning the fuel, shaping the coolant flow, or combining the two methods can be used. The cold frit provides the best place to shape the

flow distribution. Varying the porosity and/or thickness effectively controls the pressure drop across the frit to achieve the desired flow characteristic. The cold frit essentially serves as a distribution manifold. This approach is most easily applied if the flow through the packed bed of fuel is essentially inward (radial not axial).

The majority of the pressure drop in the open cycle is in the moderator block (B-1). Within the fuel assembly, the cold frit is the greatest resistance to flow. The hydrogen enters the fuel element at approximately 300 K and at 2 to 6 MPa depending on the design. At full power the exit gas is in excess of 2,000 K. The pressure drop through the element is on the order of 50 kPa.

The packed bed reactor can operate at very high power with relatively small temperature changes across the gas film and the fuel particle (because of the close proximity of the coolant and the heat deposition). This design gives a heat transfer area of 7,000 to 10,000 m^2/m^3 of fuel (P-1). Powell's analysis shows that power densities of 10 GW/m^3 of fuel can be achieved with gas film ΔTs of approximately 150 K (P-1). The packed bed design also responds well to the rapid transients associated with pulsed operation (P-1). The fuel particles are capable of enduring repeated temperature ramps of 1,000 K/s. The reactor postulated by Sandia is expected to execute a power up ramp with a period of about 0.6 s.

2.3 THE PIPE EXPERIMENT

Investigators at the Sandia National Laboratory are conducting a series of experiments titled the Pulsed Irradiation of a Particle Bed Element (PIPE). The objective of the tests is to evaluate a packed bed fuel element and determine if the design is viable from the standpoints of temperature distributions, flow distributions and coolant/fuel compatibility (V-1). The

experiments place a prototype fuel element for the reactor design discussed previously in the Annular Core Research Reactor and pulse the reactor. This will create power densities up to 2 GW/m^3 in the packed bed element. The element is full size in the radial direction; in the axial direction it has been reduced by two thirds.

The PIPE fuel element is the basis for the model being developed in the work reported here, since it provides a complete set of consistent dimensions and performance predictions.

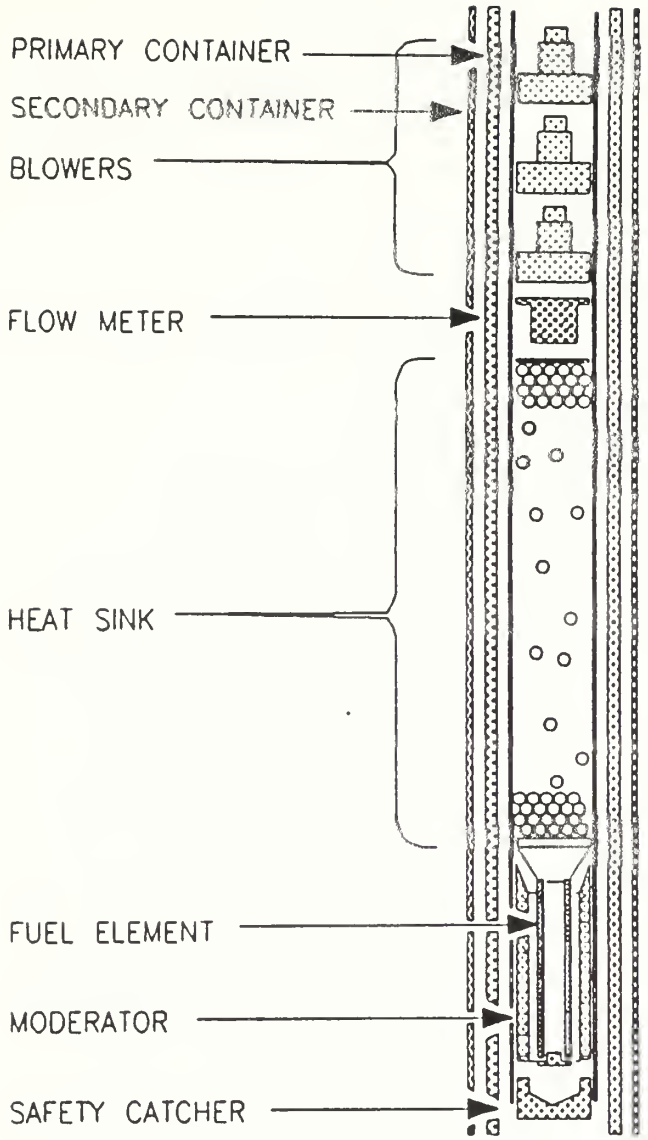

Figure 2.3a

Pipe Experiment Hardware

(V-1)

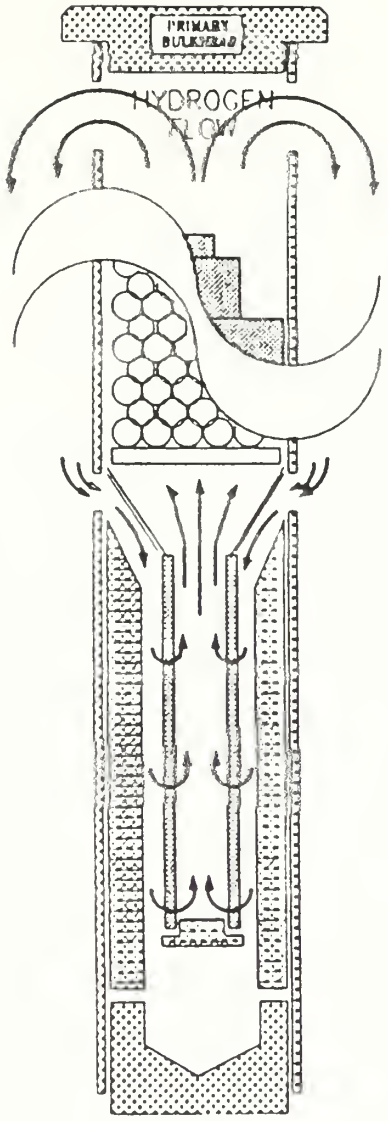

Figure 2.3b

Pipe Experiment
Hydrogen Coolant Flow

(V-1)

A cylinder .35 m in diameter and 4.19 m long houses the experimental apparatus, Fig. 2.3. It consists of a self contained pressurized hydrogen circulation system. The hydrogen flows from blowers in the upper portion of the cylinder down around the middle section components to the lower section. There it enters the top of an inlet plenum formed by the cold frit and an annulus of moderator. Flow continues radially inward through the cold frit, fuel and hot frit before entering the central outlet plenum. This plenum discharges the hot gas to a heat sink contained in the middle section. The heat sink is formed by a bed containing a number of steel balls (originally at a low temperature). From the heat sink it passes through a flow meter and back to the suction side of the blowers. Parahydrogen is used, because of its better heat transfer properties.

The coolant entering the inlet plenum is pressurized to 2 MPa and is at a temperature of 300 K. Figure 2.4 shows the dimensions of the PIPE fuel element.

The cold frit acts as a distribution manifold to match the hydrogen flow and axial power profiles. In this case, the frit is of uniform porosity, .685, but varies in thickness from 1.70 to 2.36 mm to adjust the pressure drop. It is fabricated by sintering 2.5 μm diameter particles of 316 stainless steel. The hot frit is a uniform rhenium tube with electro-arced oblong holes which provide 23.3% open area for flow of the 2,000 K exit gasses.

The fuel pellet used for the experiment is shown in Fig. 2.5. The uranium carbide fuel kernel is enriched to 93% and is coated with two layers of pyrographite. The inner one is low density to accommodate fission products. An outer coating of zirconium carbide, which was developed to improve fuel coolant compatibility in the NERVA project, is also present.

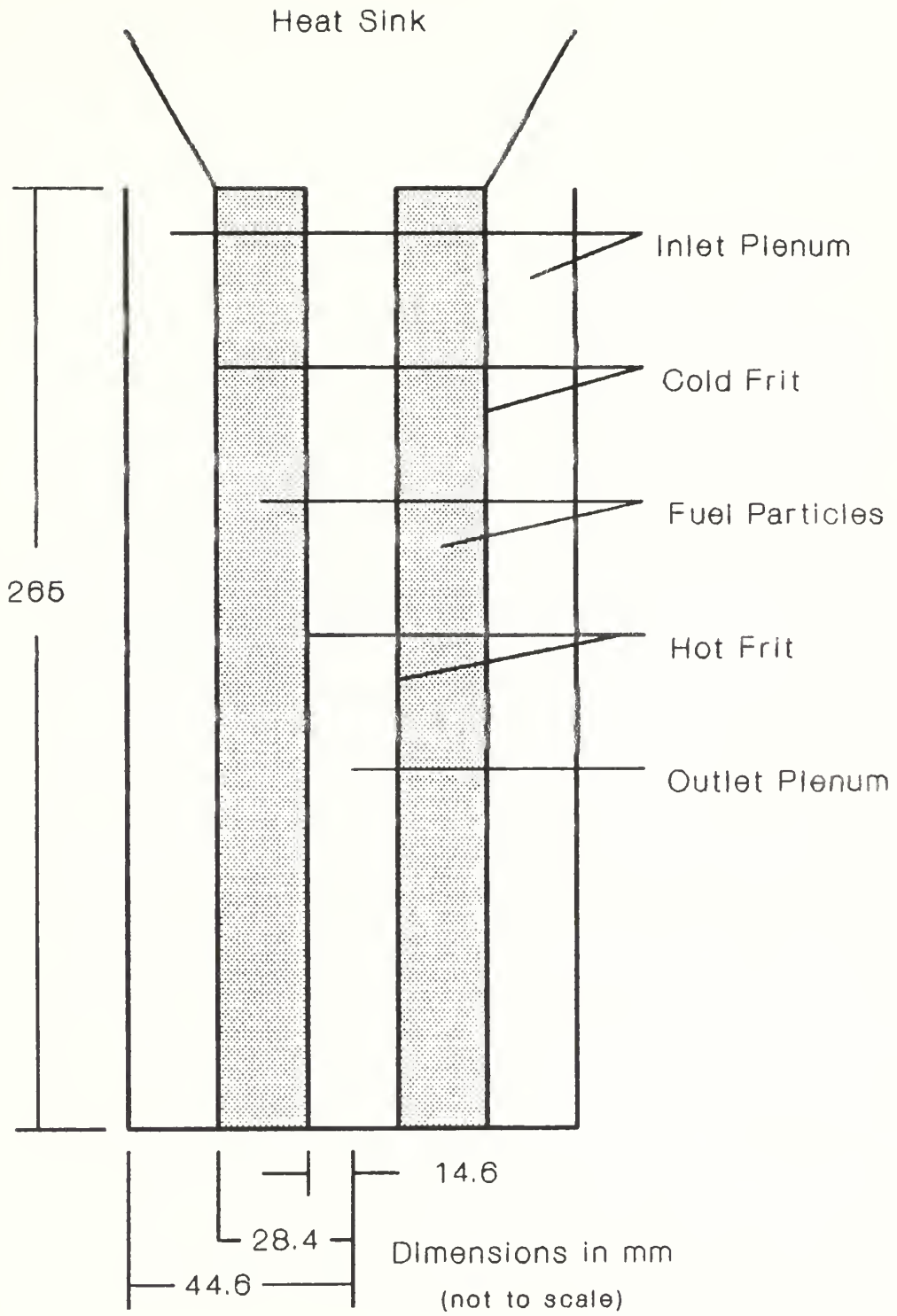

Figure 2.4

The PIPE Fuel Element

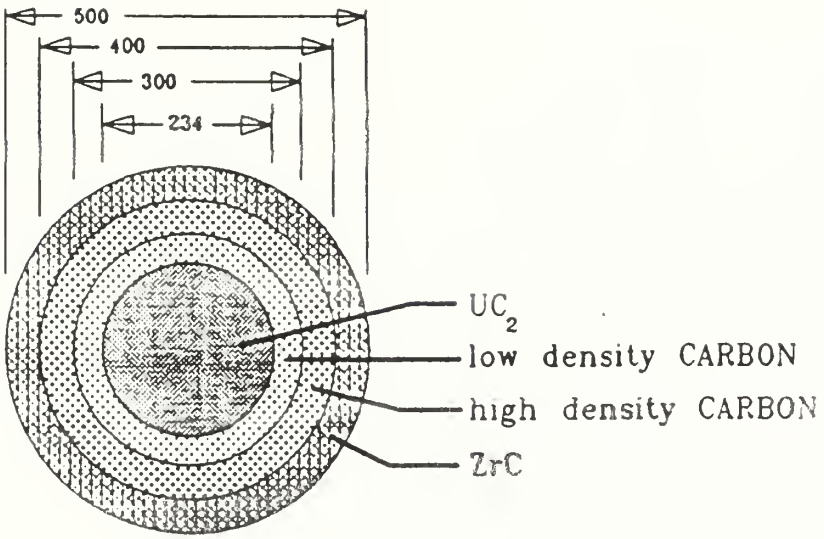

Figure 2.5

Fuel Particle Design (V-1)

(Dimensions in μm)

2.4 EXISTING MODELS

Several models have been developed for annular fuel elements. One early model was formulated in Britain for the design of a gas-cooled fast reactor (A-2, B-2). More recently, Brookhaven researchers (B-1, L-1)(in conjunction with their designs for space reactors) have modeled packed bed elements similar to those being tested at Sandia.

Each of these models was targeted to a specific purpose which in turn influenced the assumptions made and the detail included. The British model was concerned only with flow distribution calculations and did not address the heat transfer issues. One of the Brookhaven models coupled the neutronics and heat transfer to create the control codes KINETIC and SPHEAT (L-1). In these, the fuel element is partitioned radially and axially to allow for variation in the power distribution. However, hydraulics was handled by assuming that the coolant flow matched the power in each axial slice. The thermal-hydraulic code described in references (A-1) and (B-1) uses the same partitioning scheme, effectively giving a 2 dimensional model, but again assumes the flow in the fuel matches the power distribution and uses this to back calculate the required pressure drop characteristic of the cold frit.

The model developed in this investigation is dedicated only to the thermal hydraulics. Its interaction with the neutronic model is limited to passing results such as hydrogen temperatures, pressures and densities. With this in mind, the intention is to build a more general model that operates using only input information that can be supplied by system instrumentation (the inlet coolant temperature, the inlet pressure and the discharge pressure). In this way, one can determine if the flow and power match for actual operating conditions and not just for expected design conditions. The model is also general enough to allow axial as well as radial flow and to include heat transfer between the particles of the solid phase.

2.5 MODEL STRUCTURE

2.5.1 The Premise

The natural tendency in modeling is break the problem down, look at the individual pieces and then reassemble them. In the case of the packed bed fuel element, two subdivision methods are available, separation by component or by phase (solid or gas). These can be combined in several ways. The most detailed is to consider each phase in each component. But this makes it difficult to put the components back together. Another option works with each phase in its entirety and then joins them. The latter lends itself to the application of the fundamental laws of physics and easy model unification.

The model developed in this investigation treats each phase independently and joins them at the common point, solid to gas heat transfer. Thus one could look at the fuel element as a large heat exchanger. The gas phase represents the shell side and the solid phase with its heat deposition is the tube side. Heat flow in the gas phase can be convective and/or conductive and is independent of the solid phase except at the connection point. Similarly, heat flow by conduction and radiation in the solid phase is only influenced by the gas phase at the point of heat transfer. This representation is one of the basic tenets of the Momentum Integral Network method developed by Van Tuyle (V-2, V-3).

The model is based on the premise that the fuel element must obey the fundamental principles described by mass, momentum and energy balances. To facilitate the application of the balances the element is divided into an array of control volumes. The volumes are arranged to coincide with the components of the fuel element. The physical features of the components determine the way the terms of the balance equations are computed in their

respective volumes. Thus, differences between model components can be easily incorporated. For example in the momentum balance, a Darcy friction factor for pipe flow is used to calculate the frictional losses in the plenum control volumes, and an Ergun relation for packed beds is used in the volumes containing fuel particles. The matrix of control volumes and the continuity of conditions at the interfaces provide the required unifying structure.

The gas phase model uses all of the balances: mass, radial momentum, axial momentum, and energy. The inclusion of these balances accounts for the coolant compressibility. However, since the solid phase is fixed and virtually incompressible, only a heat balance is required. For transient analysis, each phase is advanced through the time steps in parallel. The connection is made in the source (sink) term of the energy balances. Using the new time step solid and gas temperatures, the heat transfer is calculated implicitly and used as the source (sink) term for the current time step calculation.

Although the basic equations are easily derived and manipulated in continuous form, an analytical solution for the fuel element would be very difficult. Therefore, the balances are discretized in a finite difference form based on the control volumes. This is readily adaptable to computer solution.

2.5.2 The Staggered Grid

In flow problems, the discretization process is greatly enhanced by defining the variables at different points. For example, velocities are defined at points between points at which pressures are defined. The resulting arrangement is often referred to as a staggered grid. Its advantage lies in the fact that the variables are defined where they are needed. In the momentum balances, the pressure difference across the velocity control volume provides

the source term. Using the staggered grid, pressure is defined on all faces of the velocity control volume. An aligned grid would require an estimation of the face pressures. This frequently introduces large errors in the numerical solution (P-2). The same is true for the mass balance where the control volumes are centered on the pressure nodes. The balance requires the mass fluxes crossing the volume faces. The staggered grid provides a velocity at each face for computing the required mass flux.

Figure 2.6 shows the staggered grid used in this model and the control volumes used in each of the fundamental balances. Cylindrical coordinates are be used throughout the model.

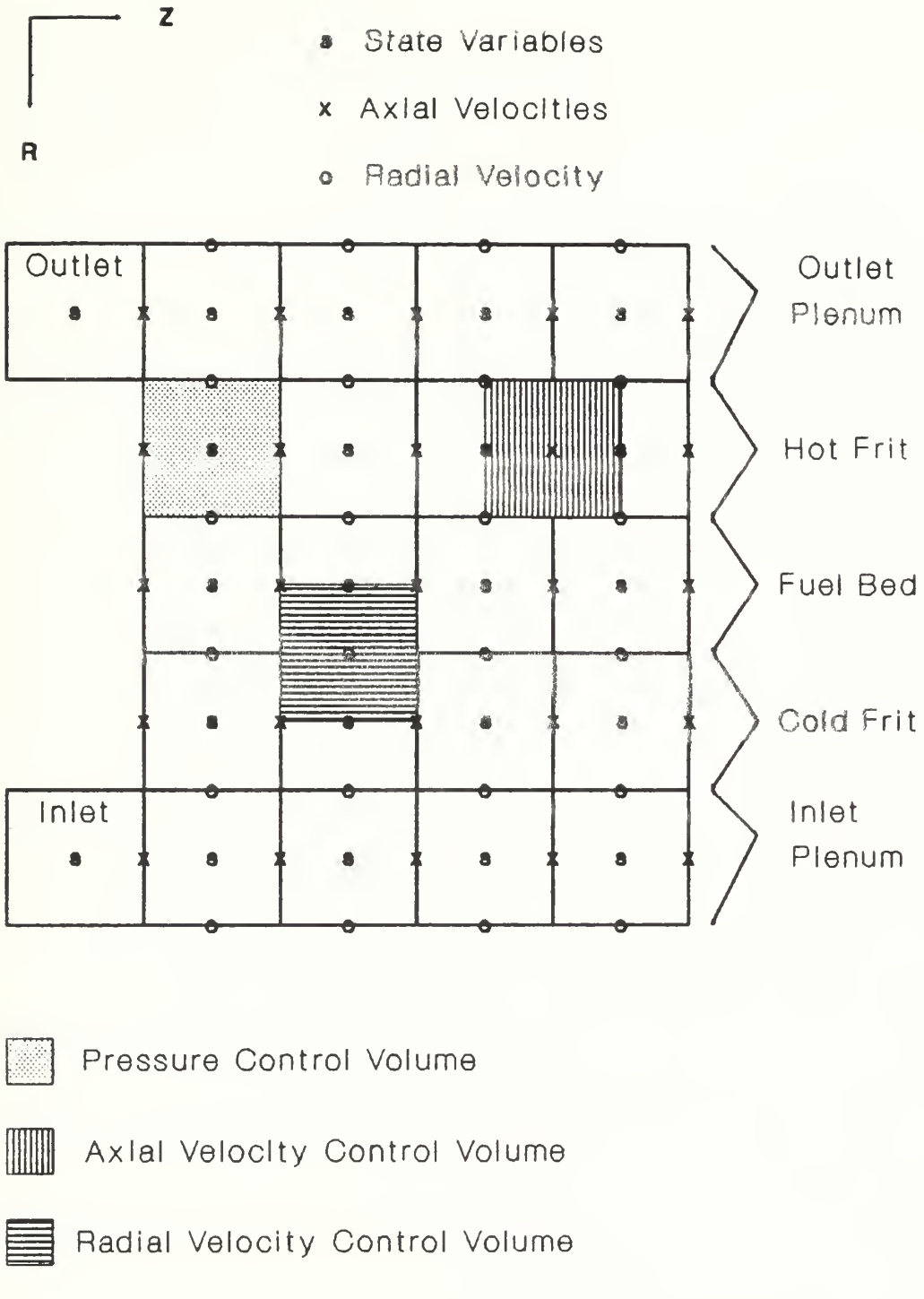

Figure 2.6 **The Staggered Grid**

2.6 SUMMARY

Proposed space based reactor designs are centered on the packed bed fuel element with its high power density. Although the entire reactor has never been built, Sandia National Laboratory has constructed and tested annular particle fuel elements. These prototypes are the basis for the modeling and the analysis performed during this investigation.

The model determines the temperature, pressure, density and velocity distributions for both the gas and solid phases through the solution of discretized mass, momentum and energy balances applied to the staggered grid of control volumes shown in Figure 2.6.

CHAPTER 3

THE GAS PHASE

3.1 OBJECTIVE

The gas phase is the most complicated part of the model, since it contains both hydraulic and heat transfer considerations. This chapter describes the underlying assumptions and modeling of the gas phase. The discussion uses the continuous form of the equations. The discretized form and solution method will be presented in chapter 4.

3.2 CHARACTERISTICS INCLUDED IN THE MODEL

The model of the packed bed fuel element should include all of the features that significantly affect the hydraulic or heat transfer response of the system. Additionally, it should be able to track transients as well as solve for the steady state condition. So, the time dependent terms must be considered. The primary physical features of interest are:

a. Friction effects

b. Manifold "action" of the plenums

c. True two dimensional flow

d. Pressure losses due to changes in direction

e. Spatial acceleration due to reduced flow area and due to density changes

f. Gas film temperature differences

g. Enthalpy changes due to pressure changes and heat transfer

In order to incorporate these aspects in the model, the basic equation for each of the balances, momentum, mass and energy is developed. Then each term is reviewed and modeled including these characteristics when appropriate. The description of the model details that follow

uses a similar approach. However, items strongly affected by the geometry and approximations used in the solution method are not specifically addressed until the model is discretized. Spatial acceleration is one example.

Several assumptions are made to keep the problem tractable and eliminate insignificant effects. Given the fuel elements inherent symmetry, it is assumed that the entire problem can be treated as cylindrically symmetric. Thus, only the radial and axial variations are included.

Gas velocities are expected to range from one to several hundred meters per second. As a result, the primary heat transfer mechanism in the gas phase is convection. Conduction and radiative processes are only considered significant in the solid phase. The model contains other assumptions that are specific to certain aspects. These are discussed when encountered in the model development.

Boundary conditions are also factored into the modeling process. The model assumes that only the inlet pressure, inlet temperature and outlet pressure are known in addition to the physical dimensions and the initial temperature, pressure and velocity distributions.

3.3 THE MOMENTUM BALANCES

3.3.1 The General Form of the Equation

The model contains two separate momentum balances, one for radial flow and one for axial flow. The development and application of the two is identical; the only difference being the direction of the velocity field. The momentum balance discussed below is the general one which can be applied to either the radial or axial velocity field.

The general form of the balance equation is based on a lumped parameter fixed control volume approach. It is derived from the General Transport Equation, Eq. 3.1 (T-1).

$$\frac{D}{Dt}\int\int_V\int f(\vec{r},t)dV = \frac{d}{dt}\int\int_V\int f(\vec{r},t)dV + \oint_S f(\vec{r},t)\vec{v}_r \cdot \vec{n}dS \qquad 3.1$$

$f(\vec{r},t)$ is a general transport function and $\vec{v}_r$ is the velocity of the fluid relative to the control volume. In this case, since the volume is fixed, it is the just the velocity of the fluid. V, S and t represent the volume, surface area and time respectively. This equation can then be made specific to the momentum balance by substituting $\rho\vec{v}$, the linear momentum per unit volume, for the transport function and realizing that

$$\dot{m} = -\oint_S \rho\vec{v}_r \cdot \vec{n}dS \qquad 3.2$$

where $\dot{m}$ is the net mass flow rate into the control volume and m is the mass in the control volume. The result is:

$$\frac{D}{Dt}m\vec{v} = \left(\frac{d}{dt}m\vec{v}\right)_{cv} - \sum_{i=1}^{I}\dot{m}_i\vec{v}_i \qquad 3.3$$

where $\dot{m}_i$ is inward the mass flux through the ith face of the control volume (cv) and $\vec{v}_i$ is its velocity component in the direction of the momentum balance. The product then represents the momentum flux through the ith face. According to Newton's second law the time rate of

change in momentum is equal to the sum of the applied forces. Applying this to Eq. 3.3 gives the final form of the momentum equation (This is a synopsis of the more detailed derivation given in reference T-1).

$$\left(\frac{d}{dt} m\vec{v}\right)_{cv} = \sum_{k=1}^{K} \vec{F}_k + \sum_{i=1}^{I} \dot{m}_i \vec{v}_i \qquad 3.4$$

In other words, the rate of change of momentum within the control volume is equal to the sum of the forces acting on the control volume and the net change in the contained momentum due to flow through the boundaries. Therefore, the effects to be included in the model fall into 2 general categories the source terms (pressure, friction) and the flux term.

The control volume used in the momentum calculations is centered on the appropriate velocity as shown in Fig. 2.6.

3.3.2 The Source Term

The source term accounts for two effects, friction and pressure. Because of the geometry and the variation in the structure of the fuel element components, the evaluation of this term is dependent on the control volume and the velocity variable involved.

The most easily analyzed force in the source term is the effect of pressure. The net force in a given direction is simply the pressure difference between opposing faces multiplied by the effective area. The staggered grid arrangement defines pressure on each of the faces,

so estimation is not required. However, geometry creates some pitfalls that must be understood to prevent introducing errors. Pressure in particular is difficult to work with in cylindrical coordinates and still maintain the proper vector relationships. Therefore, rather than resolve the pressure forces to an x-y coordinate system, the fuel element is treated as though it were slit axially and then flattened like a sheet. This way all radial forces act in the same direction. Care must be taken to ensure that this treatment does not distort other physical features such as control volume face areas.

The control volumes of the gas and the solid phase are intimately intertwined. The dimensions of the volume include the space occupied by the gas and the solid. The volume of the gas and its associated control volume are related by the void fraction, ε, a geometric parameter of the system.

$$V_{gas} = \varepsilon V_{total} \qquad 3.5a$$

$$V_{solid} = (1 - \varepsilon) V_{total} \qquad 3.5b$$

The same relationship also holds for the area of a control volume face and the effective area of the gas. It must be remembered that in a momentum balance on the gas phase that the pressure difference of interest acts on the gas area not the combined gas solid area.

This relationship is also important when velocities are being considered. This model works with the so called "superficial velocity" which is the velocity the gas would have if the control volume were completely empty. Again, superficial velocity is just the product of the void fraction and the velocity of the gas in the spaces between the solid phase, the interstitial velocity.

The geometrical arrangement of the fuel cell and coordinate system also means that the differential control volumes shown in Fig. 3.1a are not rectangular parallelepipeds. In a zero gradient pressure field, a net force would appear to be exerted on the volume if only the top and bottom faces were included in the area calculation. This is not physically correct as a zero pressure gradient should yield zero for the pressure force. The model remedies this by including the side faces in the following manner.

Given the pressure diagram, Fig 3.1b, for a two dimensional differential volume, the area of the top and bottom faces is approximated by the chords T and B respectively. The downward direction force balance is:

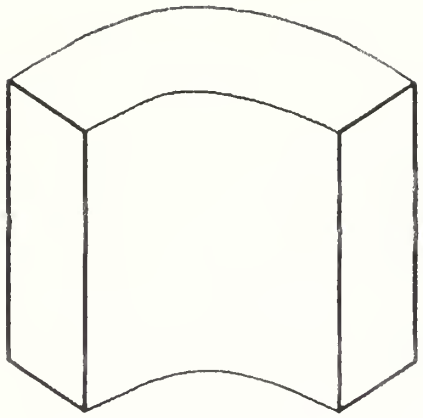

Figure 3.1a **A Typical Control Volume**

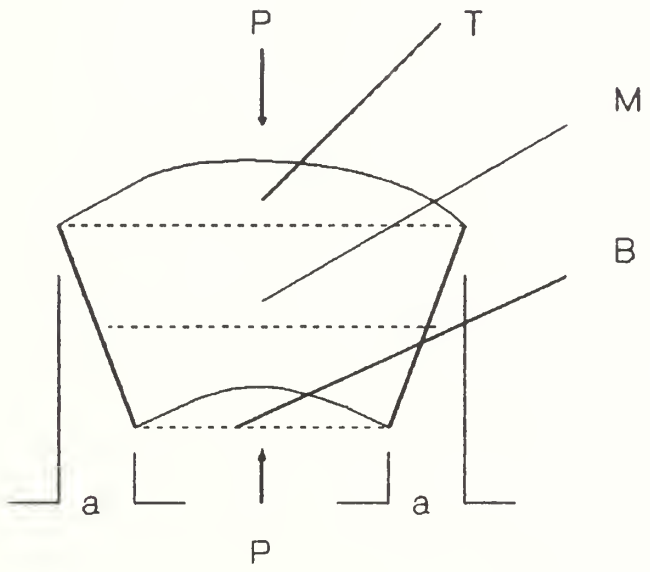

Figure 3.1b **Control Volume and Pressure Field**

$$\text{Net} \quad \text{Force}=P_{top}T - P_{bottom}B - 2aP_{avg} \tag{3.6}$$

This can be reduced to

$$\text{Net} \quad \text{Force} = P_{top}M + P_{bottom}M \tag{3.7}$$

where M is the mean chord length, $(T+B)/2$. This is not a problem for axial pressure forces, since the opposing faces are of equal area and the side faces are parallel to the direction of pressure application.

Two mathematical representations of the friction forces are used, depending on the location of the control volume being considered. The flow in the inlet and outlet plenums is viewed as pipe flow with friction forces proportional to a friction factor. The frits and the fuel particles are treated as packed beds using the pressure gradient described by the Ergun relation.

The inlet and outlet plenum pressure drops due to friction are given by the relation

$$\Delta P = f\left(\frac{L}{D}\right)\frac{\rho v^2}{2} \tag{3.8}$$

where:

P = Pressure

f = Friction factor (Darcy)

ρ = Density

v = Velocity

L = Length over which the pressure drop is experienced

D = Equivalent pipe diameter

Once the pressure drop is known, the frictional force can be determined by multiplying by the appropriate area.

All of the values required to calculate the friction force are either known from the geometry of the control volume and the previous time step values of the unknowns or are variables in the final solution. The exception is the friction factor which requires an intermediate computation.

Blasius and McAdams proposed two of the more common correlations for the friction factor of smooth pipe.

$$f = -0.184\mathrm{Re}^{-0.2} \qquad \text{(McAdams)} \qquad 3.9a$$

$$f = -0.316\mathrm{Re}^{-0.25} \qquad \text{(Blasius)} \qquad 3.9b$$

The McAdams is generally used at Reynolds number, Re, greater than 30,000 and the Blasius at lower values of Re. However, direct use of these relations can be improved upon. The Moody diagram shows friction factors as a function of the pipe wall roughness as well as the Re. As pipe wall roughness increases the exponent becomes less negative.

In an effort to preserve the easily computed form of the McAdams and Blasius equations and account for the roughness of the frits, a new correlation line was fit to the log-log based Moody plot. The result was.

$$f = 0.138\mathrm{Re}^{-0.151} \qquad 3.10$$

This revised correlation also has the advantage that it is applicable over a wider range of Re values (10^3 to 10^8), thus preventing the potential problems of discontinuities in the friction term associated with the standard application of the Blasius and McAdams formulas. For Re less than 1,000, a constant value of 0.0482 was assumed for the friction factor. A plenum Re this low should only be encountered near zero flow initial conditions.

The Colebrook equation (C-1) would also have worked and does include the surface roughness dependence. But its transcendental form makes it difficult to compute. Although the friction model for the plenums appears crude, it is probably as accurate as required. The numerical method will use previous time step velocities to calculate the Re as friction losses in the plenums are small compared to those in the frits and packed bed.

There are two ways to look at flow in packed beds, either as flow through tubes with irregular cross sections or as flow around objects. The former approach has generally been more successful (B-3). The Ergun relation, Eq. 3.11, is a widely used example of the tube model (E-1).

$$\frac{\Delta P}{L} = \frac{150\mu\vec{v}_0}{D_p^2}\frac{(1-\varepsilon)^2}{\varepsilon^3} + \frac{1.75\rho\vec{v}_0|v|}{D_p}\frac{(1-\varepsilon)}{\varepsilon^3} \qquad 3.11$$

where:

$\Delta P/L$ = Pressure drop per unit length

D_p = Particle diameter

$\vec{v}_0$ = Component of the superficial velocity in direction of the momentum balance

$|v|$ = Superficial velocity magnitude

This relation is really the smooth blending of two correlations, the Blake-Kozeny for low Re and the Burke-Plummer for high Re. So in essence, the first term is a laminar term and the second is a turbulent term (B-3). In extremes of flow, one of the terms will dominate. As with the plenum calculations, the force on the control volume is determined by multiplying the pressure difference by the appropriate area.

Several assumptions are implicit with the use of Eq. 3.11. First the cross sectional area for flow is assumed to be constant. This is approximated in the model by using the mean cross sectional area of the control volume for radial flow. The condition is satisfied exactly for axial flow. Second, the packing is uniform everywhere in the fuel element. This removes the effects of channeling (B-3).

Third, the ratio of the particle diameter to the effective bed diameter is small (B-3). Thus wall bypass effects are assumed to be negligible. These effects arise from the variation in void fraction as a function of radial position. It is a maximum of 1 at the wall where there is only a single point of contact between the wall and each sphere. The minimum of 0.2 occurs half a particle diameter in from the wall. The void fraction then shows a damped oscillatory variation as one moves radially inward and eventually reaches the mean value.

The unity void fraction at the wall essentially creates a low resistance channel which allows flow to bypass the bed. Reducing the particle diameter to bed diameter ratio minimizes this effect.

The Ergun equation uses the superficial velocity. In order to preserve the vector nature of the calculation, the velocity component in the direction of the balance is used. When velocity is squared in the second term, the magnitude of the velocity vector as well as the velocity component along the direction of the balance are used.

The Ergun relation forms the basis of the model's friction calculations in the frits and fuel particle bed. All of the terms in the Eq. 3.11 are known either from the geometry or the previous time step. The method of solution discussion will address how the gradient is computed given this basic relation.

Achenbach (A-2) also proposed a relation to predict packed bed pressure drops which was adopted by the Brookhaven researchers. It gave 25% higher gradients than the Ergun relation and was chosen as the conservative method (B-1). This model uses the Ergun which has worked well in the Sandia PIPE experiment preparations.

3.3.3 The Flux Term

The net momentum flux into a control volume is determined by looking at the mass flow rate through each face and its velocity then combining them vectorialy. The mass flow rate is computed by equation 3.12.

$$\dot{m}_i = \rho v_0 a \qquad 3.12a$$

$$\dot{m}\vec{v}_i = \rho v_0 a \vec{v}_i \qquad 3.12b$$

In this case, the area, a, is the overall area of the control volume face. Note also, that v_0 is the component of the superficial velocity perpendicular to the face of the control volume. $\dot{m}$ is positive for flow into the volume and negative for outward flow. Since velocity is a vector with a sign convention, care must be taken when determining the sign for this term.

Once the mass flow rate is known, multiplying by the velocity component in the direction of the momentum balance, $\vec{v}_i$, yields the momentum flux for the face, Eq 3.12b[1]. Figure 3.2 illustrates the momentum flux for a typical control volume and a radial momentum balance.

Figure 3.2 shows the use of the staggered grid and its complications. Fluids enter the West face with two different velocities and densities depending on which control volume they enter from. No attempt is made to model a more detailed gradation of density and velocity, since the lumped parameter approach assumes the value of a variable to be the same everywhere in the volume. All variables in Eq. 3.12b are known or are a variable in the final set of solution equations.

---

1 $\vec{v}_i$ as used in the model development and results that follow is defined to be the superficial velocity. This is incorrect. The formulation of the momentum balance used in the model requires that $\vec{v}_i$ be the interstitial velocity. As a result, the model evaluates the time derivative and momemtum flux terms incorrectly. Refer to section 7.5, Recommendations.

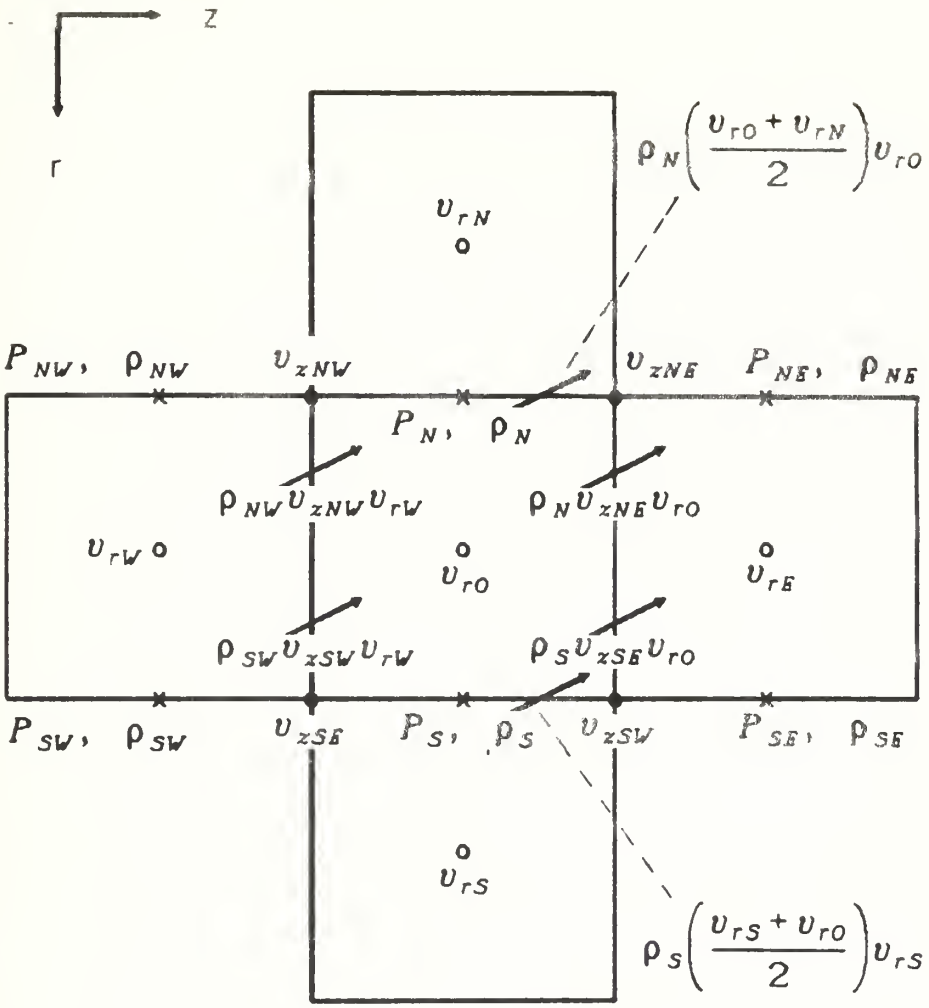

—— Control Volume Boundary

⟶ Radial Momentum Flux

v_r Radial Velocity P Pressure

v_z Axial Velocity ρ Density

Figure 3.2

Radial Momentum Flux and Control Volume

3.3.4 The Manifold Effect

One of the principal functions of the inlet plenum and cold frit is to serve as a flow distribution manifold. Similarly, the outlet plenum serves as a collection manifold. This raises the question of whether or not the general momentum balance accurately predicts the radial flow as a function of position and whether or not improvements can be made. This is especially important given the requirement to match the power and flow distributions.

Rephrasing the question for the inlet plenum, is the average axial component of momentum of the radial (lateral) stream leaving the control volume in Fig 3.3 the same as that of the fluid at the center of the volume where the predominant flow is axial? The model as constructed to this point assumes that the averages are the same. In other words, the axial velocity component of exiting fluid, v_x, is equal to v_1 in Fig 3.3. The other extreme says v_x is 0 and the exiting stream carries no axial momentum. Bajura noted this issue and included it in his models for piping distribution manifolds (*B*-4,5 and 6).

Bajura derived an analytical expression for manifold flow based on an axial momentum balance which included factors to account for deviations from ideal behavior. He then performed a series of experiments to evaluate the constants. He assumed steady state conditions and started with the following balance for the dividing header volume shown in Fig 3.3:

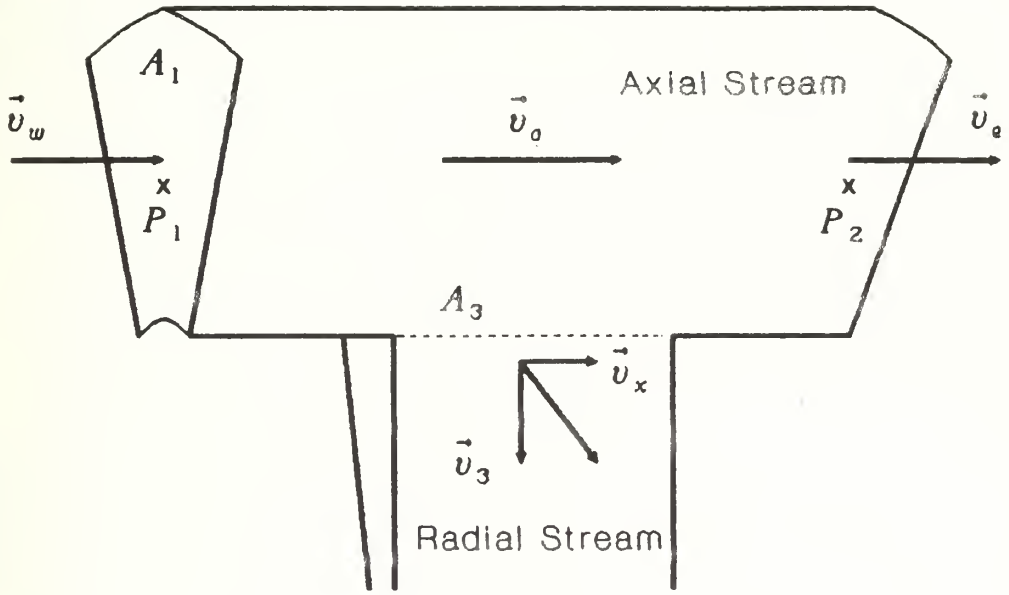

Figure 3.3

Manifold Control Volume

(Adapted from B-4, B-5, B-6)

$$\oint_{A_1} P_1 dA - \oint_{A_1} P_2 dA + \oint_{A_{cv}} \tau_w dA = \oint_{A_w} \rho v_2^2 dA - \oint_{A_w} \rho v_1^2 dA + \oint_{A_3} \rho v_x v_y dA \qquad 3.13$$

The Left hand side contains the source terms and the right hand side the flux terms. Then he defined two correction factors that involve an area weighting and the relationship between v_x and v_1.

$$\beta = \frac{1}{\bar{v}_O^2 A_1} \oint_{A_1} v_O^2 dA \qquad 3.14a$$

$$\gamma = \frac{1}{\bar{v}_O \bar{v}_3 A_3} \oint_{A_3} v_x v_y dA \qquad 3.14b$$

β and γ are the axial momentum correction factors for the axial and radial streams respectively. β Accounts for any deviations from a flat flux profile in the axial stream and γ is a measure of the axial momentum of the radial flow stream as a function of the axial momentum per unit volume in the control volume. Substituting these relations, applying a continuity constraint and assuming that conditions on opposite sides of the control volume are related by a first order Taylor series expansion, Bajura's balance becomes after considerable algebra:

$$\text{SourceTerms} = -\rho v_O^2 A_1 \delta x \frac{d\beta}{dx} - (2\beta - \gamma) v_O \rho A_1 \delta x \frac{dv}{dx} \qquad 3.15$$

$\frac{d\beta}{dx}$ accounts for changes in the flux profile due to plenum entrance effects as a function of position. β becomes constant within the first 20% of the header length when fully devel-

oped flow is established. It is very dependent on the header geometry. $(2\beta - \gamma)$ is the overall momentum correction factor, θ. If v_x equals v_O and the velocity profile is flat across A_3, then γ equals 1. If the velocity profile across A_1 is flat, then β equals 1. A similar analysis can also be made for the outlet header. This particular condition is exactly that contained in the model if the momentum correction factors were not included. Bajura's experiments found that for fully developed incompressible flow the values of γ were 0.95 and -0.66 for the inlet and outlet headers respectively (B-4). The corresponding values of θ were 1.05 and 2.66 (B-6). These are consistent with plug flow and a β of 1.

The fact that γ for a dividing header is approximately .95 says that v_x is less than v_O (B-4). This can be explained if one assumes that the lower kinetic energy boundary layer is preferentially turned to radial flow by the virtue of its position relative to the bulk axial flow and the radial flow openings. γ for a combining, outlet, header tends to -.66 and represents a fundamentally different interaction between the radial and the axial streams. In a combining header, the radial stream carries virtually no axial momentum into the plenum control volume. But it does add to the mass in the header and effectively reduces the flow area available to axial flow stream entering the volume at the upstream face. This necessitates a velocity increase and a further pressure drop in addition to that required to accelerate the incoming flow and counter friction effects, thus the large value of θ in a combining header (B-4). γ should not be viewed as implying the axial momentum of the radial flow stream is in the opposite direction of the plenum flow and momentum.

Datta and Majumdar (D-1, M-1) took Bajura's results one step further. They transformed the equation to a finite difference form and relaxed the requirements for constant

porosity and lateral (radial) flow resistance. Using this and Bajura's recommended values for θ they found that the entrance effect term, $\frac{d\beta}{dz}$, did not significantly affect the results and assumed β was constant for a given header configuration and flow.

The model of the fuel element combines the preceding formulations and adds the time dependency to transform the general momentum equation, 3.4, to the following form for the inlet and outlet plenums.

$$\left(\frac{d}{dt} m \vec{v}_{axial}\right)_{cv} = \vec{F}_{press} + \vec{F}_{friction} + \theta\left[\oint_{A_1} \rho v_w^2 dA - \oint_{A_1} \rho v_e^2 dA - \oint_{A_3} \rho v_z v_3 dA\right] \qquad 3.16$$

Refer to Fig 3.3 for notation. The radial momentum balance for the plenums retains the form of Eq. 3.4.

Although this model is based on incompressible flow, it still represents an improvement to the unmodified momentum balance. Anticipated gas velocities do not exceed 30 to 40% of the speed of sound, so the compressive effects should be minimal. The value of β is assumed to be 1. However, if solutions indicate flows are near the laminar turbulent transition β can be adjusted to achieve a better fit of predictions to the data.

From the designer's perspective, the two variables with the greatest influence on flow distribution are the ratio of axial to total radial flow area and the resistance to radial flow. Ideally, the larger the radial flow resistance and the smaller the area ratio the easier it is to achieve the desired distribution of flow (B-6). The fuel element uses the radial flow

resistance of the cold frit to control the flow distribution. The cold frit pressure drop is over 10 times the pressure drop of the rest of the fuel element. This high pressure drop is the price of maintaining flow distribution stability under a wide range of operating conditions.

3.4 THE MASS BALANCE

3.4.1 The General Form of the Equation

The mass balance accounts for the amount of hydrogen in the system and ensures that in steady state the mass entering the system equals the mass leaving of the system.

The general equation describing the mass conservation is derived from the General Transport Equation, Eq. 3.1. In this case the transport function, $f(\vec{r},t)$ is replaced by ρ, the density. The equation becomes:

$$\frac{Dm}{Dt}\int\int_V\int \rho dV = \frac{d}{dt}\int\int_V\int \rho dV + \oint_S \rho\vec{v}\cdot\vec{n}dS \qquad 3.17$$

Substituting Eq. 3.3 this reduces to:

$$\frac{Dm}{Dt} = \left(\frac{dm}{dt}\right)_{cv} - \sum_{i=1}^{I}\dot{m}_i \qquad 3.18$$

Since the substantial derivative of the mass equals zero, the continuity balance can be stated as:

$$\left(\frac{\mathrm{d}}{\mathrm{d}t}m\right)_{cv} = \sum_{i=1}^{I} \dot{m}_i \qquad 3.19$$

The time rate of change of the mass in the control volume is equal to the net mass flux into the volume.

There are no source terms in the equation. This is consistent with the absence of any chemical or nuclear reactions that produce a significant amount of hydrogen.

The continuity balance could theoretically be used on any arbitrarily defined control volume. However, for the convenience of the solution algorithm, it will be applied to a pressure centered control volume as shown in Fig 2.6.

3.4.2 The Flux Term

As done with the momentum balances, the mass flux across a control volume surface is the product of the density, velocity perpendicular to the face and the face area, Eq. 3.12. Since it is the superficial velocity, the total face area should be used. The difference from the momentum case is that the velocities are defined on each face of the control volume in accordance with the staggered grid simplifying the evaluation of the flux terms. Thus, everything required is known from geometry or is a defined variable obtained when the overall solution is completed.

3.5 THE ENERGY BALANCE

3.5.1 The General Form of the Equation

The energy balance serves two purposes. First it provides the additional equation required to solve for the state variables of the hydrogen. The momentum and mass balances are sufficient to obtain a hydraulic solution for an adiabatic incompressible flow system. However, for compressible flows, since density is a function of temperature and pressure, the third equation in conjunction with the equation of state is necessary to obtain velocity, temperature, density and pressure. Second the enthalpy balance is the primary heat transfer relationship representing the connection between the solid, heat producing, phase and the coolant gas phase.

The energy balance is also derived from the General Transport Equation, Eq. 3.1. This time the transport function is ρh, where h is the specific enthalpy. Substituting and integrating Eq. 3.1 yields

$$\frac{DH}{Dt} = \left(\frac{dH}{dt}\right)_{cv} - \sum_{i=1}^{I} \dot{m} h \qquad 3.20$$

The substantial derivative (follows motion of a given mass) of the total enthalpy, H, is:

$$\frac{DH}{Dt} = Q + V\frac{dP}{dt} \qquad 3.21$$

where Q, the heat input, and $V\frac{dP}{dt}$, the change in the pressure volume product, are the source terms. Substituting in Eq. 3.20 and rearranging gives:

$$\left(\frac{d}{dt}H\right)_{cv} = Q + V\frac{dP}{dt} + \sum_{i=1}^{I} \dot{m}h \qquad 3.22$$

Thus, the time rate of change of the enthalpy in the a fixed control volume is the sum of the heat input, change in the PV product and the net enthalpy flux into the volume.

The staggered grid defines all the state variables at the same points. Therefore, enthalpy, pressure, temperature and density are co-located and the control volume is identical to that used for the continuity equation.

3.5.2 The Source Term

There are two "sources" of enthalpy within the control volume. One is the heat generated in the solid and transferred to gas phase. The other is the change in control volume pressure.

The pressure dependence is the simpler to analyze. Since the control volume size is constant, the change in the enthalpy is the product of the volume and the change in pressure. The change is the pressure increment since the last time the enthalpy was evaluated.

When the fuel element is in operation, the larger source will be the energy transfer from the solid phase. As with most transport phenomena, the heat transferred to the hydrogen is proportional to a driving force. In this case, the driving force is the temperature difference between the fuel surface and the bulk coolant temperature.

$$Q = \mathrm{h}\mathrm{A}_{\mathrm{V}} V (T_S - T_G) \tag{3.23}$$

where Q is the total energy transferred per unit time in the control volume. h is the heat transfer coefficient and A_{V} is the total particle surface area per unit volume of the bed.

The heat transfer coefficient is a function of the mass flow rate, the shape of the particles and the physical properties of the hydrogen. Empirical correlations have proven most effective for determining h. The relation used in this model is (B-3)

$$j_H = 0.91 \mathrm{Re}^{-0.51} \psi (\mathrm{Re} < 50) \tag{3.24a}$$

$$j_H = 0.61 \mathrm{Re}^{-0.41} \psi (\mathrm{Re} > 50) \tag{3.24b}$$

$$j_H = \frac{\mathrm{h}}{\hat{\mathrm{C}}_{pb} G_0} \left(\frac{\hat{\mathrm{C}}_{pf} \mu_f}{\mathrm{k}_f} \right)^{2/3} \tag{3.24c}$$

$$\mathrm{Re} = \frac{G_0}{\mathrm{a} \mu_f \psi} \tag{3.24d}$$

j_H = Colburn j factor

$\hat{\mathrm{C}}_{pb}$ = Heat capacity at constant pressure of the gas at bulk temperature

$\hat{\mathrm{C}}_{pf}$ = Heat capacity at constant pressure of the gas at film temperature

k = Thermal conductivity of the gas film

μ_f = Viscosity of the gas film

G_0 = Superficial mass velocity

ψ = Particle shape factor, 1.0 for spheres

The film is the boundary layer of coolant next to the surface of the fuel particle. The correlation approximates the film temperature by averaging the solid surface temperature and the bulk gas temperature. The Reynolds number used in this correlation is different than the one used in the momentum equation pipe flow friction term. Here, the length term is the inverse of the particle area per unit volume as opposed to the equivalent diameter for flow. The result is that the Re should range from 5 to 20 in the packed bed.

3.5.3 The Flux Term

The flux through each face of a control volume is the product of the density, superficial velocity, area and the specific enthalpy. These are added vectorialy to determine the net enthalpy flux. The final form of the balance is:

$$\left(\frac{\mathrm{d}}{\mathrm{d}t}H\right)_{cv} = \mathrm{h}\mathrm{A}_{\mathrm{v}}V(T_S - T_G) + V\frac{\mathrm{d}P}{\mathrm{d}t} + \sum_{i=1}^{I}\dot{m}_i h_i \qquad 3.25$$

All of the terms in the balance can now be either evaluated or expressed as the product of a constant coefficient and a variable that will be determined when the balances are solved. The physical properties are generally evaluated using previous time step values for the state variables.

3.6 SUMMARY

The gas phase model of the packed bed fuel element consists of four lumped parameter conservation equations simultaneously applied to an array of control volumes. The balance equations are shown in Table 3.1.

Table 3.1

The Gas Phase Conservation Equations		
Axial Momentum	$\left(\frac{d}{dt} m \vec{v}_{axial}\right)_{cv} = \vec{F}_{press} + \vec{F}_{friction} + \theta \sum_{i=1}^{I} \dot{m}_i \vec{v}_{axial,i}$	note1
Radial Momentum	$\left(\frac{d}{dt} m \vec{v}_{radial}\right)_{cv} = \vec{F}_{press} + \vec{F}_{friction} + \sum_{i=1}^{I} \dot{m}_i \vec{v}_{radial,i}$	
Mass	$\left(\frac{d}{dt} m\right)_{cv} = \sum_{i=1}^{I} \dot{m}_i$	
Energy	$\left(\frac{d}{dt} H\right)_{cv} = hA_V V(T_S - T_G) + V\frac{dP}{dt} + \sum_{i=1}^{I} \dot{m}_i h_i$	
Note 1: θ: Inlet Plenum 0.95, Outlet Plenum 2.66, Otherwise 1.0		

The basic equations are the same for all of the volumes. The differences between components are reflected in the way the individual source terms are evaluated and the dimensions of the control volumes.

CHAPTER 4

SOLUTION METHOD FOR THE GAS PHASE THERMAL HYDRAULICS

4.1 OBJECTIVE

The fundamental gas phase balances described in chapter 3 contain sufficient information to solve for the hydrogen temperature, pressure, velocity and density as a function of position when they are combined with appropriate boundary conditions and fuel element geometry. Many numerical schemes have been developed for the solution of fluid dynamics problems. This chapter describes the method chosen for this analysis, including the required transformation of the equations to finite difference form and the approximations imposed on the model.

4.2 SOLUTION METHODS

4.2.1 Choice of a Numerical Method

The basic problem in computational fluid dynamics is to reduce a highly nonlinear set of equations to a set of simultaneous linear equations that still retain the properties of the originals and can be solved using standard matrix techniques. All methods which are applied to digital computers require transformation of the continuous equations to a discrete form, finite difference in this model. In the discrete form, the variables can not vary continuously. Rather the values are defined at specific points which are paired with a control volume. Consistent with the lumped parameter approach, the value of the variable is assumed to be the same everywhere in the associated control volume.

The discretization is also the step that performs the linearization and determines how time is handled. Implicit differencing uses the unknown values of the next time step and the current time step values; where, explicit differencing uses only current and past values to advance to the next time step. Implicit equations require greater computational effort than explicit ones.

Solution of the discretized equations can be accomplished by iterative, predictor-corrector or shooting techniques. Each type has its strengths. In the end, the choice of a method is a trade off between stability, accuracy and computing time.

Three numerical methods commonly found in the solution of heat transfer and fluid flow problems are the Semi-Implicit Method for Pressure Linked Equations (SIMPLE)(P-2,P-3 and P-4). The Pressure Implicit with Splitting of Operators method (PISO) (I-1,I-2) and the Implicit Continuous-fluid Eulerian method (ICE) (H-3). All of these methods use the same basic balance equations but manipulate them differently to achieve the final solution. Some degree of implicitness is included in all of them for numerical stability.

The SIMPLE algorithm is an iterative technique developed by S. V. Patankar and his co-workers (P-2,P-3,P-4). In this method, one first guesses the pressure field values at the advance time, n+1. Then, the corresponding velocities are calculated using the momentum equations. The mass and energy balances are used to correct the pressure and velocity fields. The new pressure is compared to the initial guess and iteration continues until the desired degree of convergence is obtained.

The PISO method is similar to SIMPLE except that it starts with the current pressure field and is noniterative. The technique uses the mass balance and a predictor corrector format to remove the linkage between the pressure and velocity equations.

ICE is also noniterative and has been employed successfully for the solution of two phase flow problems in the THERMIT code (K-1).

The PISO algorithm developed by R. I. Issa (I-1,I-2) has been adopted for this model of a packed bed fuel element. Since it is noniterative, the solution time is expected to be the shortest giving the greatest potential for use in a real time digital controller. The semi-implicit structure of the finite difference equations provides the necessary stability. The ICE method would also be acceptable. Although PISO does not allow the arbitrary accuracy available in iterative procedures, it is considered as accurate the differencing scheme used to discretize the equations (I-1).

Unlike SIMPLE and related methods which use density corrections or update density at the end of an iteration, PISO forces the final pressure and velocity fields to satisfy the momentum and mass balances simultaneously. This feature is the key to avoiding the need for iteration (I-1). For a compressible flow test problem, Issa found that PISO required 19% of the computing time of SIMPLE and that the method was stable over a much wider range of time step size (I-2).

4.2.2 The PISO Algorithm

The following summary of the PISO procedure is presented to motivate the discretization of the balance equations. Sections 4.6 and 4.7 contain the detailed sequencing of the equations and the boundary conditions.

PISO uses two predictor corrector stages to advance the values of the variables from time n to n+1 through a series of ever more refined approximations. The first predictor uses the momentum balances to make the first estimate of the n+1 velocity field. It uses the current (already computed) time n values for all variables except the desired velocity.

The radial and axial velocities calculated in the first predictor satisfy the momentum balance but usually not the mass balance. The first corrector applies the continuity equation to the momentum balances. The resulting pressure equation is used to provide the first approximation to the new pressure and density. The second estimate of the velocities is also obtained.

The second predictor is accomplished using the energy conservation equation. In this case, the enthalpy balance is used. It advances the temperature and serves as the heat transfer link to the solid phase. The new temperature allows one to update the equation of state relationship between temperature, density and pressure.

The second corrector is similar to the first corrector. It is derived by combining the momentum equations, mass balance and the new equation of state. The result is the second determination of the pressure and density at n+1 and the third approximation of the velocity field.

If one desired, a third predictor corrector stage could be added. The method discussed here uses only two stages. Thus, to advance the variables one time step the method makes three successive estimates of the velocities, two updates of the pressure and density and one approximation for the new temperature field. To see how this scheme works one must first look at the discretized form of the equations.

4.3 DISCRETIZATION OF THE MOMENTUM AND ENERGY BALANCES

4.3.1 The General Equation

The built in stability of the PISO method starts with the transformation of the balance equations to an implicit finite difference form which is amenable to a computer based numerical solution. The equations are arranged to advance the values of the variables from the current time step, n, to the n+1 time step.

A review of Table 3.1 shows a useful similarity in the momentum and enthalpy conservation equations. All of them equate the time rate of change of a quantity in a control volume to the sum of the sources and the fluxes crossing the control volume surfaces. Therefore, discretizing a general equation using the dummy variable ϕ essentially discretizes all of the equations. The radial and axial velocities or the specific enthalpy can be substituted for ϕ. Thus, one starts the transformation with the general conservation equation

$$\left(\frac{\mathrm{d}}{\mathrm{d}t}\rho\phi\right)_{cv} = source + \sum_{i=1}^{I} \dot{m}\phi \qquad 4.1$$

The time derivative can be represented in discrete form by the following implicit finite difference

$$\left(\frac{d}{dt}\rho\phi\right)_{cv} = \left(\frac{\rho^{n+1}\phi^{n+1} - \rho^{n}\phi^{n}}{\delta t}\right)\delta V \approx \rho^{n}\left(\frac{\phi^{n+1} - \phi^{n}}{\delta t}\right)\delta V \qquad 4.2$$

The time n density is used, since the density at n+1 is not determined in the first predictor step of the PISO method.

The flux terms are the product of the mass flow rate across the control surface and the quantity ϕ . The mass flow is evaluated using the expression

$$mass \quad flow \quad rate \quad = \quad \rho v a \qquad 4.3$$

where v is the velocity normal to the control volume surface of area a . For the control volume shown in Fig. 4.1 the ϕ flow rates across the control volume surfaces are

$$(\rho^{n} v^{n}_{axial} a\phi)_{w} \qquad 4.4a$$

$$(\rho^{n} v^{n}_{axial} a\phi)_{e} \qquad 4.4b$$

$$(\rho^{n} v^{n}_{radial} a\phi)_{n} \qquad 4.4c$$

$$(\rho^{n} v^{n}_{radial} a\phi)_{s} \qquad 4.4d$$

where the lower case letters identify the surfaces.

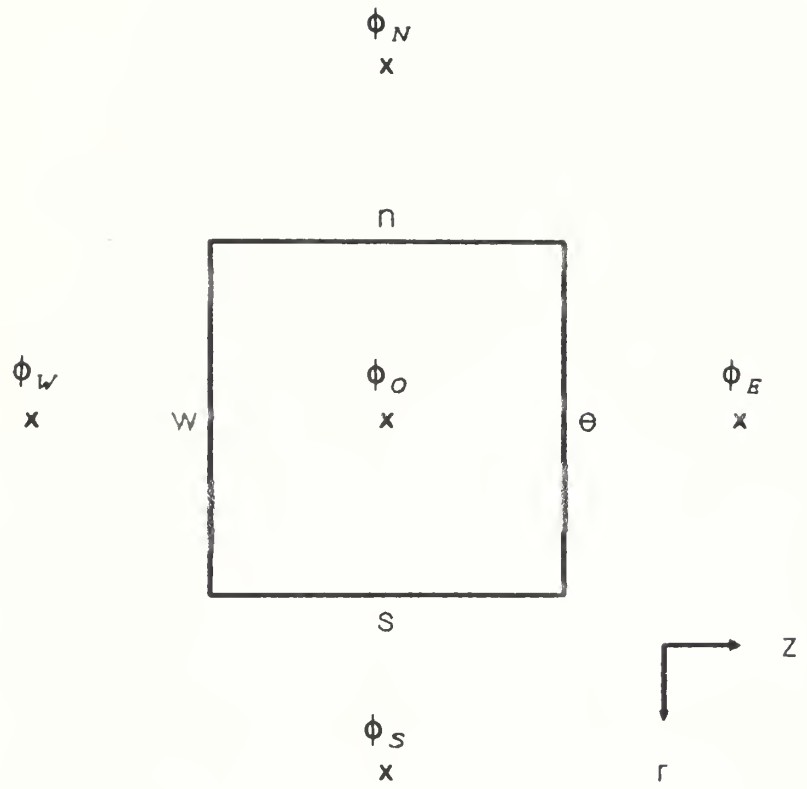

Figure 4.1

The Control Volume for the General Variable Phi

A complication occurs in the momentum equations when ϕ represents a velocity. This results in making the flux term a function of the square of the velocity and hence nonlinear. Fully implicit differencing would have all of the ϕs, except the one in the time derivative, evaluated at time n+1. In order to obtain a linear equation a compromise is made. The velocity in the mass flow calculation is evaluated at the current time, n, and ϕ is evaluated at the n+1 time step. This also resolves another problem. If the axial momentum balance is performed before the radial balance, v_{radial}^{n+1} is required to compute the flow through the north and south faces of the control volume but is not known. The compromise allows the use of the current time value of the radial velocity. The same situation exists in the radial balance. As a result, the flux term remains a function of velocity squared yet linear in terms of v^{n+1}. This approximation is made in the flow calculations in both the momentum and enthalpy equations.

The question now becomes how to evaluate a variable if it is not defined at the control volume interface, for example ϕ in Fig 4.1. One scheme would be to average the values on either side the interface. This works in some instances and is done to estimate the current velocity in the mass flow term. However, this often breaks down when convection due to fluid flow is present. If the gas phase flows from W to O, the value of the gas density at the interface much more nearly resembles the density ϕ_W than ϕ_O. Several methods, varying from exact to simple estimations, are available to describe this effect.

For simplicity the donor cell or upwind method is chosen here. This procedure looks at the direction of the convective flow and assumes that the value of a quantity at the interface is its value in the upstream control volume. Mathematically, the donor cell method evaluates ϕ at the west interface by

$$(0.5+\alpha)\phi_W + (0.5-\alpha)\phi_O \quad = \quad \phi|_w \qquad 4.5$$

Where:

$\alpha = 0.5$ if the flow is from W to O

$\alpha = -0.5$ if the flow is from O to W

α is the upwinding factor. It is evaluated using the time n value of the velocity whose sign indicates the direction of flow. If density is not defined on the interface, the procedure is followed again using velocity as the flow reference. Combining the results above, Eq. 4.1 is transformed to:

$$\begin{aligned}\delta V \rho^n \left(\frac{\phi^{n+1}-\phi^n}{\delta t}\right) = source &+(\rho^n v^n_{axial} a)_w ((0.5+\alpha_w)\phi^{n+1}_W + (0.5-\alpha_w)\phi^{n+1}_O) \\ &+(\rho^n v^n_{axial} a)_e ((0.5+\alpha_e)\phi^{n+1}_O + (0.5-\alpha_e)\phi^{n+1}_E) \\ &+(\rho^n v^n_{radial} a)_s ((0.5+\alpha_s)\phi^{n+1}_S + (0.5-\alpha_s)\phi^{n+1}_O) \\ &+(\rho^n v^n_{radial} a)_n ((0.5+\alpha_n)\phi^{n+1}_O + (0.5-\alpha_n)\phi^{n+1}_N) \qquad 4.8\end{aligned}$$

Rearranging and making the following substitutions

$$M_x = (\rho^n v^n a)_x$$

$$A_w = (0.5+\alpha_w) M_w$$

$$A_e = -(0.5-\alpha_e) M_e$$

$$A_s = (0.5+\alpha_s) M_s$$

$$A_n = -(0.5-\alpha_n) M_n$$

reduces Eq. 4.6 to

$$\delta V \rho^n \left(\frac{\phi^{n+1} - \phi^n}{\delta t} \right) = source - \phi_O^{n+1}(A_e + A_w + A_n + A_s + M_e - M_w + M_n - M_s)$$
$$+ A_e\phi_E^{n+1} + A_w\phi_W^{n+1} + A_n\phi_N^{n+1} + A_s\phi_S^{n+1} \qquad 4.7$$

This is the discretized form of the general equation. However, to put it in a more tractable form the operator H' and the coefficient A_O are defined and substituted into the equation. The H' operator is also used in several of the other discrete conservation equations.

$$A_O = -(A_e + A_w + A_n + A_s + M_e - M_w + M_n - M_s)$$
$$H'(\phi) = A_e\phi_E^{n+1} + A_w\phi_W^{n+1} + A_n\phi_N^{n+1} + A_s\phi_S^{n+1}$$
$$\left(\frac{\rho^n \delta V}{\delta t} - A_O \right) \phi^* = source + H'(\phi^*) + \frac{\rho^n \phi^n \delta V}{\delta t} \qquad 4.8$$

Eq. 4.8 is discretized with the exception of the source term which is specific to the balance being studied. Note, that the superscript * has been used in lieu of n+1. Since the momentum and energy balances compute only an approximation of the n+1 value, the single asterisk designates it as the first guess.

4.3.2 The Momentum Balance and Source Terms

The discrete form of the momentum balances can be obtained by substituting the appropriate velocity for ϕ and transforming the source terms.

Fig. 4.2 shows a control volume associated with radial velocity and locates where the principal variables are defined. The pressure force acting as a source of radial momentum is discretized by estimating the derivative and multiplying by the area.

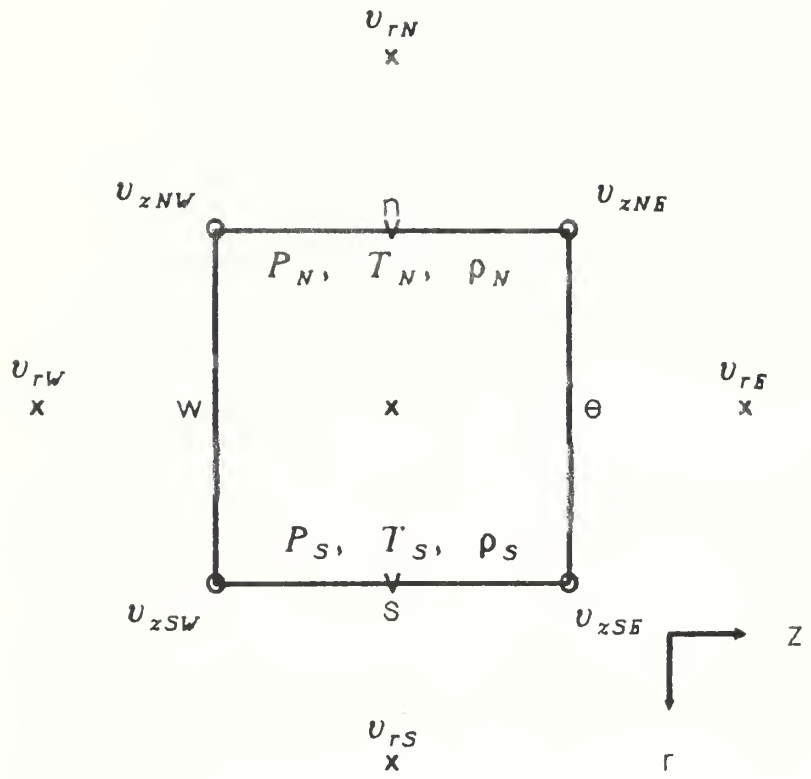

x Radial Velocity

o Axial Velocity

v State Variables

Figure 4.2

The Radial Momentum Balance

Control Volume and Variables

$$pressure \quad force \quad = \quad -\frac{dP}{dr}La \quad = \quad -(P_N^n - P_S^n)a \tag{4.9}$$

The current time step values of pressure are used since the PISO algorithm solves for velocity using the momentum conservation equations before advancing the pressure variable. The mean gas phase area is used as discussed in section 3.3.2.

The other source term in the momentum equations is the friction force. In the frits and the fuel particles this is characterized by the Ergun relation, Eq. 3.11. Rearranging this to calculate the pressure force yields

$$\Delta P a = aL\left(\frac{150\mu\vec{v}_0}{D_p^2}\frac{(1-\varepsilon)^2}{\varepsilon^3} + \frac{1.75\rho\vec{v}_0|v|}{D_p}\frac{(1-\varepsilon)}{\varepsilon^3}\right) \tag{4.10}$$

Since the friction force is a function of velocity squared, it must be linearized. The same technique used in the flux term is applied. Using Fig. 4.2

$$\vec{v}_O = v_O^{n+1} \tag{4.11}$$

$$|v^n| = \sqrt{\left(.25(v_{aNW}^n + v_{aNE}^n + v_{aSE}^n + v_{aSW}^n)\right)^2 + (v_{rO}^n)^2} \tag{4.12}$$

This maximizes the implicitness of the relation. As a result, the left hand side of Eq. 4.8 becomes

$$\left(\frac{\rho^n \delta V}{\delta t} - A_O + aL\left(\frac{150\mu}{D_p^2}\frac{(1-\varepsilon)^2}{\varepsilon^3} + \frac{1.75\rho|v_O^n|}{D_p}\frac{(1-\varepsilon)}{\varepsilon^3}\right)\right) = \left(\frac{\rho^n \delta V}{\delta t} - A_O + Fric\right) \tag{4.13}$$

The friction term for the plenums is treated similarly with the Re calculated based on the time n velocity.

The discrete form of the radial momentum conservation equation used in the PISO solution algorithm is:

$$-\left(\frac{\delta V}{\delta t}-\frac{A_O}{\rho^n}+\frac{Fric}{\rho^n}\right)\rho^n v_{rO}^{*}+H'(v_r^{*})=(P_N^n-P_S^n)a-\frac{\rho^n v_{rO}^n \delta V}{\delta t} \qquad 4.14$$

Eq. 4.14 has been arranged to facilitate solution of the resulting system of simultaneous equations when each of the radial velocity control volumes is considered. The left hand side can be factored into a matrix of coefficients multiplied by a vector containing the radial velocities for each of the control volumes. The right hand side is a constant vector, since all values are known for time n. The axial momentum is handled analogously.

4.3.3 The Energy Balance and Source Terms

Heat transferred from the solid phase and the change in the pressure volume product are the source terms in the energy balance for the control volume shown in Fig 4.3. The energy transferred from the fuel particles couples the solutions of the solid and the gas phase models.

The heat source term is simply:

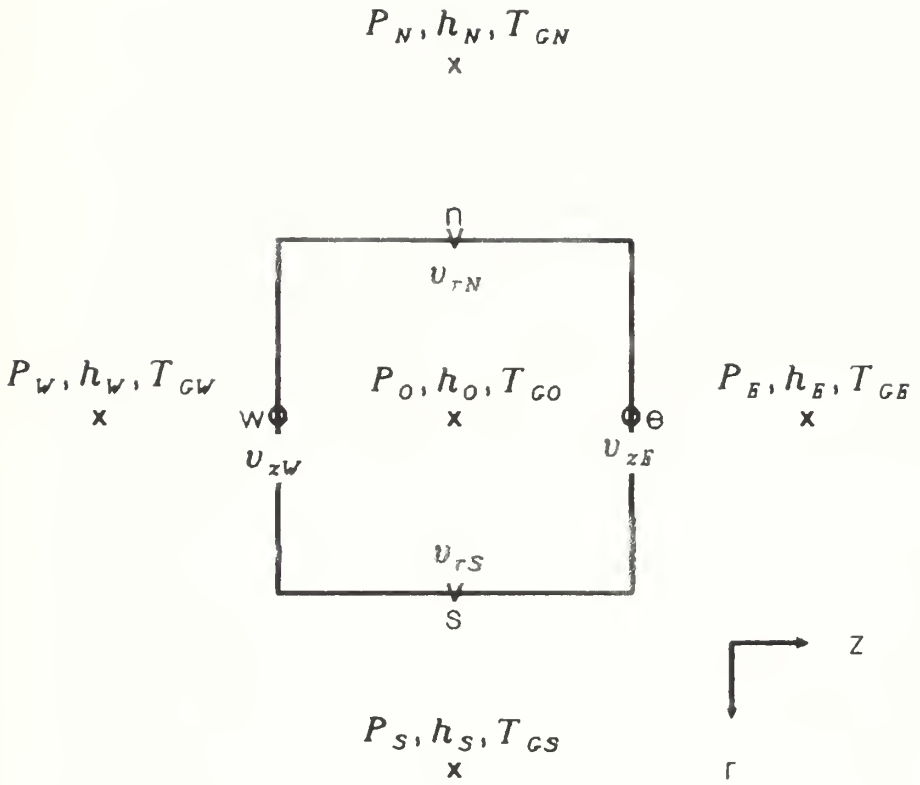

x State Variables

o Axial Velocity

v Radial Velocity

Figure 4.3

The Energy and Mass Balance

Control Volume and Variables

$$Q = hA_v V_{cv}(T_S^n - T_G^n) \qquad 4.15$$

The problem is whether to use the time n or n+1 values for the temperatures. A heat source term based on time n would be the easiest to handle. However, this introduces the stability problems associated with explicit differencing. These are magnified by the small gas volume and heat capacity. The authors of the THERMIT code (R-1) developed a fully implicit method for treating the heat transfer from the fuel which is used in this model.

In order to treat both the solid and gas temperatures implicitly, the procedure consists of three steps which combine the results of the solid and gas energy conservation equations.

First, the model assumes T_G^n equals T_G^{n+1} and solves the solid phase energy balance for T^* and $\partial T_S^{n+1}/\partial T_G^{n+1}$ where T^* is the first approximation to the new solid temperature.

Second with T^* substituted for T_S^{n+1} the fluid phase enthalpy balance is solved for the enthalpy at n+1. To do this, Eq. 4.15 is modified to account for the fact that $T^*$is not the final value of T_S^{n+1}. This results in Eq. 4.16a which is transformed to the conservation variable used in the rest of the equation by substituting 5.16b. Eq. 5.16c shows the final form of the heat source term in the gas phase model.

$$Q = hA_V V_{cv}(T_S^* - T_G^{n+1}) + hA_V V_{cv}\left(\frac{\partial T_S^{n+1}}{\partial T_G^{n+1}}\right)(T_G^{n+1} - T_G^n) \qquad 4.16a$$

$$T_G^{n+1} - T_G^n = \frac{h^{n+1}}{C_P} - \frac{h^n}{C_P} \qquad 4.16b$$

$$Q = hA_V V_{cv}\left(T_S^* - \frac{h^{n+1}}{C_P} + \frac{h^n}{C_P} - T_G^n\right) + hA_V V_{cv}\left(\frac{\partial T_S^{n+1}}{\partial T_G^{n+1}}\right)\left(\frac{h^{n+1}}{C_P} - \frac{h^n}{C_P}\right) \qquad 4.16c$$

Lastly, now that the true value of T_G^{n+1} is known, T^* is updated to T_S^{n+1} using Eq. 4.17.

$$T_S^{n+1} = T_S^* + \frac{\partial T_S^{n+1}}{\partial T_G^{n+1}}(T_G^{n+1} - T_G^n) \qquad 4.17$$

Chapter 5 presents the fuel particle model and how to evaluate T^* and the temperature derivative. The fuel temperature and heat transfer coefficient are further modified and replaced by $\overline{T}$ and $\overline{U}$ when the exact definitions of the solid phase model are applied.

The pressure volume term is less complicated. The discretized form is

$$V\frac{dP}{dt} = \frac{\delta V(P.I.)_O}{\delta t} \qquad 4.18$$

Here $(P.I.)_O$ is the estimate of the pressure change between n and n+1 calculated by the first corrector in the PISO method. This value is available, since the energy balance is used as the second predictor.

Combining the enthalpy source terms with the general discretized balance equation results in the following discrete energy conservation equation:

$$\left(\frac{\delta V\rho^{*}}{\delta t}-A_{O}+\left(\frac{\overline{U}V_{cv}A_{V}}{C_{P}}\right)\left(1+\frac{\partial\overline{T}^{n+1}}{\partial T_{G}^{n+1}}\right)\right)h^{*}=\overline{U}A_{V}V_{cv}\left(\overline{T}^{*}+\frac{h^{n}}{C_{P}}+T_{G}^{n}-\frac{\partial\overline{T}^{n+1}}{\partial T_{G}^{n+1}}\frac{h^{n}}{C_{P}}\right)$$

$$+\frac{\delta V(P.I.)_{O}}{\delta t}+H'(h^{*}) \qquad 4.19$$

ρ^{*} is the first approximation of ρ^{n+1} which is calculated in the first corrector step and A_V is the particle surface area per unit volume of the packed bed.

4.4 THE MASS BALANCE

The mass balance is implemented by using the control volumes centered on pressure and the other state variables. This in conjunction with the staggered grid, which conveniently defines the velocities on the faces of the control volume as shown in Fig. 4.3, makes the conservation of mass flow calculation straight forward.

Since no sources exist within the control volume, only the mass flows and the time derivative terms of the continuity equation require transformation. The techniques used on the similar terms in the momentum balances yield Eq. 4.20 which is the form of the mass balance used in the first corrector.

$$-\left(\frac{\rho^{*}-\rho^{n}}{\delta t}\right)\delta V+(\rho^{*}v_{a}^{**}a)_{w}-(\rho^{*}v_{a}^{**}a)_{e}+(\rho^{*}v_{r}^{**}a)_{s}-(\rho^{*}v_{r}^{**}a)_{n}=0 \qquad 4.20$$

Note that the second estimate of v^{n+1} is used. No requirement for a mass balance was imposed on the first predictor. As a result, the v^{*} values do not satisfy this relation.

4.5 THE PRESSURE EQUATION

The pressure equation is the core of the PISO method. It is the relation that forces both mass and momentum to be conserved simultaneously. The derivation of the equation outlined below is adopted from references (I-1,I-2).

The continuity equation, 4.20, for the control volume and variables shown in Fig. 4.3 forms the foundation of the pressure equation. To this several substitutions developed from the momentum equations are made. Focusing on the east face axial velocity for a moment, the first momentum predictor and corrector relations take the form of Eq. 4.21 and 4.22 respectively. Note that the corrector form is explicit.

$$\left(\frac{\delta V}{\delta t}-\frac{A_O}{\rho^n}\right)\rho^n v_{aE}^{*}=H'(v_{aE}^{*})-(\Delta P^n a)_e+\rho^n v_{aE}^n\frac{\delta V}{\delta t} \qquad 4.21$$

$$\left(\frac{\delta V}{\delta t}-\frac{A_O}{\rho^n}\right)\rho^{*} v_{aE}^{**}=H'(v_{aE}^{*})-(\Delta P^{*} a)_e+\rho^n v_{aE}^n\frac{\delta V}{\delta t} \qquad 4.22$$

Subtracting Eq. 4.21 from 4.22 and solving for $\rho^{*} v_{aE}^{**}$ one obtains:

$$\rho^* v_{aE}^{**} = K^{-1}(\Delta P^* a)_e - K^{-1}(\Delta P^n a)_e + \rho^n v_{aE}^* \qquad 4.23$$

$$K = \left(\frac{\delta V}{\delta t} - \frac{A_O}{\rho^n} \right)$$

$$\Delta P^* = P_E^* - P_O^*$$

Multiplying by the area then gives the mass flow rate through the east face of the control volume. Substituting this and the similar expressions derived from the velocities at the other faces yields:

$$-\frac{\delta V}{\delta t}(\rho^* - \rho^n) - (P_O^* - P_O^n)(D_e + D_w + D_n + D_s)$$

$$+ D_e(P_E^* - P_E^n) + D_w(P_W^* - P_W^n)$$

$$+ D_n(P_N^* - P_N^n) + D_s(P_S^* - P_S^n) = (\rho^n v_a^*)_e - (\rho^n v_a^*)_w + (\rho^n v_r^*)_n - (\rho^n v_r^*)_n$$

$$D_x = (K^{-1} a^2)_x \qquad 4.24$$

The last step relates the density difference to the pressure using the equation of state, $P = \rho R T$, to obtain the following:

$$\rho^* = \frac{P^* \rho^n}{P^n} \qquad 4.25$$

This combined with Eq 4.24 and some algebra gives the final form of the first corrector pressure equation.

$$-\left(\frac{\rho^n \delta V}{P^n \delta t}+D_c\right)(P_O^*-P_O^n)+D_e(P_E^*-P_E^n)+D_w(P_W^*-P_W^n)+D_n(P_N^*-P_N^n)+D_s(P_S^*-P_S^n)$$

$$=(\rho^n v_a^*)_e-(\rho^n v_a^*)_w+(\rho^n v_r^*)_n-(\rho^n v_r^*)_n \qquad 4.26$$

$$D_c=D_e+D_w+D_n+D_s$$

The pressure equation used in the second corrector is derived in the same fashion. Using Eq. 4.22 and the second corrector for momentum, Eq 4.27, gives Eq. 4.28 which is the second corrector pressure equation.

$$\left(\frac{\delta V}{\delta t}-\frac{A_O}{\rho^n}\right)\rho^{**}v_{aE}^{***}=H'(v_{aE}^{**})-(\Delta P^{**}a)_e+\rho^n v_{aE}^n\frac{\delta V}{\delta t} \qquad 4.27$$

$$-\left\{(D_e+D_w+D_n+D_s)+\frac{\rho^*}{P^*}\frac{\delta V}{\delta t}\right\}(P_O^{**}-P_O^*)+D_e(P_E^{**}-P_E^*)+D_w(P_W^{**}-P_W^*)+D_n(P_N^{**}-P_N^*)$$

$$+D_s(P_S^{**}-P_S^*)=\left(\frac{\delta V}{\delta t}-\frac{A_O}{\rho^*}\right)^{-1}(H'(v_{aE}^{**}-v_{aE}^*)-H'(v_{aW}^{**}-v_{aW}^*)+H'(v_{rN}^{**}-v_{rN}^*)-H'(v_{rS}^{**}-v_{rS}^*)$$

$$-\left(A_O\left(\frac{\rho^*-\rho^n}{\rho^n}\right)v^{**}a\right)_e+\left(A_O\left(\frac{\rho^*-\rho^n}{\rho^n}\right)v^{**}a\right)_w-\left(A_O\left(\frac{\rho^*-\rho^n}{\rho^n}\right)v^{**}a\right)_n$$

$$+\left(A_O\left(\frac{\rho^*-\rho^n}{\rho^n}\right)v^{**}a\right)_s)+\frac{\delta V}{\delta t}\left(\frac{\rho^*}{P^*}-\frac{\rho^n}{P^n}\right) \qquad 4.28$$

Where:

$$D_x=\left(\left(\frac{\delta V}{\delta t}-\frac{A_O}{\rho^*}\right)^{-1}\right)_x$$

The pressure equation roots in the momentum and mass conservation equations force the pressure and velocity fields to satisfy the two conditions simultaneously, thereby giving one the option of using a noniterative solution procedure.

4.6 THE SOLUTION ALGORITHM

Sections 4.3 through 4.5 developed the equations required for the PISO solution scheme outlined in section 4.2.2. The following steps provide the solution sequence used for the gas phase in the fuel element model.

First Predictor

1. Solve the radial momentum balance, Eq. 4.14, for the radial velocity field, v_r^*.
2. Solve axial momentum balance, Eq. 4.14, for the axial velocity field, v_a^*.

First Corrector

3. Solve the pressure equation, 4.26, for the pressure increment, $P^* - P^n$.
4. Calculate the P^* field by adding the pressure increment to P^n.
5. Use the equation of state as modeled in the H2EOS program to compute ρ^* given P^* and T^n.
6. Compute the new radial velocities, v_r^{**}, using Eq. 4.23.
7. Calculate the new axial velocity field, v_a^{**}, using an equation similar to 4.23.

Second Predictor

8. Obtain h^* from the enthalpy balance.
9. Use the H2EOS program to get T_G^* given P^* and h^*.

Second Corrector

10. Solve the second pressure equation, 4.28, for $P^{**} - P^{n}$.

11. Calculate P^{**}. This is now P^{n+1}

12. Compute ρ^{**} using the equation of state given P^{**} and T_G^{*}. This is ρ^{n+1}.

13. Calculate the radial velocity, v_r^{***}, using a relation equivalent to Eq. 4.27. This is the time n+1 value.

14. Calculate the axial velocity, v_a^{***}, using a relation similar to Eq. 4.27. This is the n+1 time step value.

The equations solved in steps 1, 2, 3, 8 and 10 are actually sets of M times N simultaneous linear equations, where M is the number of radial nodes and N is the number of axial nodes. These steps are most easily accomplished by treating the equations in matrix form.

[Matrix of Coeff.][Variable Vector] = [Constant Vector]

A wide variety of methods exist to solve this problem. For large numbers of nodes iterative techniques are probably most efficient. Issa recommends the use of ADI or Stone's Strongly Implicit Procedure (I-2). For smaller matrices direct solution methods such as LU decomposition can be used.

4.7 BOUNDARY CONDITIONS

Once the equations and physical data are available, problem definition is completed by adding the appropriate boundary conditions. Figures 4.4 a, b and c show the control volume arrays for typical momentum and pressure equation solutions.

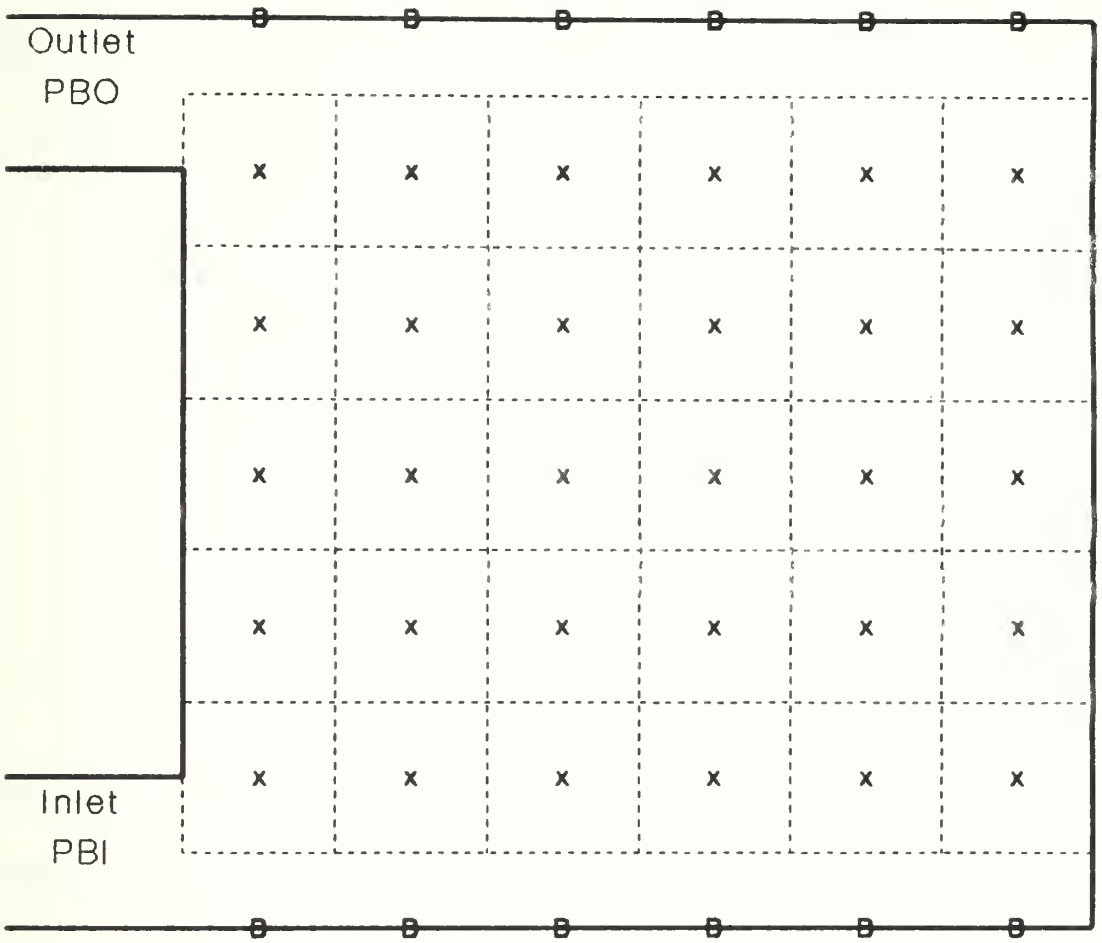

x Calculated Radial Velocity

B Boundary Condition

PBI Inlet Pressure

PBO Outlet Pressure

Figure 4.4a

Radial Velocity

Control Volume Array

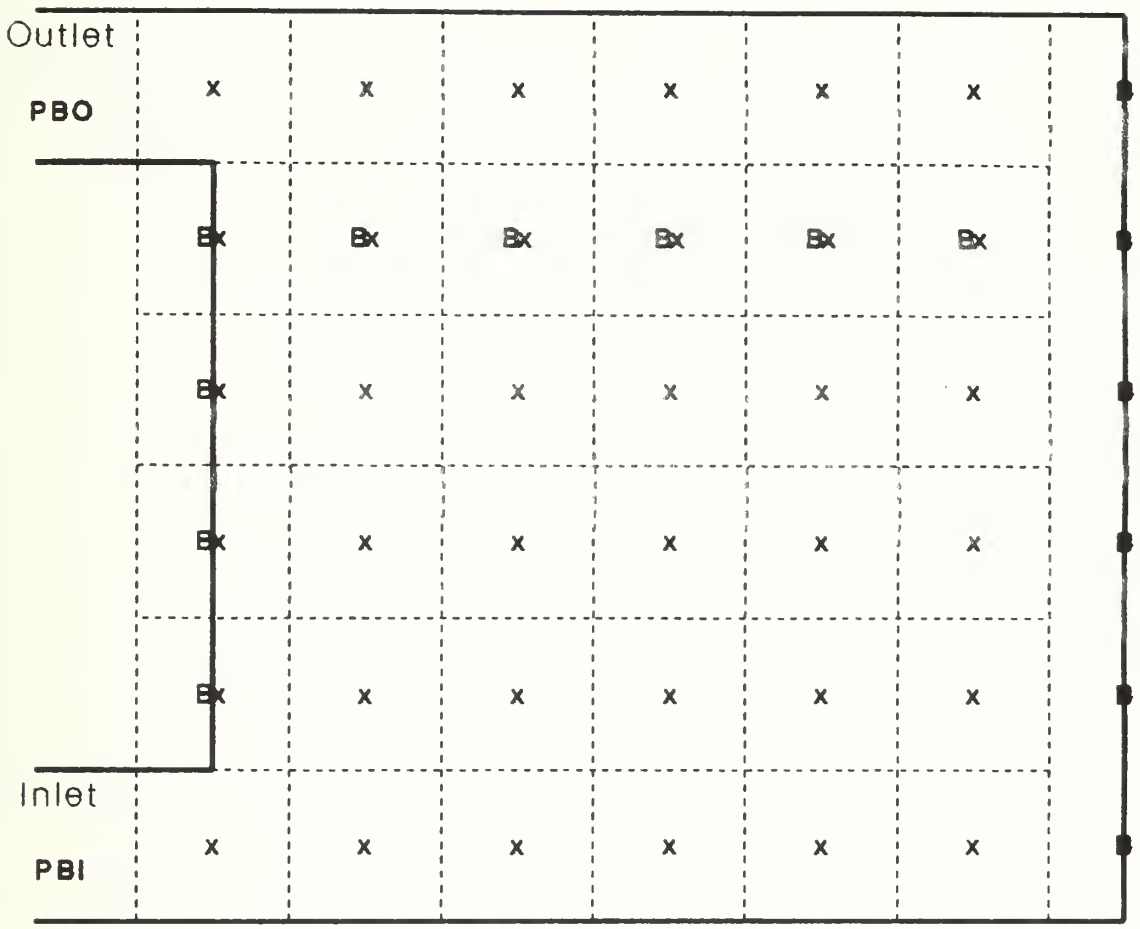

Figure 4.4b

Axial Velocity

Control Volume Array

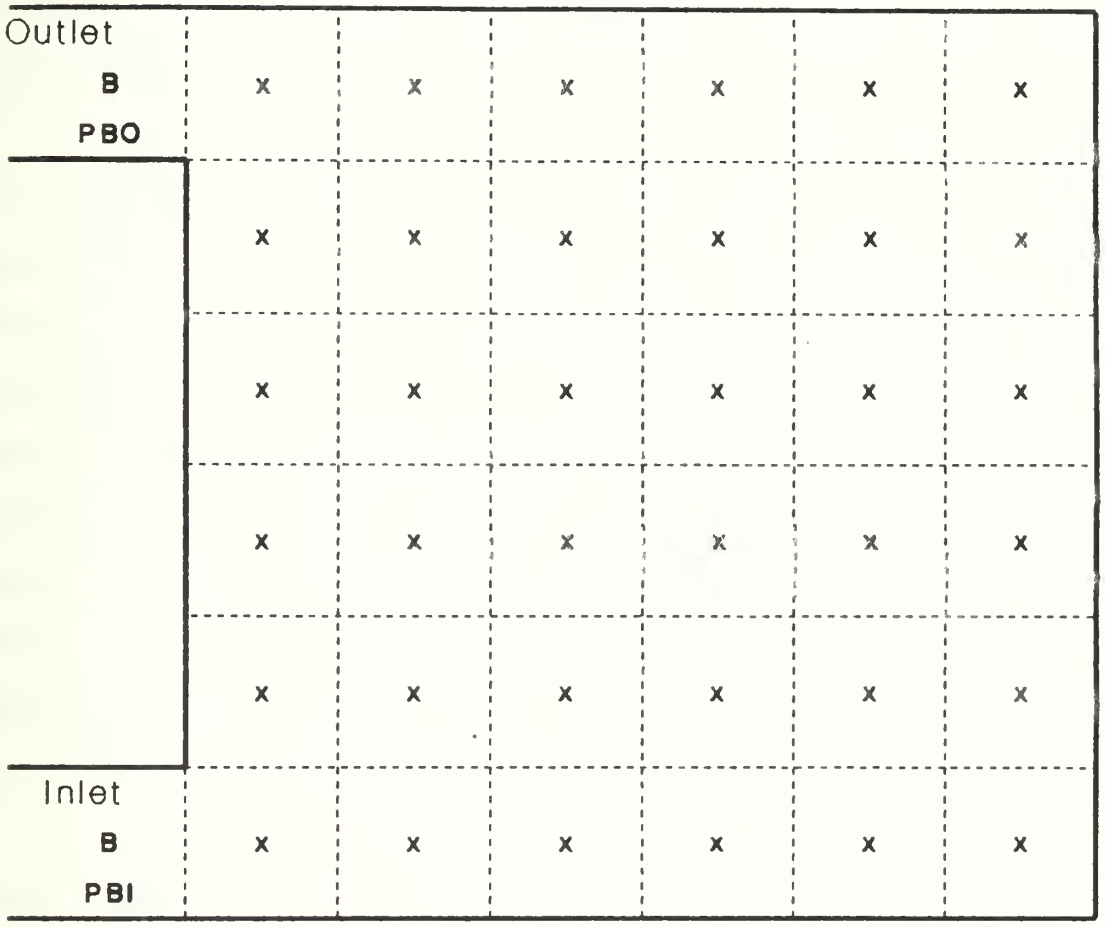

Figure 4.4c

Pressure Control Volume Array

The user determines the inlet pressure and temperature (PBI and TBI) and the outlet pressure (PBO) when the transient is defined. The other boundary conditions are imposed by the fuel element geometry. One constraint common to all equations is that the velocity perpendicular to a solid surface is 0 on the surface. Thus, the radial velocities that would be defined on the outer surface of the inlet plenum (B in Fig. 4.4a) are known to be 0 and the points are not included in the solution matrix. Symmetry also requires this condition on the fuel element center-line.

A constraint similar to the radial case exists for the axial momentum at the west and east ends, Fig 4.4b. However, the arrangement of the fuel element and control volumes impose some complications. The first occurs in the region of the hot frit. The design prevents axial flow in the frit, since it is constructed from a solid piece of metal drilled to allow radial flow. The second occurs along the west end. The inlet and outlet port control volumes are separated by a series of control volumes which contain half solid boundary and half particle bed. The axial velocities are defined on the solid surface and are therefore 0. The problem is how to maintain an array of control volumes with a solution matrix that retains the appropriate coupling and mass balances, yet still gives correct solutions for the boundary values.

Two methods exist to handle this problem. One is to eliminate the control volumes for known boundary values. The resulting nonrectangular array complicates the programing if the user still has the option to define the number of axial and radial nodes. It also risks decoupling the outlet plenum from the rest of the fuel element. The other method, the one used here, includes the boundary volumes necessary to achieve a rectangular control volume array and forces the solution to the correct value by controlling the source terms in the boundary control volumes. Using an artificially high friction term effectively reduces the

included boundary velocities to 0. This has the advantage that anisotropic friction characteristics can be used to adjust the axial velocity with minimal effect on the radial velocity. As a result radial flow is still allowed in the west end volumes and the hot frit.

One other boundary value issue that affects the two pressure equations is the evaluation of the pressure gradient across the boundary control volumes. The model assumes that there is no difference between the pressure at the boundary surface and the pressure in the center of the control volume. If the pressure at the center of the control volume changes, so does the pressure at the solid surface. This gives a zero pressure gradient at the boundary. The pressure gradient across the opposite side of the control volume can still vary in accordance with the variable pressure on either side of the interface. This is consistent with the lumped parameter approach. Figure 4.5 illustrates the principle.

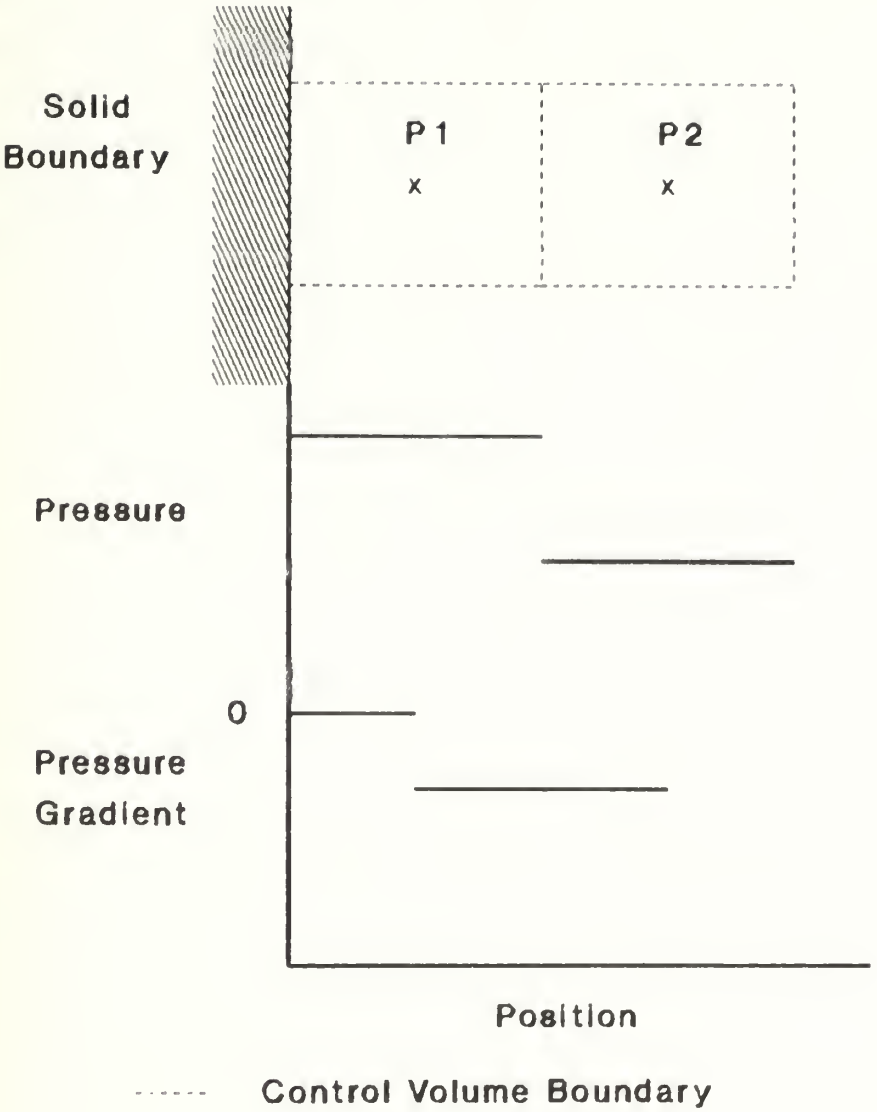

Figure 4.5

The Boundary Pressure Gradient

4.8 SUMMARY

Discretization and linearization of the control volume balance equations results in sets of simultaneous equations which can be solved for the pressure, velocity, temperature and density in each control volume. The PISO method is used to accomplish the numerical solution. It uses a 2 stage predictor corrector technique which advances the variables from one time step to the next by calculating a series if successively refined approximations. Its semi-implicit, noniterative structure provides ease of solution and numerical stability.

CHAPTER 5

THE SOLID PHASE MODEL

5.1 OBJECTIVE

Chapters 3 and 4 present the gas phase part of the model. Equally critical to the success of the fuel element code is the modeling of the fuel particles. They are the source of the heat and contain the majority of the stored energy. This chapter presents the development of the solid phase model equations and the solution method.

5.2 THE MODEL

The solid phase is simpler than the gas phase, since no motion is present. As a result, predicting the solid phase temperatures requires only a heat balance. The energy conservation model must account for three processes, heat deposition, storage and dissipation. The first two can be described on the scale of a single fuel particle. The third represents the fuel particle's interaction with surrounding particles and the hydrogen coolant.

The lumped parameter, control volume approach used in the gas phase model is also used here. Because this method assumes all particles in a control volume are the same, the single particle processes can be analyzed on an individual basis, then rescaled to account for the total solid mass in the control volume. The lumped parameter approach is also convenient for the dissipation mechanisms of conduction and radiation. These processes are dependent on a temperature gradient. Since no gradient exists within a control volume, they can be considered as occurring between control volumes in the overall energy balance. Eq. 5.1 is the general form of the energy conservation equation for a control volume.

$$\left(mC_P\frac{dT_S}{dt}\right)_{cv} = q - hA_V V(T_S - T_G) + \sum_{i=1}^{I} k_i a_i \nabla T_{Si} \qquad 5.1$$

k = effectivity conductivity

q = heat source

5.2.1 The Fuel Particle

The temperature distribution within a fuel particle is a function of the heat deposition rate, heat removal rate and fuel particle dimensions and materials. The most accurate model would divide a fuel particle into at least four nodes (based on composition), then create and solve a set of finite difference equations. This process would have to be repeated for one particle in each control volume, making the model extremely cumbersome. To simplify the particle model, the single node approach is adopted. This reduces the fuel particle to a single composite control volume which retains all of the properties of the original.

Reference M-2 derives the single node model for a cylindrical fuel pin. The same technique is used here except that spherical geometry has been substituted. The single node analysis homogenizes the fuel particle by assuming a steady state temperature distribution and constant material properties in each region of the fuel particle. The resulting particle heat balance takes the form of Eq. 5.2

$$m_a \overline{C}_P \frac{d}{dt}\overline{T} = q'' - \overline{U}(\overline{T} - T_G) \qquad 5.2$$

Where:

m_a = particle mass per unit outside surface area (kg/m^2)

$\overline{C}_P$ = average particle specific heat (J/kg K)

$\overline{T}$ = effective fuel particle temperature (K)

q'' = heat generation per unit outside surface area (W/m^2)

$\overline{U}$ = effective overall heat transfer coefficient (W/m^2 K)

The second term on the right side represents the heat transfer to the gas phase. The model code uses the following equations to evaluate the terms in the single node relation. These are easily derived using the procedure of reference M-2. The number subscripts refer to regions identified in Fig 5.1

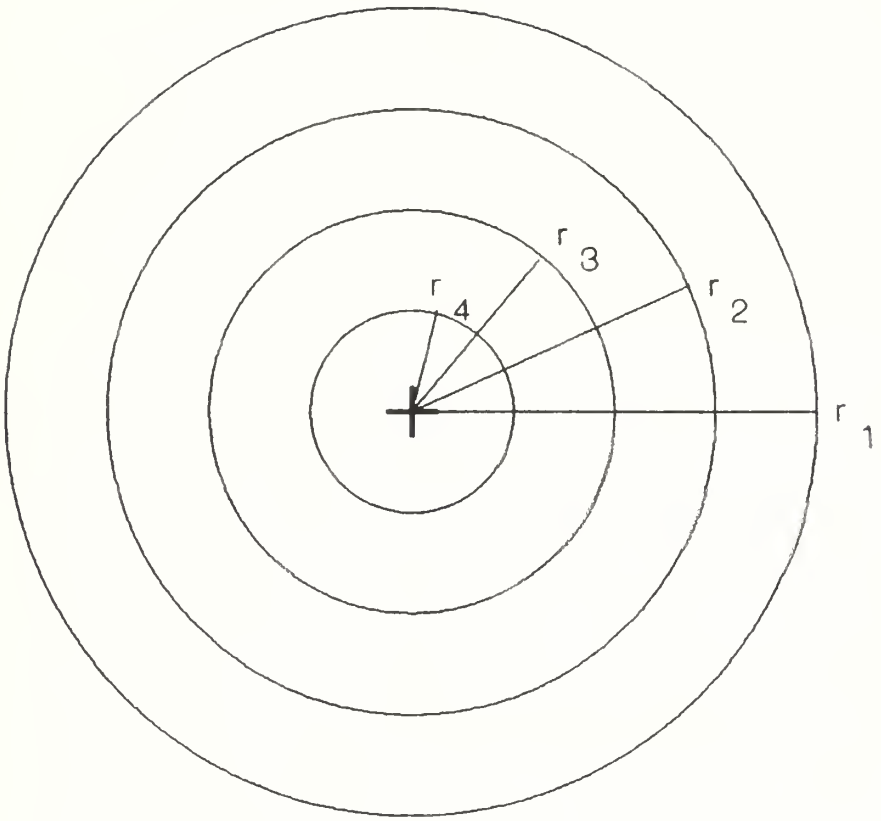

Figure 5.1

The Fuel Particle

$$m_{ax} = \frac{(r_x^3 - r_{x+1}^3)\rho_x}{r_1^2} \qquad m_a = m_{a1} + m_{a2} + m_{a3} + m_{a4} \qquad 5.3a$$

x = region number

$$\bar{C}_P = \sum_{x=1}^{4} \frac{m_{ax}}{m_a} \qquad U_x = \left(\frac{r_x r_{x+1}}{r_x - r_{x+1}} \right) \frac{k_x}{r_1^2} \qquad U_4 = \frac{2k_4}{3r_1} \qquad 5.3b$$

$$U_T = \left(\sum_{x=1}^{4} \frac{1}{U_x} \right)^{-1} \qquad f_1 = \frac{U_T}{U_1} \qquad f_2 = \frac{U_T}{U_2} + f_1 \qquad f_3 = \frac{U_T}{U_3} + f_2 \qquad 5.3c$$

$$\bar{f} = \frac{1}{2m_a \bar{C}_P} [m_{a1} C_{P1} f_1 + m_{a2} C_{P2}(f_1 + f_2) + ma_{a3} C_{P3}(f_2 + f_3) + m_{a4} C_{P4}(f_3 + 1)] \qquad 5.3d$$

$$\bar{U} = \frac{U_T h}{\bar{f} h + U_T} \qquad 5.3e$$

$\bar{T}$ is, in effect, defined to be the temperature that satisfies the requirements of the single node heat balance. It is not a true average or associated with any particular point in the fuel particle. The determination of the heat transfer coefficient, h, is discussed in chapter 3. These relations assume that the average temperature of a region in the fuel particle can be approximated by the arithmetic average of the regions inner and outer interface temperatures.

The material properties of the fuel particle components vary with temperature. This model assumes fixed values for the product of the density and specific heat. Thermal conductivities are allowed to vary with temperature and are evaluated using the correlations of reference D-2. Even with these correlations, the values of the physical parameters are only estimates. For example, estimates of the carbide fuel conductivity vary by as much as 30% between references.

The single node analysis also permits easy estimation of the heat flux time constant, τ. If power is increased linearly, Tau is the time delay between achieving a given power level and having its equivalent steady state flux on the outside surface of the particle. This assumes that the coolant temperature remains constant (M-2). Fig 5.2 diagrams the relationship. As such, it is a measure of the time for the energy to move from the fuel kernel to the surface of the particle and into the gas phase.

$$\tau = \frac{m_a \bar{C}_P}{\bar{U}} \qquad 5.4$$

In this case, τ is a function of coolant flow and temperature and varies from 30 to 105 ms.

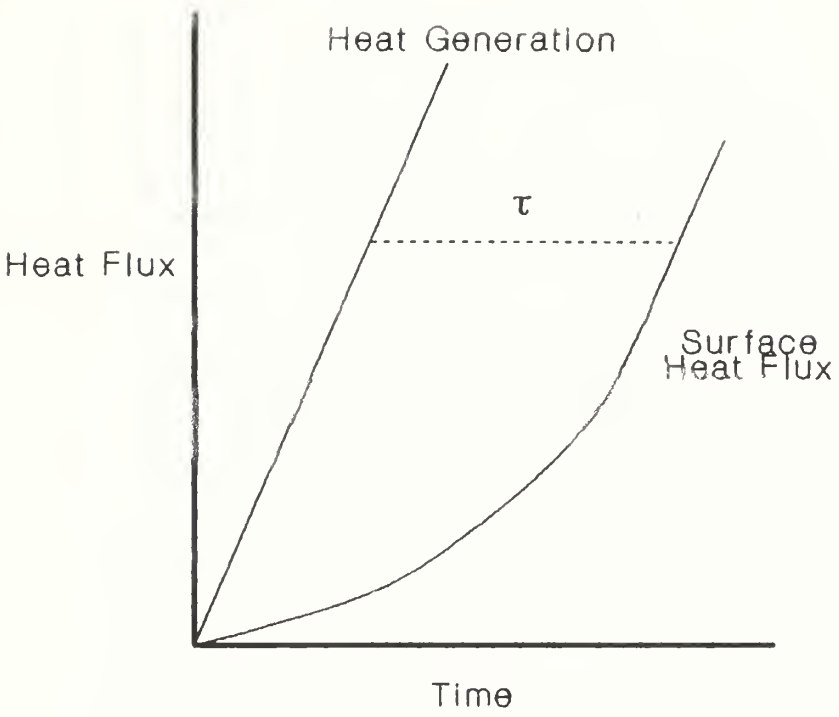

Figure 5.2

The Heat Transfer

Time Constant

(From M-2)

5.2.2 Solid Phase Conduction and Radiation

Heat transfer between adjacent solid particles occurs via several mechanisms. Conduction can take place through particle to particle contact points or through the gas trapped between the particles near the points of contact. If temperatures are sufficiently high, radiative heat transfer also contributes (Y-1). The effective conductivity of the solid phase is the sum of these components.

The dominant mode of conduction is through the fluid near the point of contact. Because the fluid is in the boundary layer, its conduction properties are relatively insensitive to the gas flow rate except at very high Reynolds numbers (Y-1). The packed bed element Reynolds numbers are low because of the high fuel particle surface area to bed volume ratio. Direct conduction via the points of contact is only significant at low pressures. As a result, the conductivity of the solid phase is highly dependent on the fluid and is therefore a function of the gas and solid conductivities. Kunii and Smith proposed the following relation to determine the effective conductivity. It is the one incorporated in the fuel element code.

$$k^{O} = k_{G}\left(\varepsilon + \frac{\beta(1-\varepsilon)}{\phi + \frac{2}{3}\left(\frac{k_{G}}{k_{S}}\right)}\right) \qquad 5.5$$

Where:

k^{O} = effective bed thermal conductivity

k_{G} = gas thermal conductivity

ε = bed void fraction

β = packing parameter, assumed to be one for a randomly packed bed

ϕ = a measure of the effective thickness of the liquid film between particles near the contact point

ϕ is calculated using the following equation:

$$\phi = .5\frac{\left(\frac{\kappa-1}{\kappa}\right)^2 \sin^2\theta}{\ln(\kappa-(\kappa-1)\cos\theta)-\frac{\kappa-1}{\kappa}(1-\cos\theta)}-\frac{2}{3\kappa} \qquad 5.6$$

$$\kappa = \frac{k_S}{k_G}$$

$$\theta = \frac{1}{n}$$

n is the number of points of contact with other particles and represents the number of possible paths for conduction. Because the number of points of contact is not known exactly in a randomly packed bed, ϕ is calculated for the most open packing, ϕ_1 , and a maximum close packing, ϕ_2 . The values are averaged, weighting them by the true bed void fraction as shown in Eq. 5.7.

$$\phi = (\phi_1 - \phi_2)\frac{\varepsilon - .0260}{0.216} + \phi_2 \qquad 5.7$$

The temperature required for significant radiative effects is a function of particle size. For 1 mm particles thermal radiation is important at temperatures greater than 700 K and 1,800 K for .1 mm diameter particles (S-4). With anticipated fuel temperatures of 2,000 K radiative heat transfer is significant and is included in the model.

Schotte includes two paths in his model of the radiation effects. One is the radiation across the void space to an adjacent particle, k_r^o, and the other is the radiative transfer between particles in series with conduction through the particles. The applicable equations for SI units are:

$$k_r^o = 0.229(EM)\varepsilon D_p \frac{\bar{T}^3}{10^6} \qquad 5.8a$$

$$k_r = \frac{1-\varepsilon}{\frac{1}{k_{solid}} + \frac{1}{k_r^o} + \varepsilon k_r^o} \qquad 5.8b$$

k_r is the effective radiation conductivity of the bed and EM is the emissivity of the fuel particles. The fuel element code uses the properties of the outer layer, zirconium carbide, for the conduction parameters because it is the material in contact with the other particles and its surface characteristics determine the emissivity. The code uses an emissivity of .78. The radiation component of conduction is a function of the surface temperature as well. The model program approximates this with the effective solid temperature, $\bar{T}$. The actual surface temperature is less than $\bar{T}$ but the size and spherical shape of the particles minimize the ΔT within the particle, mitigating the error of the model.

Combining the conduction and radiation conductivities yields the overall effective conductivity of the solid phase, k_{total}.

$$k_{total} = k^{O} + k_{r} \tag{5.9}$$

5.2.3 The Solid Phase Solution Method

The solid phase energy balance is solved by applying a discretized form of the energy balance to an array of control volumes, just as is done with the gas phase model. The control volumes are coincident with their gas phase counterparts.

Assimilating the discussion of the previous sections into the energy balance requires rescaling the single node analysis of the heat deposition, storage and transfer to the gas phase from an isolated particle to a control volume basis. The terms of Eq. 5.2 were derived on a per unit particle surface area. The rescaling is accomplished by multiplying both sides of the product of the control volume size, V_{cv}, and particle surface area per unit volume, A_V. The units for each term in Eq. 5.10 then become Watts.

$$m_a \bar{C}_P V_{cv} A_V \frac{d}{dt}\bar{T} = q'' V_{cv} A_V - \bar{U} V_{cv} A_V (\bar{T} - T_G) \tag{5.10}$$

The area per volume for spheres is a function of the particle diameter and the void fraction.

$$A_V = \frac{6(1-\varepsilon)}{D_P} \tag{5.11}$$

The last step in assembling the continuous form of the control volume energy conservation equation is to add the conduction terms which account for the heat transferred through the control volume boundaries. This yields:

$$m_a \overline{C}_P V_{cv} A_V \frac{d}{dt} \overline{T} = q'' V_{cv} A_V - \overline{U} V_{cv} A_V (\overline{T} - T_G) - \sum_{i=1}^{l} k_{total} a_i \nabla \overline{T}_i \qquad 5.12$$

Note that the area used in the conduction term is the area of the control volume face, not the surface area of the particles.

Equation 5.12 must be discretized to make it compatible with numerical solution techniques. Since the control volumes are the same as those of the gas phase, the solid temperatures are defined at the same points as the gas state variables. Solid temperatures are *not* defined in the plenum areas. No *solid exists in these* control volumes and conduction to the moderator block is not considered.

The discretization procedure is the same used in chapter 4. The last term on the right hand side is the only new term which has not been discretized earlier. The temperature gradient across an interface is approximated by the difference in the temperatures on either side of the interface divided by the distance between the temperature points. The problem now is how to evaluate the conductivity at the interface.

Conductivity is a function of temperature, void fraction and material. Therefore, significant differences may exist on opposing sides of the interface. The first impulse is to use the arithmetic average of the two values. However, this has been shown to give erroneous results (P-2). The harmonic mean is a better choice and has several physical arguments in its

favor. Patankar equates the heat flow on either side of the interface to derive the relation for the harmonic mean (P-2). Eq. 5.13 shows the relation for the east face of a control volume. f is the ratio of the distance between the east interface and T_E to the distance between the centers of the two control volumes. Similar relations can be derived for the other faces.

$$(k_{total})_e = \left(\frac{f}{k_E} + \frac{1-f}{k_O} \right)^{-1} \qquad 5.13$$

The source term representing the heat transfer from the solid to the coolant is treated implicitly as discussed in chapter 4. Therefore the n+1 values of the temperatures are used. In accordance with the THERMIT implicit method, T_G^n is used as an estimate of the T_G^{n+1}. A correction is made later in the solution process.

Substituting the discrete forms of the terms into Eq. 5.12 results in the following form of the heat balance:

$$m_a \bar{C}_P V_{cv} A_V \left(\frac{\bar{T}^{n+1} - \bar{T}^n}{\delta t} \right) = \left(k_{total} a \frac{(\bar{T}_E^{n+1} - \bar{T}_O^{n+1})}{\delta z} \right)_e + \left(k_{total} a \frac{(\bar{T}_O^{n+1} - \bar{T}_W^{n+1})}{\delta z} \right)_w$$
$$+ \left(k_{total} a \frac{(\bar{T}_N^{n+1} - \bar{T}_O^{n+1})}{\delta r} \right)_n + \left(k_{total} a \frac{(\bar{T}_O^{n+1} - \bar{T}_S^{n+1})}{\delta r} \right)_s$$
$$+ q'' V_{cv} A_V - \bar{U} V_{cv} A_V \left(\bar{T}^{n+1} - T_G^n \right) \qquad 5.14$$

This can be rearranged into a form similar to the gas phase balances with these substitutions:

$$\left(\frac{k_{total}a}{\delta z}\right)_e = A_e \qquad \left(\frac{k_{total}a}{\delta z}\right)_w = A_w \qquad \left(\frac{k_{total}a}{\delta r}\right)_n = A_n \qquad \left(\frac{k_{total}a}{\delta r}\right)_s = A_s$$

$$A_O = -(A_e + A_w + A_n + A_s) \qquad B = \frac{m_a \bar{C}_P V_{cv} A_V}{\delta t}$$

$$H'(\bar{T}^{n+1}) = A_e \bar{T}_E^{n+1} + A_w \bar{T}_W^{n+1} + A_n \bar{T}_N^{n+1} + A_s \bar{T}_S^{n+1} \qquad 5.15$$

Equation 5.16 is the final form of the solid phase heat balance used in the fuel element model code.

$$-(B - A_O - \bar{U} V_{cv} A_V)\bar{T}_O^* + H'(\bar{T}^*) = -q''' V_{cv} A_V - \bar{U} V_{cv} A_V T_G^n - B\bar{T}_O^n \qquad 5.16$$

Setting up this equation and evaluating the coefficients for each control volume creates a system of simultaneous linear equations. The model code can now solve these for $\bar{T}^*$ with the same matrix solution techniques used for the gas phase. The values obtained for the solid temperature are only a first estimate.

The THERMIT method for solving the coupling of the gas and solid phases also requires the evaluation of the temperature derivative, $\partial \bar{T}^{n+1} / \partial T_G^{n+1}$. Continuing with the assumptions that T_G^n and $\bar{T}^*$ equal T_G^{n+1} and $\bar{T}^{n+1}$ respectively, the code differentiates Eq. 5.16 to get:

$$\frac{\partial \bar{T}^{n+1}}{\partial T_G^{n+1}} = \frac{\bar{U} V_{cv} A_V}{(B - A_O - \bar{U} V_{cv} A_V)} \qquad 5.17$$

Before completing the solution for the solid phase temperature, the gas phase energy conservation equation must be solved for the true value of T_G^{n+1}. When this is done, all of the terms in Eq. 5.18 are known and $\overline{T}^*$ can be corrected to get $\overline{T}^{n+1}$.

$$\overline{T}^{n+1} = \overline{T}^* + \frac{\partial \overline{T}^{n+1}}{\partial T_G^{n+1}} (T_G^{n+1} - T_G^n) \qquad 5.18$$

This process is equivalent to saying

$$\text{Interphase Heat Transfer} = \overline{U} V_{cv} A_v \left(\overline{T}^{n+1} - T_G^{n+1} \right) \qquad 5.19$$

in both the gas and solid phase equations.

5.3 SUMMARY

An energy balance is applied to the fuel particles to model heat generation, storage, and transfer. Transfer includes convection to the coolant conduction to surrounding particles and radiation to adjacent material. To simplify the model a steady state temperature distribution within the fuel particle is assumed. This allows the state of the solid phase to represented by a single temperature in each control volume.

The coolant and fuel particle models are coupled by the interphase heat transfer term. In order to preserve numerical stability, the model treats both gas and solid temperatures implicitly using the technique developed for the THERMIT code.

The model of the packed bed fuel element is now complete.

CHAPTER 6

RESULTS AND CONCLUSIONS

6.1 OBJECTIVE

Chapters 2 through 5 present the details of a mathematical model of a packed fuel element. It is based on the momentum, energy and mass conservation equations. These relations are encoded in a micro computer Fortran program described in appendix B. As a partial test of the model's validity, the code is applied to a series of steady state and transient problems. This chapter presents the results of these test cases.

6.2 STEADY STATE

6.2.1 Problem Statement and Methodology

Six steady state problems test the model's ability to reach a reasonable solution under various conditions. Changing the peak power level provides the simplest means of simulating the wide range of hydraulic and thermal conditions that the fuel element would experience during pulsed high power operation. Cases with peak power densities of 2.1 and 1.0 GW/m^3 are examined as well as a zero power problem. The other boundary conditions are held constant to permit more meaningful comparisons.

In addition to power density the operator must also specify the following:

1. The physical dimensions of the fuel element
2. The control volume dimensions and arrangement
3. The initial values of all variables

4. The coolant inlet temperature and pressure
5. The initial and final outlet pressure
6. The initial and final power density

All of the test problems are conducted using a rectangular array of control volumes arranged with 5 equal sized nodes axially and 10 nodes radially. The radial nodes vary in size to match the fuel element components. One node was assigned to each plenum and frit and 6 nodes were assigned to the fuel particle bed. The control volumes and variables are identified by two indexes, I and J for the radial and axial positions respectively. Figure 6.1 shows the indexing scheme. The origin of the grid is the pressure control volume at the inlet port (1,1). Note that the velocity control volumes cross component boundaries, because of the nature of the staggered grid. For example, radial velocity (2,1) is defined on the interface between the inlet plenum and the cold frit.

The sign convention is positive for axial velocities moving from low index to high. Radial velocities are positive for flow from the outside of the fuel element toward the center. Thus, increasing I and J represent the positive directions. Under normal flow circumstances then, axial velocity is positive in the inlet plenum and negative in the outlet plenum. Radial velocity is positive in the fuel bed under these circumstances.

For steady state cases the initial conditions are arbitrary. However, they should represent an equilibrium condition to ensure initial numerical stability. The test problems are started with steady flow, zero power and an element pressure drop of 50 kPa. All temperatures are 300 K and inlet pressure is 2 MPa. The final outlet pressure is 1.915 MPa. for all cases.

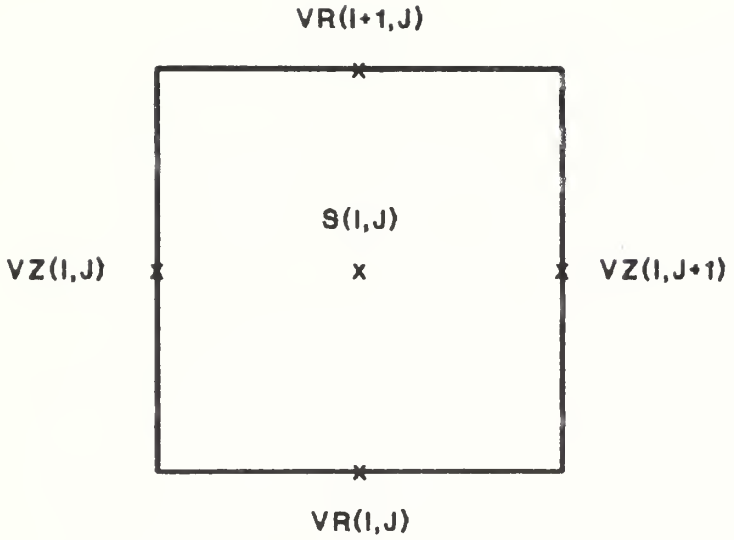

S State Variables (pressure, temperature)

VR Radial Velocity

VZ Axial Velocity

Figure 6.1

Staggered Grid

Indexing Scheme

The code takes the peak power density and applies a chopped cosine weighting to simulate the axial power profile. In this case, the factors were .89, .97, 1.0, .97, and .89 for axial nodes 1 through 5 respectively.

The cold frit thickness varies with position to match the axial flow profile and the power distribution. The thicknesses are based on the PIPE element design drawings. Values of 2.26, 1.93, 1.80, 1.78 and 1.91 mm are used for nodes 1 through 5 respectively.

The problem is completely defined without having to specify the mass flow rate. It varies as the conditions in the fuel element change.

The steady state solution is actually achieved by conducting a transient for a long enough period of time that the values of the variables become essentially non-varying. The transient is initiated by making a step change in the outlet pressure and power density to the final values. This essentially simulates instantaneously raising power and opening the fuel element outlet valve.

Steady state is identified by monitoring the overall system mass and heat balances. All problems are run for 3.75 sec. which insures that the energy transferred to the coolant is within 5% of the energy deposited by the simulated fission. The mass balances agree within 1% or less.

The test cases also provide a test of the numerical stability of the solution technique. As expected, the semi-implicit differencing used in the discretization limits the size of the

time step that can be used. Instabilities can be initiated by raising the power or increasing the fuel element pressure drop. A time step of .25 ms works well for the power densities and pressures used in the test problems.

6.2.2 Hydraulic Results

The principle hydraulic issues address the subjects of model complexity, 1 or 2 dimensions, and flow distribution prediction. Figure 6.2 shows the calculated steady state values of the variables for the 2.1 GW/m^3 case (Refer to Fig. 6.1 to meld the arrays). The zeros on the edges of the velocity arrays represent velocities defined on the fuel element boundaries. The hot frit shows zero axial velocities due to the modification of the axial friction term to simulate the frit's drilled single piece construction. The small diameter of the particles in the cold frit also result in high friction and negligible axial flow.

Steady State Fuel Element
Power Density = 2.1 GW/m^3, Inlet Temp. = 300 K,
Inlet Press. = 2.0 MPa, Outlet Press. = 1.915 MPa

Superficial Radial Velocities (m/sec)

11	.0000	.0000	.0000	.0000	.0000
10	6.6141	6.0407	6.0424	5.7759	5.3303
9	6.2537	5.7132	5.7147	5.4678	5.0468
8	5.1095	4.7442	4.7188	4.5146	4.1770
7	4.0823	3.7857	3.8043	3.6624	3.3877
6	3.1475	2.9651	2.9711	2.8551	2.6506
5	2.3003	2.1792	2.1830	2.0985	1.9494
4	1.5059	1.4474	1.4315	1.3704	1.2725
3	.5821	.5724	.5428	.5111	.4685
2	.5109	.5004	.4703	.4392	.3995
1	.0000	.0000	.0000	.0000	.0000
I/J	1	2	3	4	5

Superficial Axial Velocity (m/sec)

10	-223.3224	-173.2407	-127.9471	-82.7846	-39.6856
9	0000	.0000	.0000	.0000	.0000
8	.0000	-1.4026	-.9275	-.5075	-.1527
7	.0000	-1.5122	-.9882	-.5323	-.1485
6	.0000	-1.6399	-1.0684	-.5699	-.1488
5	.0000	-1.7937	-1.1713	-.6236	-.1550
4	.0000	-1.9537	-1.3024	-.7041	-.1697
3	.0000	-2.0629	-1.4397	-.8257	-.2017
2	.0000	-.0017	-.0010	-.0005	-.0001
1	6.4169	5.0037	3.6201	2.3196	1.1048
I/J	1	2	3	4	5

Pressure (MPa)

10	1.92157	1.93258	1.93969	1.94380	1.94538
9	1.92359	1.93461	1.94179	1.94584	1.94724
8	1.92610	1.93716	1.94441	1.94835	1.94952
7	1.92711	1.93822	1.94544	1.94931	1.95037
6	1.92788	1.93904	1.94623	1.95004	1.95102
5	1.92845	1.93966	1.94681	1.95056	1.95147
4	1.92884	1.94010	1.94721	1.95090	1.95177
3	1.92913	1.94045	1.94749	1.95112	1.95194
2	1.96743	1.97277	1.97619	1.97798	1.97849
1	2.00001	2.00002	2.00003	2.00003	2.00003
I/J	1	2	3	4	5

Figure 6.2 Steady State Results - 2.1 GW/m^3

Density (kg/m^3)

I/J	1	2	3	4	5
10	.2567	.2464	.2426	.2419	.2443
9	.2976	.2589	.2452	.2404	.2445
8	.2988	.2599	.2462	.2411	.2451
7	.3203	.2773	.2640	.2585	.2618
6	.3551	.3125	.2942	.2861	.2893
5	.4108	.3634	.3426	.3335	.3351
4	.5030	.4555	.4289	.4170	.4170
3	.6855	.6393	.6085	.5934	.5897
2	1.5111	1.5049	1.4913	1.4792	1.4678
1	1.6118	1.6118	1.6118	1.6118	1.6118

Coolant Temperature (K)

I/J	1	2	3	4	5
10	1816.8	1899.2	1931.4	1940.3	1925.0
9	1569.6	1813.3	1915.2	1954.7	1925.1
8	1565.5	1808.9	1911.0	1951.2	1922.5
7	1457.7	1688.1	1787.9	1829.8	1807.6
6	1311.3	1507.0	1603.9	1647.1	1631.8
5	1133.1	1287.8	1371.9	1411.7	1404.6
4	923.8	1027.2	1095.6	1129.4	1129.9
3	679.2	728.5	771.5	792.6	797.8
2	314.8	316.8	320.0	322.7	325.0
1	300.0	300.0	300.0	300.0	300.0

Fuel Particle Temperature (K)

I/J	1	2	3	4	5
10	.0	.0	.0	.0	.0
9	1577.0	1820.3	1921.3	1959.6	1928.7
8	1590.9	1834.2	1935.6	1974.4	1943.9
7	1491.4	1723.0	1823.0	1863.7	1839.1
6	1350.5	1549.2	1646.9	1689.1	1671.2
5	1178.5	1336.5	1423.5	1463.3	1453.3
4	977.3	1083.2	1157.9	1194.3	1192.0
3	742.5	789.2	844.2	876.1	882.0
2	314.8	316.8	320.0	322.7	325.0
1	.0	.0	.0	.0	.0

Figure 6.2 Steady State Results - 2.1 GW/m^3

In the fuel bed axial velocities are significant and vary from 17 to 360% of the radial velocity, with the maximum just inside the cold frit. The associated flow is toward the ported end of the fuel element (J=1). This implies that the high pressure drop of the cold frit forces the coolant to distribute itself over the entire surface of the cold frit. Once through the frit, the coolant redistributes as it follows the many parallel paths through the fuel bed and outlet plenum to the exit port. The axial flow increases from the closed end to the ported end of the element.

Figures 6.3a,b and c show the mass flow profiles for the three cases, comparing the axial distribution at the cold frit and the hot frit. At all power levels, the flow shifts to the ported end of the element after passing through the cold frit. This is consistent with the axial velocity field. The redistribution increases with power.

Flow Distribution
2.1 GW/m^3

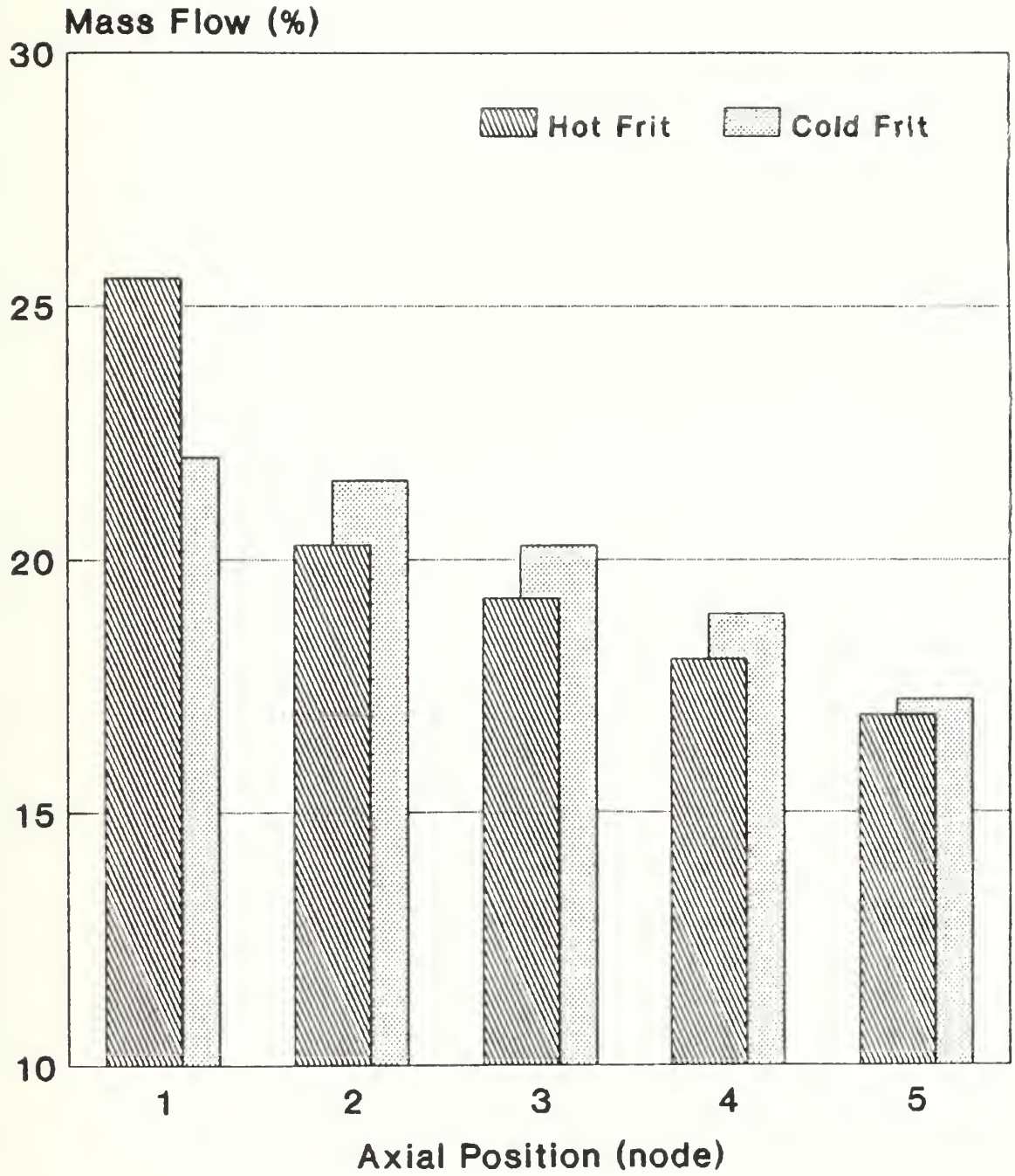

Figure 6.3a

Flow Distribution
1.0 GW/m^3

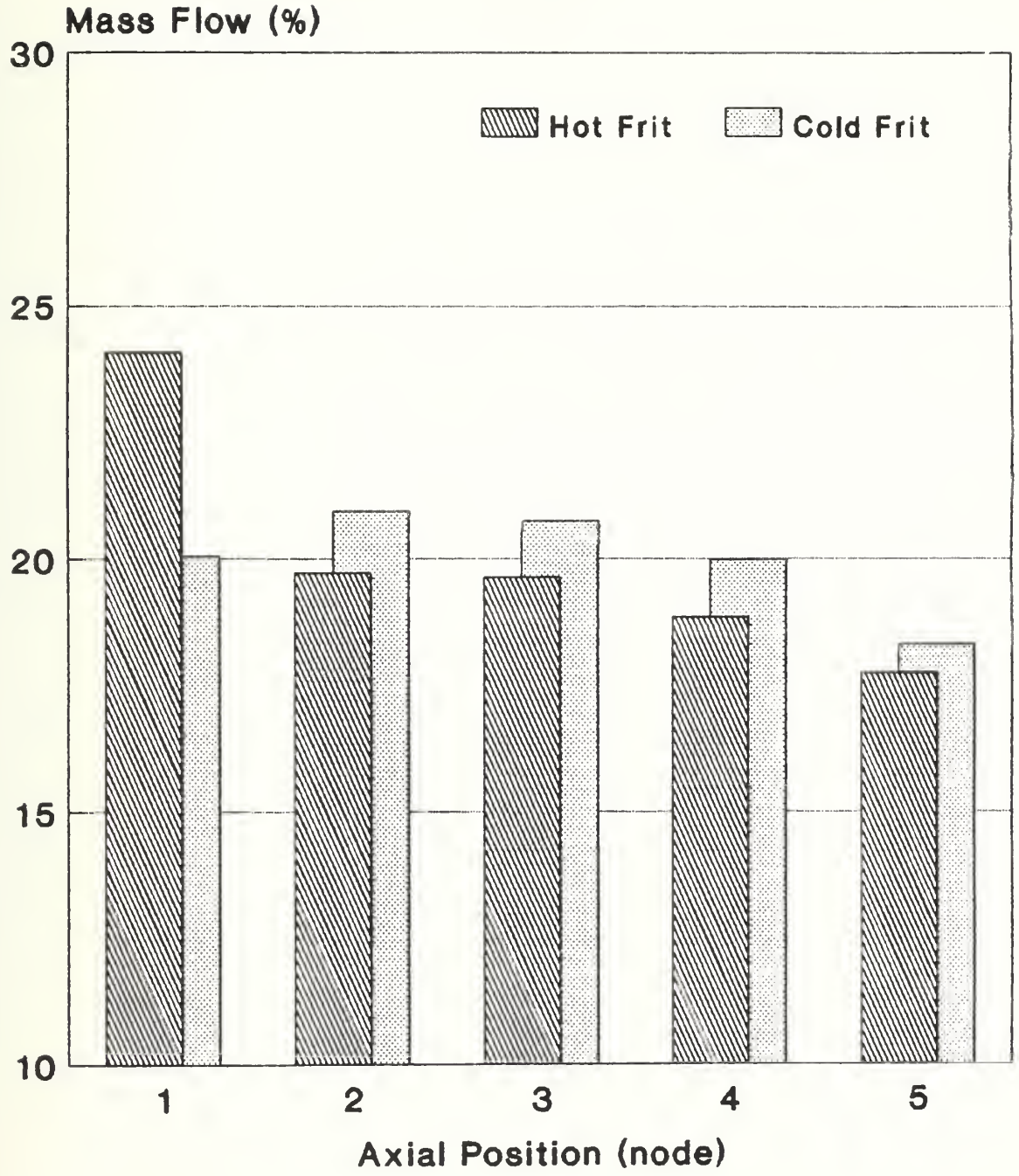

Figure 6.3b

Flow Distribution
No Heat Source

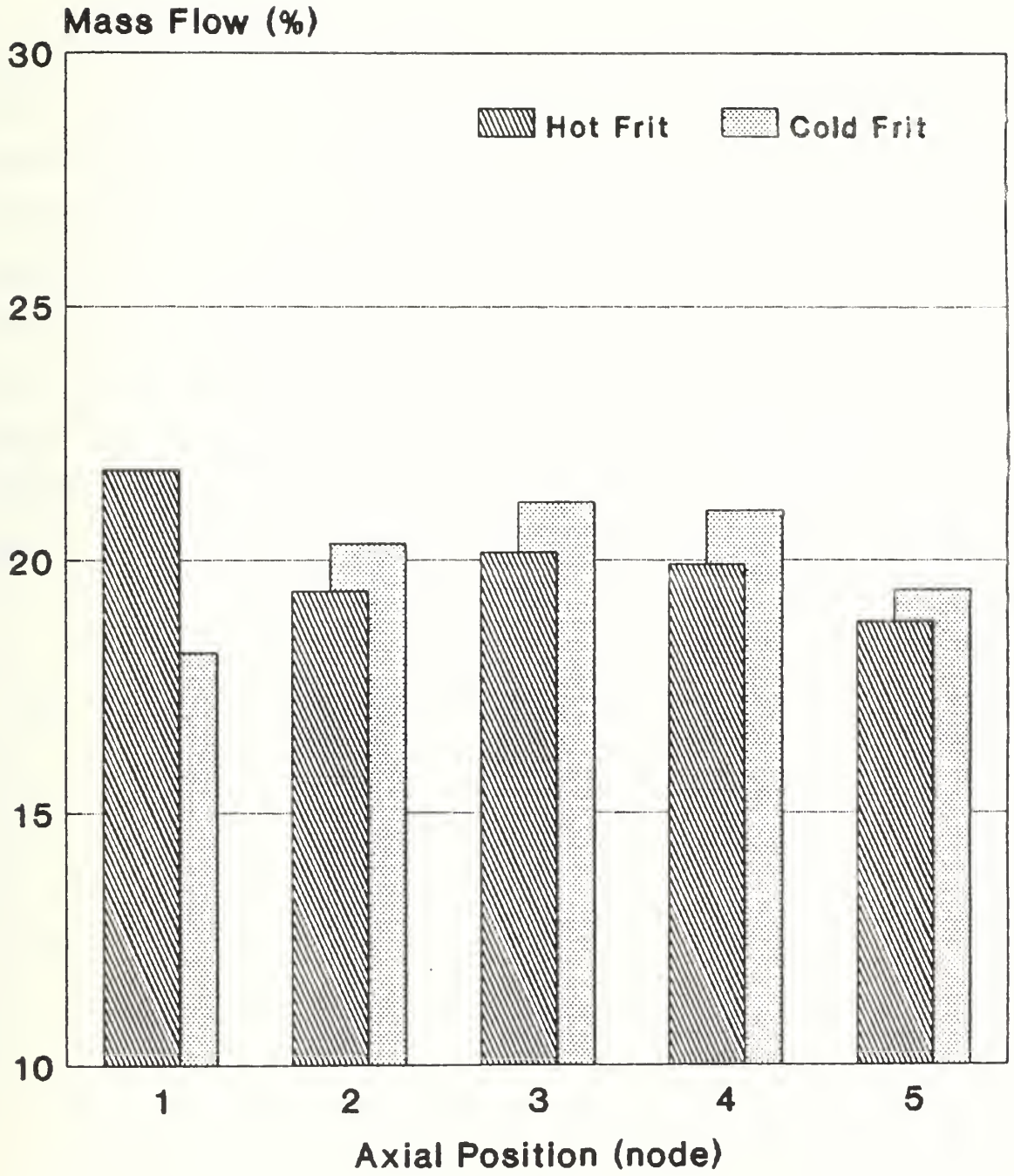

Figure 6.3c

The flow distribution through the cold frit is also a function of power. Figure 6.4a illustrates the shift from a centrally peaked flow profile at zero power to one peaked in the first axial node at 2.1 GW/m^3. The hot frit exhibits similar behavior only it is more pronounced, Fig. 6.4b.

The sources of the pressure losses in the element also change with power density. Figures 6.5 and 6.6 plot the changes in the pressure drop along the length of the outlet plenum and across the cold frit as a function of power. At zero power, 74 to 82 kPa of the 85 kPa total element pressure drop occurs across the cold frit. However, at 2.1 GW/m^3 the cold frit represents only 48 to 71 kPa of the pressure drop. The biggest change is in the closed end of the element (J=5). The cold frit changes result from increases in the pressure losses in the fuel bed, hot frit and outlet plenum as the hydrogen heats up. This is expected, since the lower density of the warmed coolant forces higher velocities to maintain the mass flow rate. Therefore, frictional losses, modeled as a function of velocity and velocity squared, increase rapidly.

Comparative Flow Distribution
Cold Frit

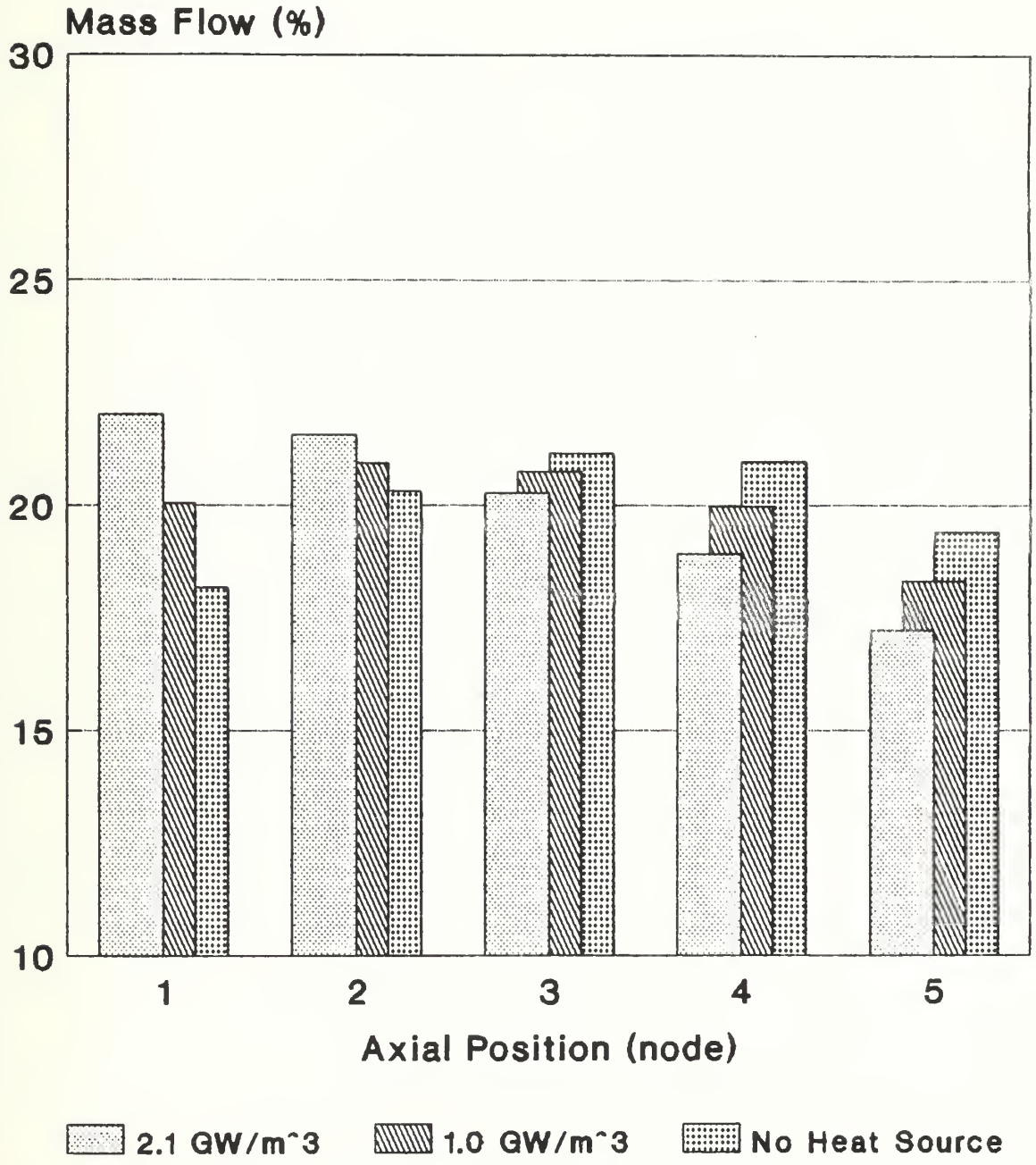

Figure 6.4a

Comparative Flow Distribution
Hot Frit

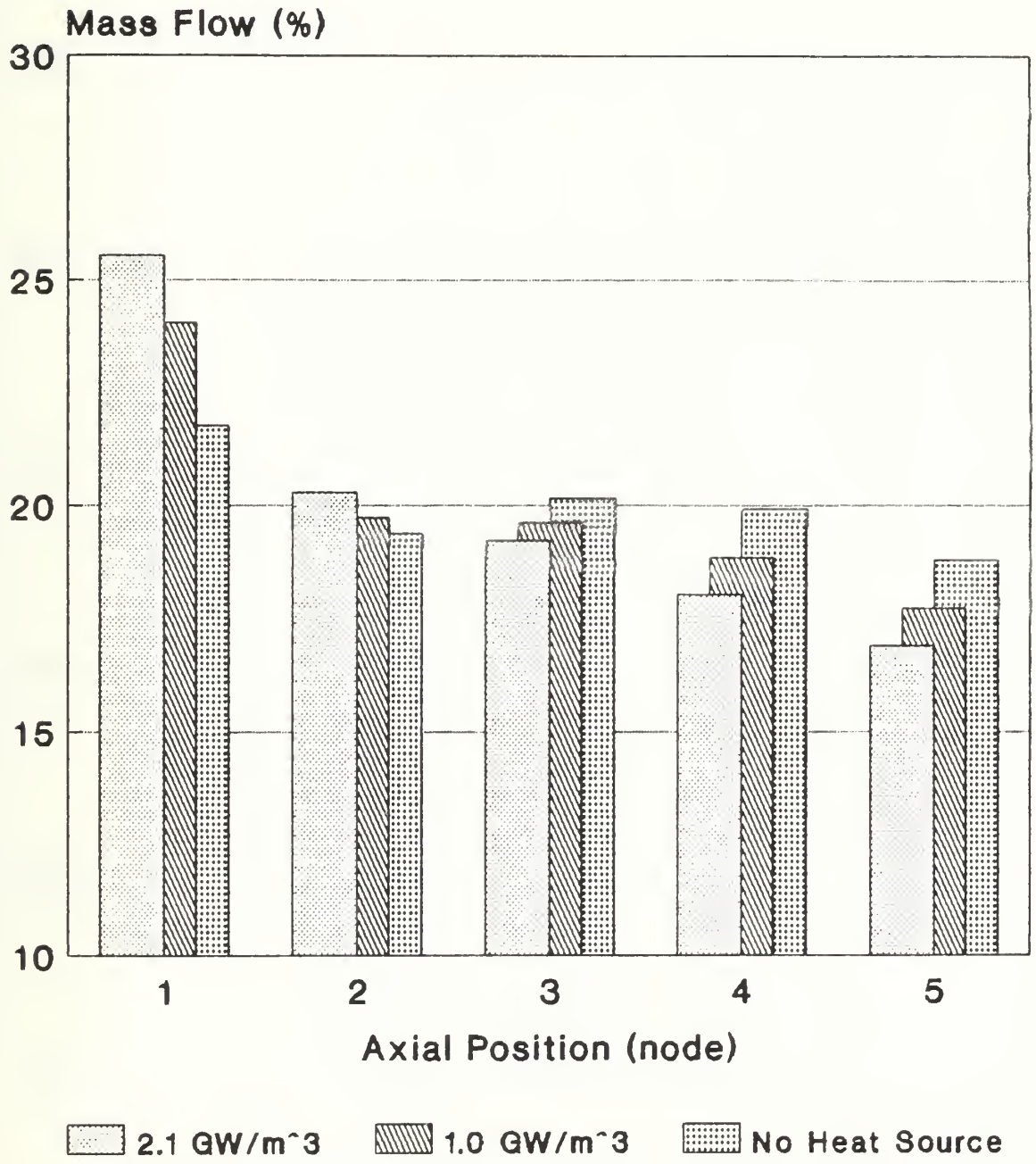

Figure 6.4b

Outlet Plenum Pressure Drop

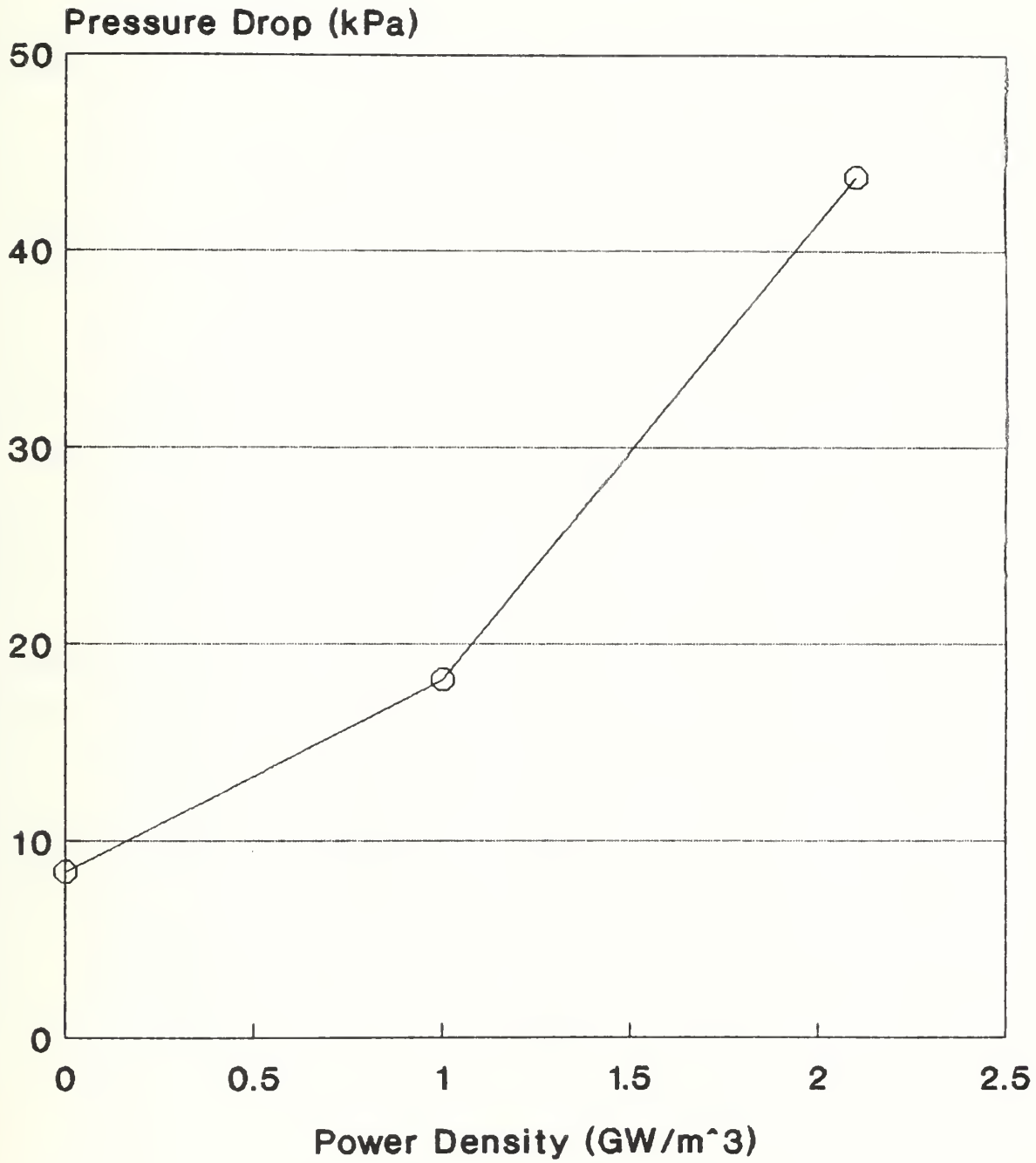

Figure 6.5

Cold Frit
Pressure Drop

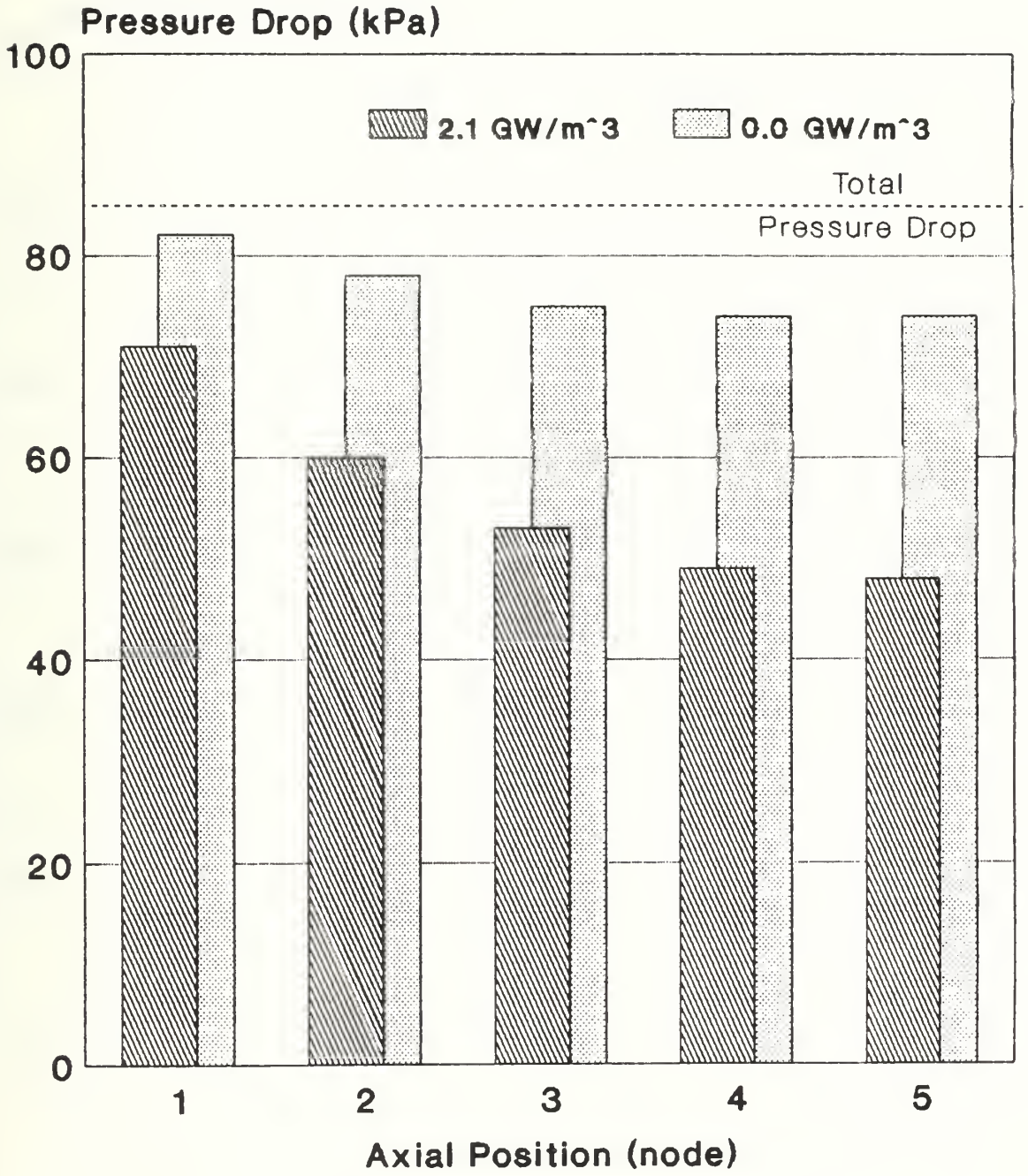

Figure 6.6

Mass Flow Rate and Power Density

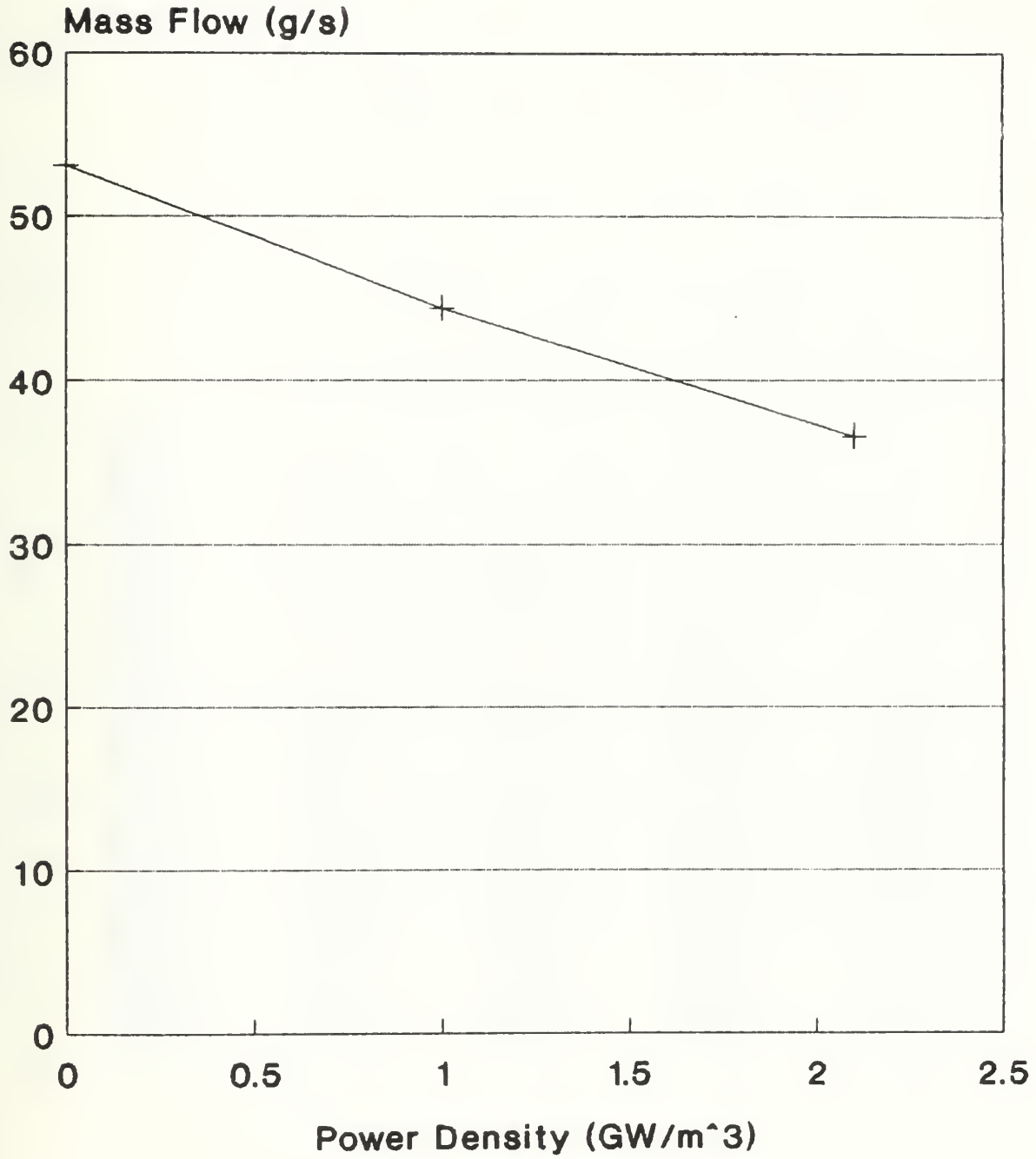

Figure 6.7

Flow Distribution
No Axial Flow

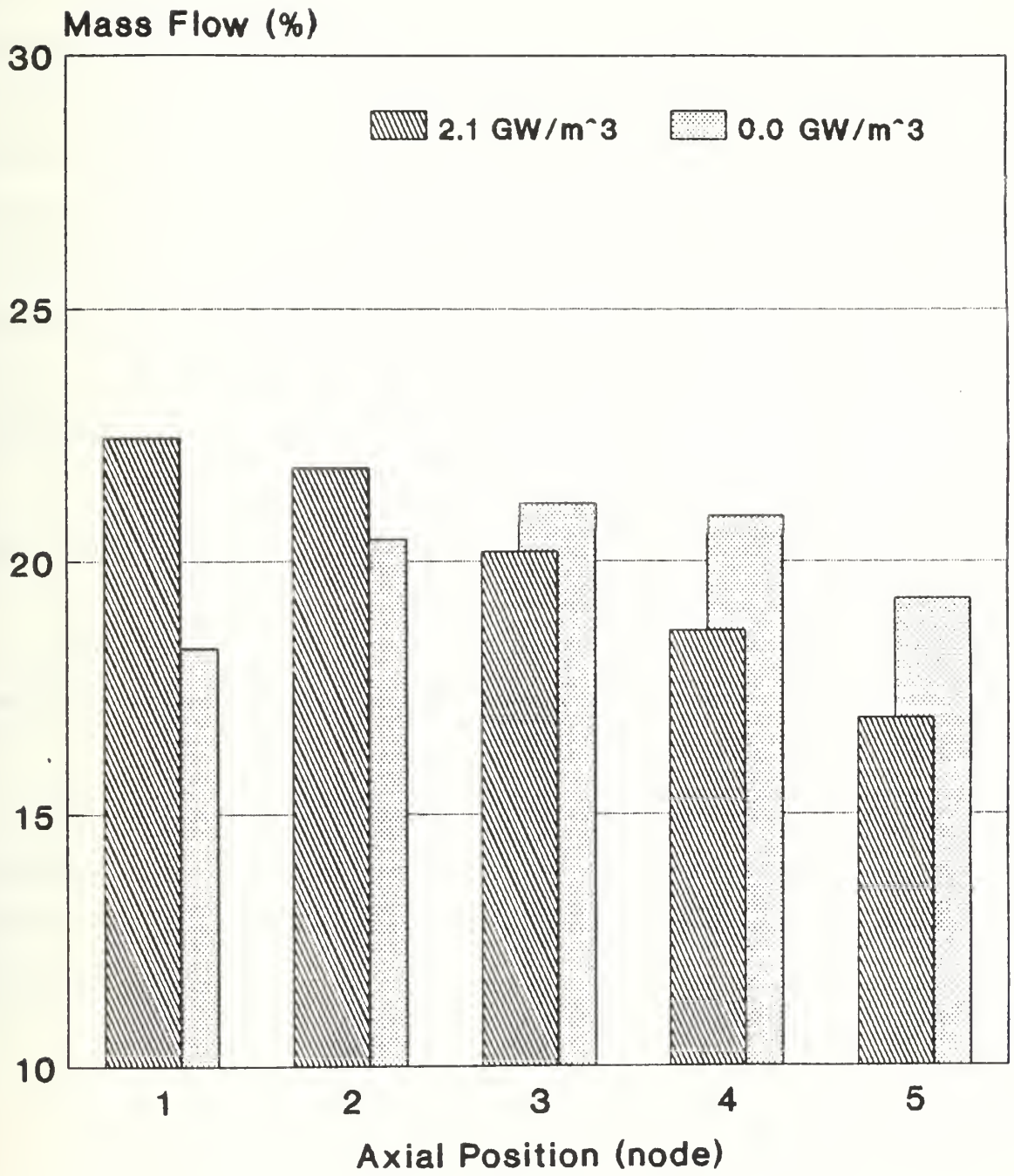

Figure 6.8

The explanation of the hydraulic behavior of the model lends itself to an electrical analogy. The fuel element can be viewed as an inlet and outlet port connected by an infinite number of parallel flow paths with different resistances, similar to parallel resistors in an electrical circuit. Just as the current distribution adjusts to give the same voltage drop across all of the resistors so does the mass flow distribution adjust to give the same pressure drop across all possible flow paths. The complication in the fuel element is that resistances are a function of power and therefore variable. As the hydrogen heats up, the relative resistance of the flow paths changes forcing a change in the flow profile. These changes favor increasing the percentage of flow in the more direct paths despite the greater thickness of the cold frit. The higher axial velocities in the fuel particle bed at high power represent increased flow in the paths that bypass the outlet plenum. However, it should be noted that the vast majority of the flow is still collected in the outlet plenum and that the total shift is less than 10% in the cases studied.

6.2.3 Thermal Results

Thermal issues examined in the test problems include the temperature profile and what heat transfer processes should be included in the model.

The temperature distribution along the hot frit shows significant variation, contrary to the design objective of approximately equal temperature gasses entering the outlet plenum, Fig.6.9. This is the result of the flow redistribution causing a mismatch in the mass flow and axial power profiles.

Coolant Temperature Distribution Along the Hot Frit

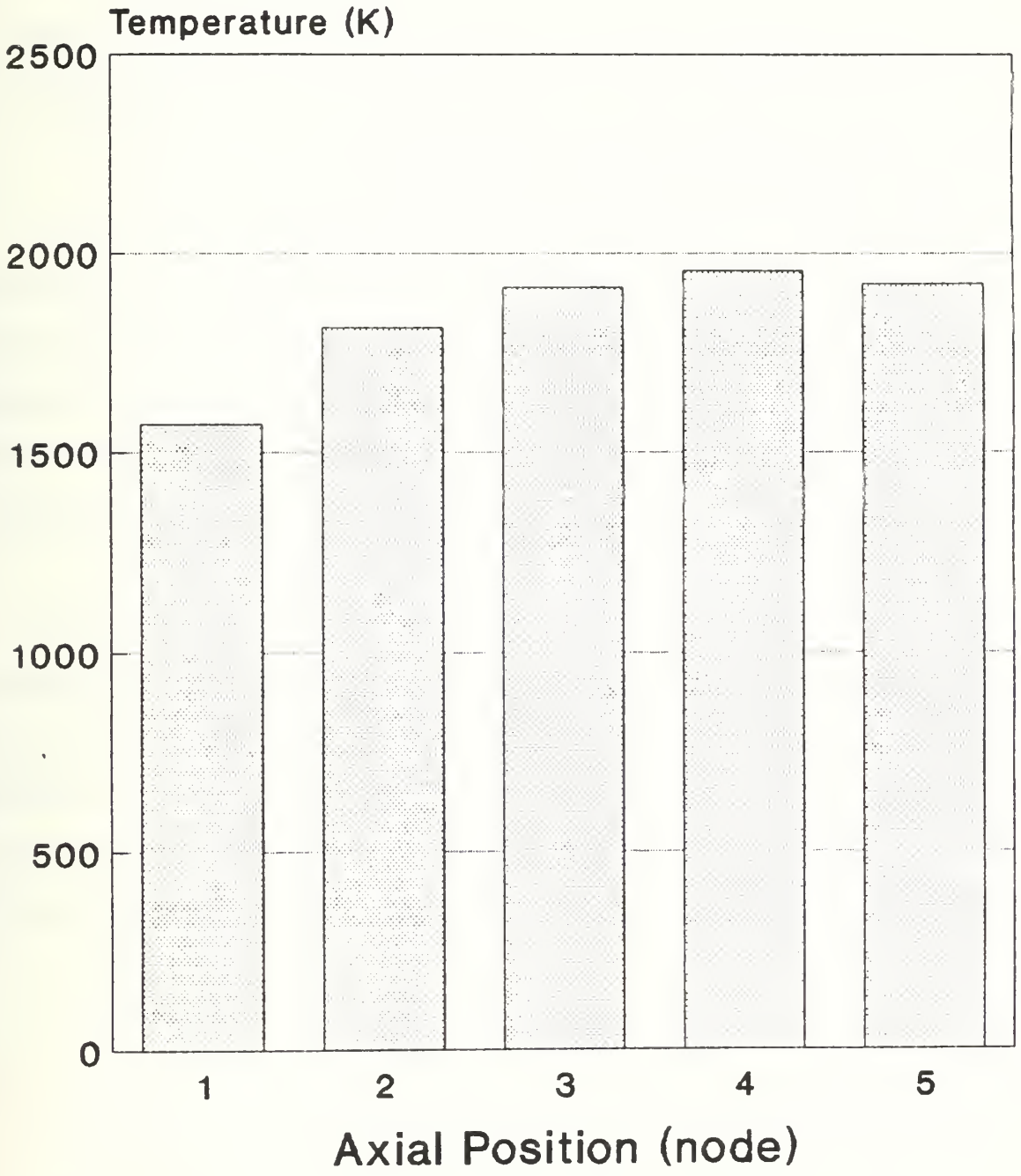

2.1 GW/m^3

Figure 6.9

Figure 6.10 shows the radial coolant and solid phase temperature distributions in the J=3 node for a peak power density of 2.1 GW/m^3. Looking at the J=1, 3 and 5 fuel control volumes next to the hot frit, the model predicts the following heat balance results:

Control Volume	(8,1)	(8,3)	(8,5)
Heat Generation (W)	19849	22273	19849
Power transferred to the gas phase (W)	15685	14870	12203

The heat transferred to the gas phase is calculated using the overall heat transfer coefficient and the difference in the fuel and coolant temperatures. If the heat balance is maintained and steady state exists, then the difference between the heat generation and the power generation must represent the energy conducted or radiated to the surrounding fuel particles and the hot frit. The elevated temperatures in the cold frit are also the result of conduction from the fuel particles.

The gas film temperature difference is a maximum in the first fuel particle control volume inside the cold frit (I=3). The zero temperature difference in the cold frit is indicative of its excellent heat transfer characteristics, especially the high surface area to volume ratio (700,000 compared to 7,200 m^2/m^3 in the fuel). The smallest film temperature drop occurs next to the hot frit and is the result of conduction which reduces the power transfer required to the coolant.

Radial Temperature Distribution

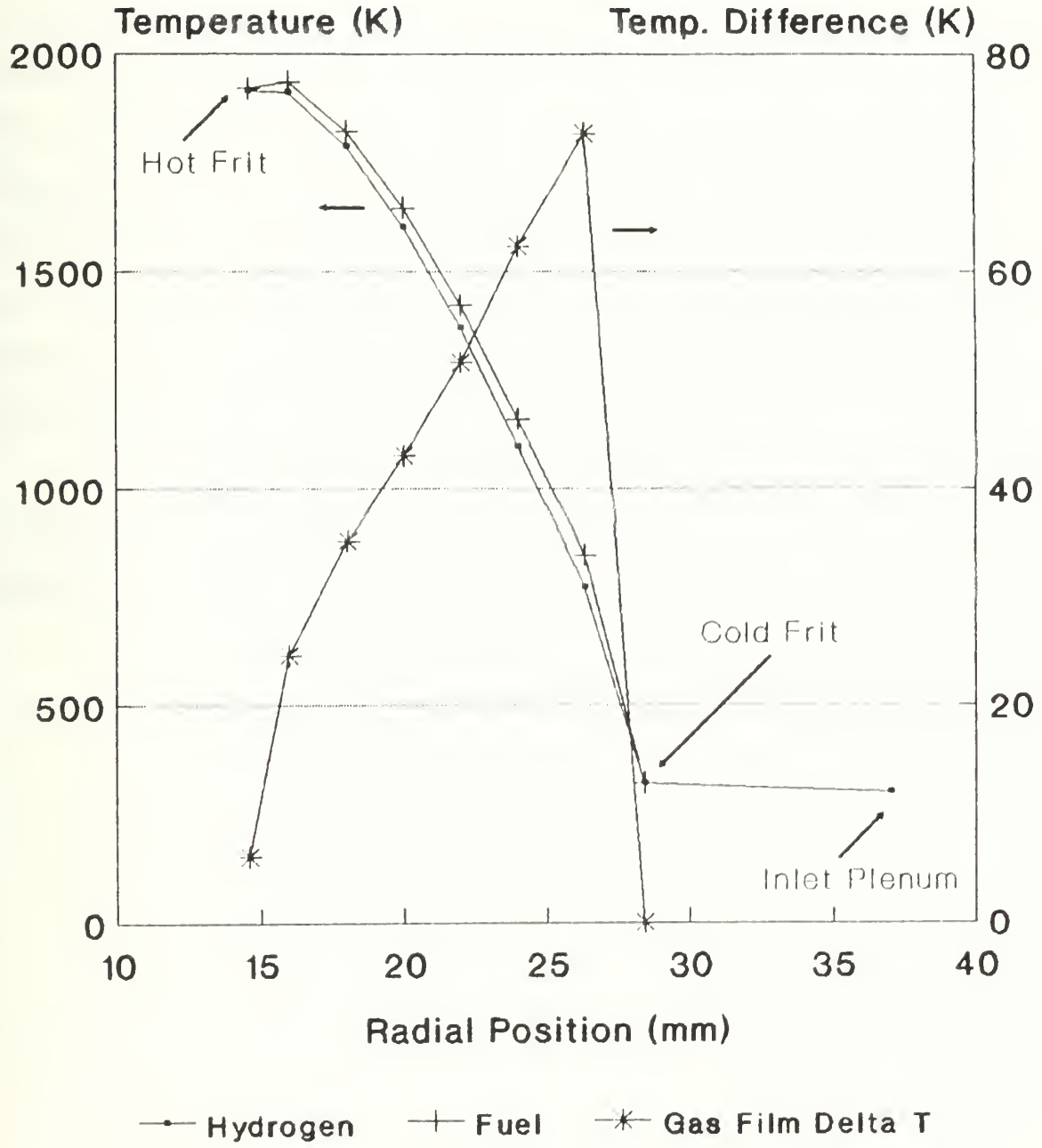

2.1 GW/m^3, J=3 node

Figure 6.10

The heat transfer time constant for the single node model also varies with temperature. At 300 K it is approximately 100 ms in the fuel particles, while at 1935 K it is 30 ms. Looking at the formula for the time constant, this reflects an increase in the overall heat transfer coefficient, $\overline{U}$.

To further check the effect of conduction and radiation, a case without conduction between control volumes was run. Figure 6.11 shows the difference in the solid phase temperatures with and without conduction included in the model for the J=3 node. The fuel temperature next to the hot frit changed relatively little. However, fuel temperatures in the rest of the bed decreased significantly. The coolant temperature follows the fuel. Near the hot frit, the lack of conduction forces higher gas film temperature drops to accommodate the larger direct heat transfer from the fuel to the hydrogen. This was confirmed by the steady state heat balance where the heat transferred to the coolant equaled the power generated.

The no conduction case also displayed a small increase in the mass flow rate from 36.7 to 37.8 g/sec. The change in flow resulted in a 25 K decrease in the outlet temperature

The Effect of Conduction and Radiation

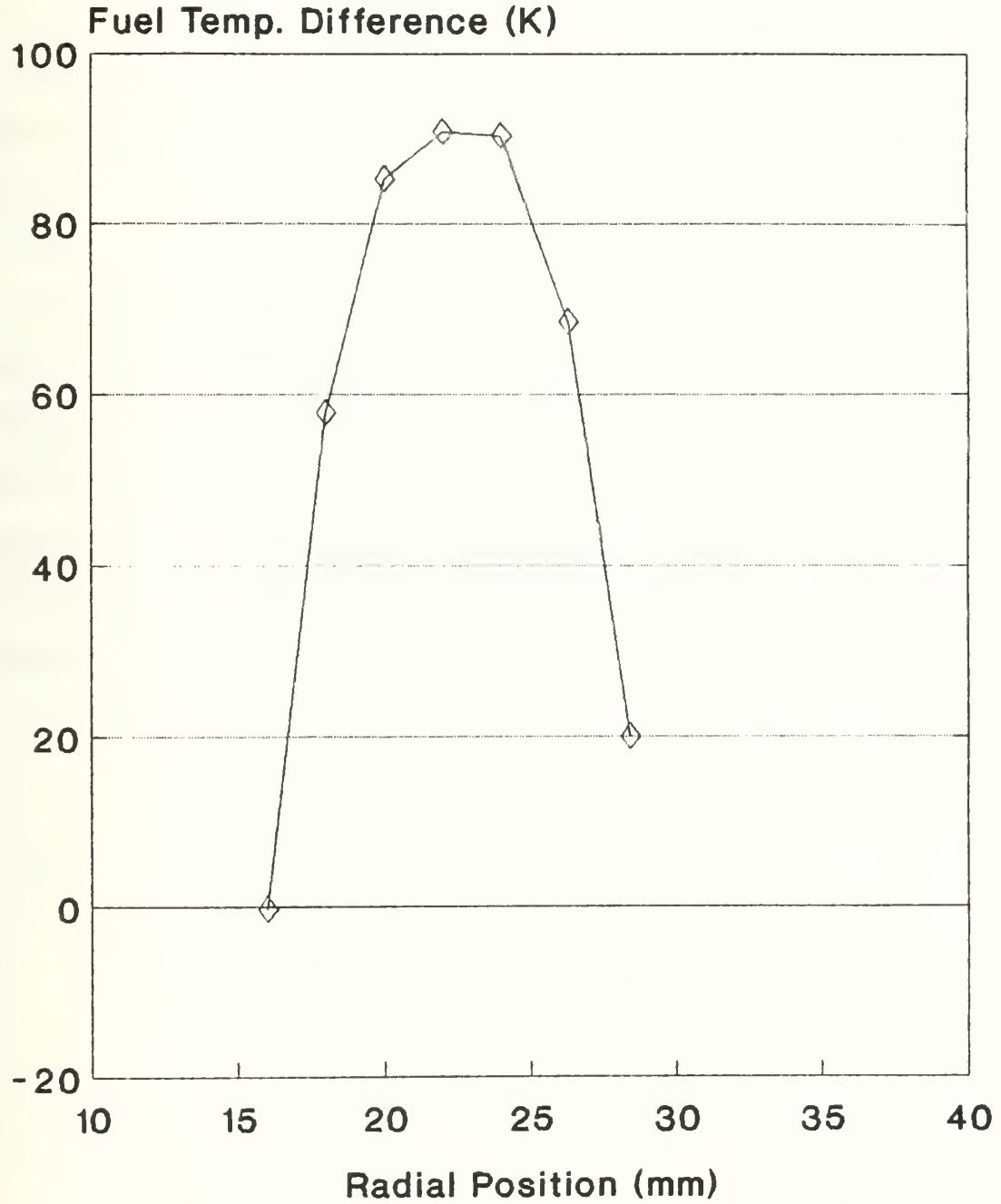

T(With Cond & Rad) - T(No Cond & Rad)

Figure 6.11

6.3 TRANSIENT RESULTS

A rapid up power transient is conducted to test the codes ability to track rapidly changing conditions. In this case, steady state flow is established then the peak power is ramped from 0.0 to 2.0 GW/m^3 over a period of one second.

Figures 6.12 through 6.16 show the time variation of the variables. The results are consistent with the trends observed in the comparison of the steady state results at various power levels.

The power plot, Fig. 6.12, also provides some insight into the characteristics of the model fuel element. During the first second of the transient while power is increasing at a constant rate, the time constant of the system can be estimated from the time difference of the curves, since they are almost parallel to each other (See section 5.2). In this case the time constant is probably between .6 and 1.0 seconds which agrees with the times required to reach steady state. This is only an approximation, because the heat transfer parameters included in the time constant are themselves functions of temperature.

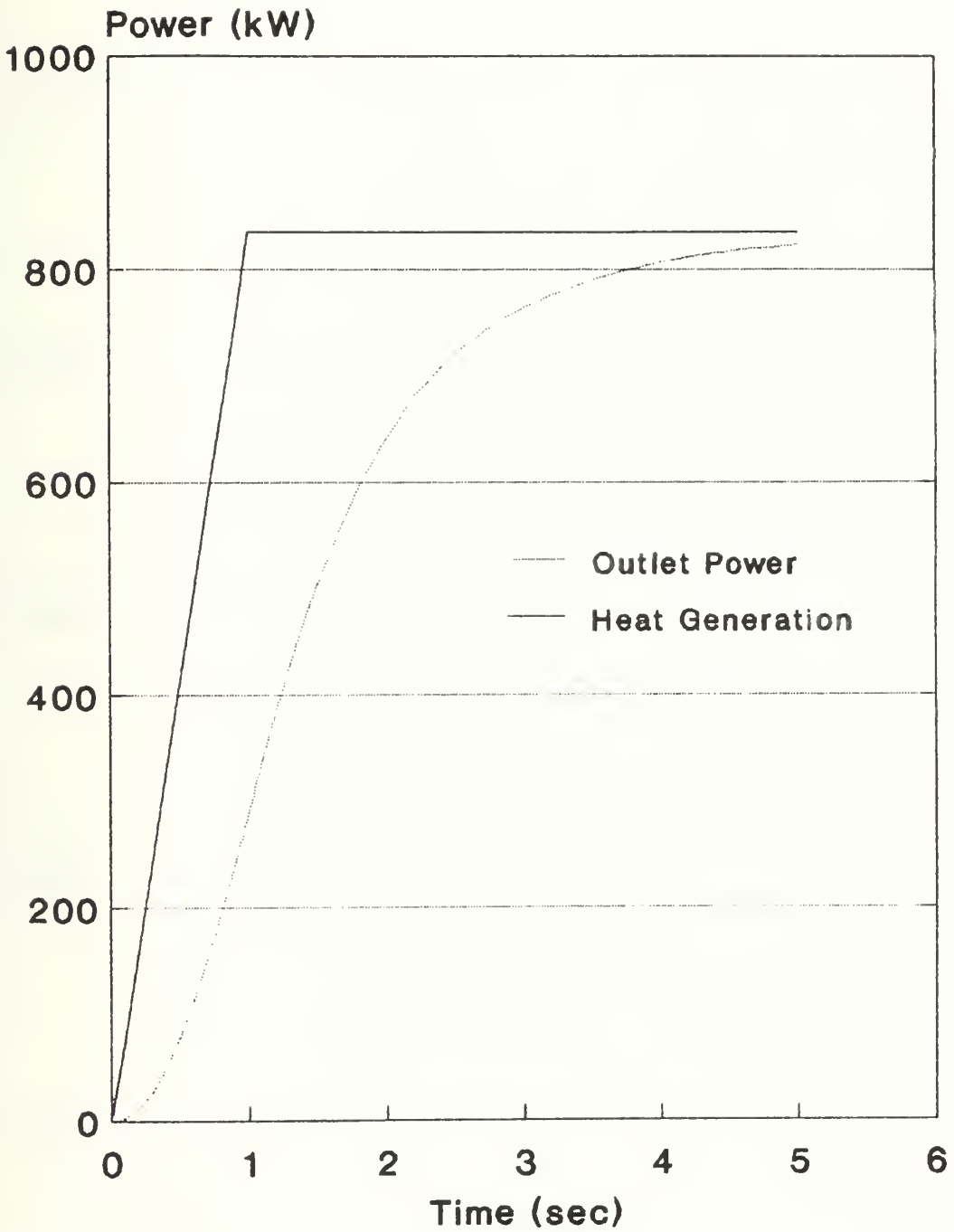
Power Transient
0.0 to 2.0 GW/m^3
Power (kW)
1000
800
600
400
200
0
0
1
2
3
4
5
6
Time (sec)
Outlet Power
Heat Generation

Figure 6.12

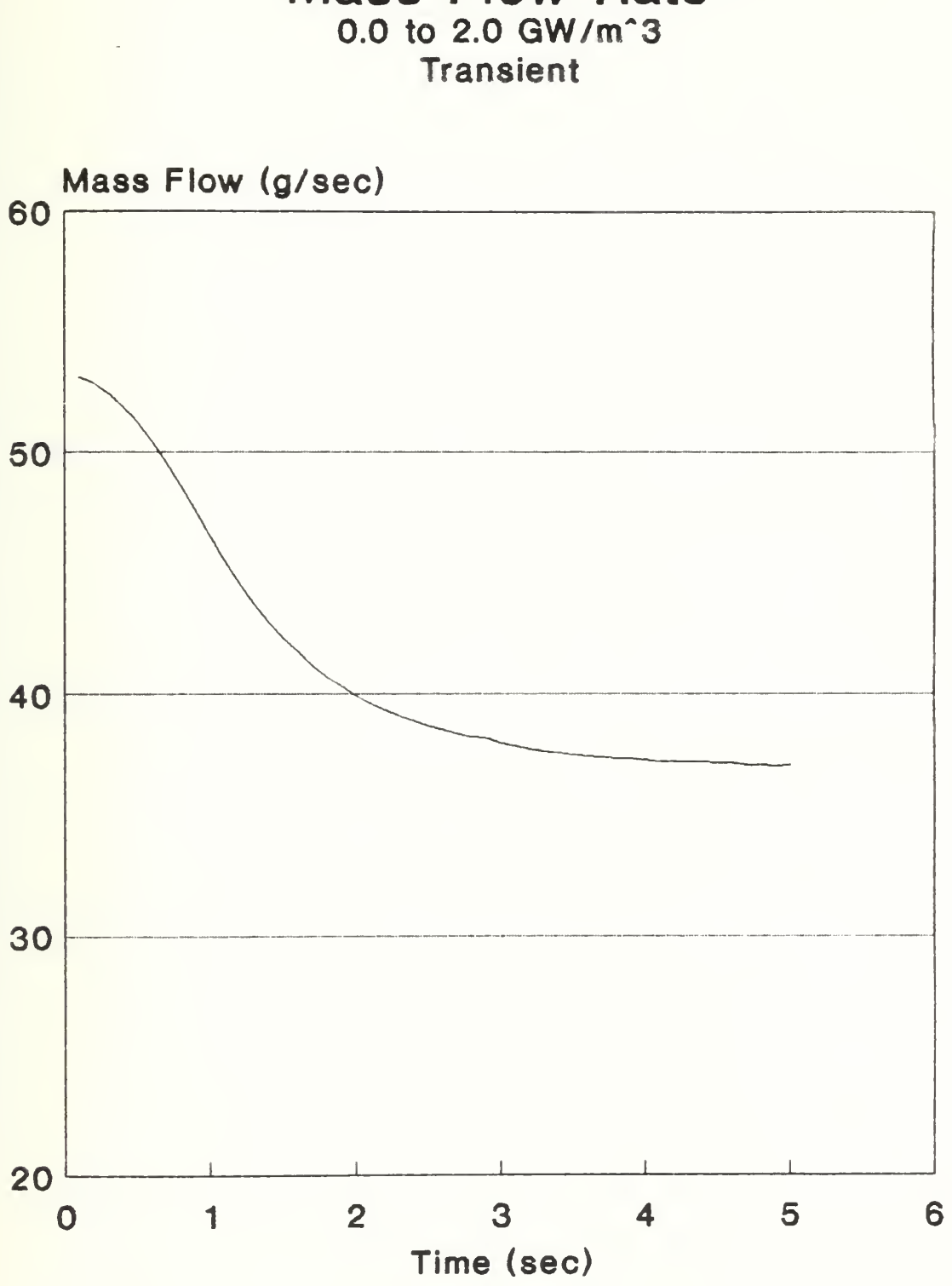
Mass Flow Rate
0.0 to 2.0 GW/m^3
Transient
Mass Flow (g/sec)
60
50
40
30
20
0
1
2
3
4
5
6
Time (sec)

Figure 6.13

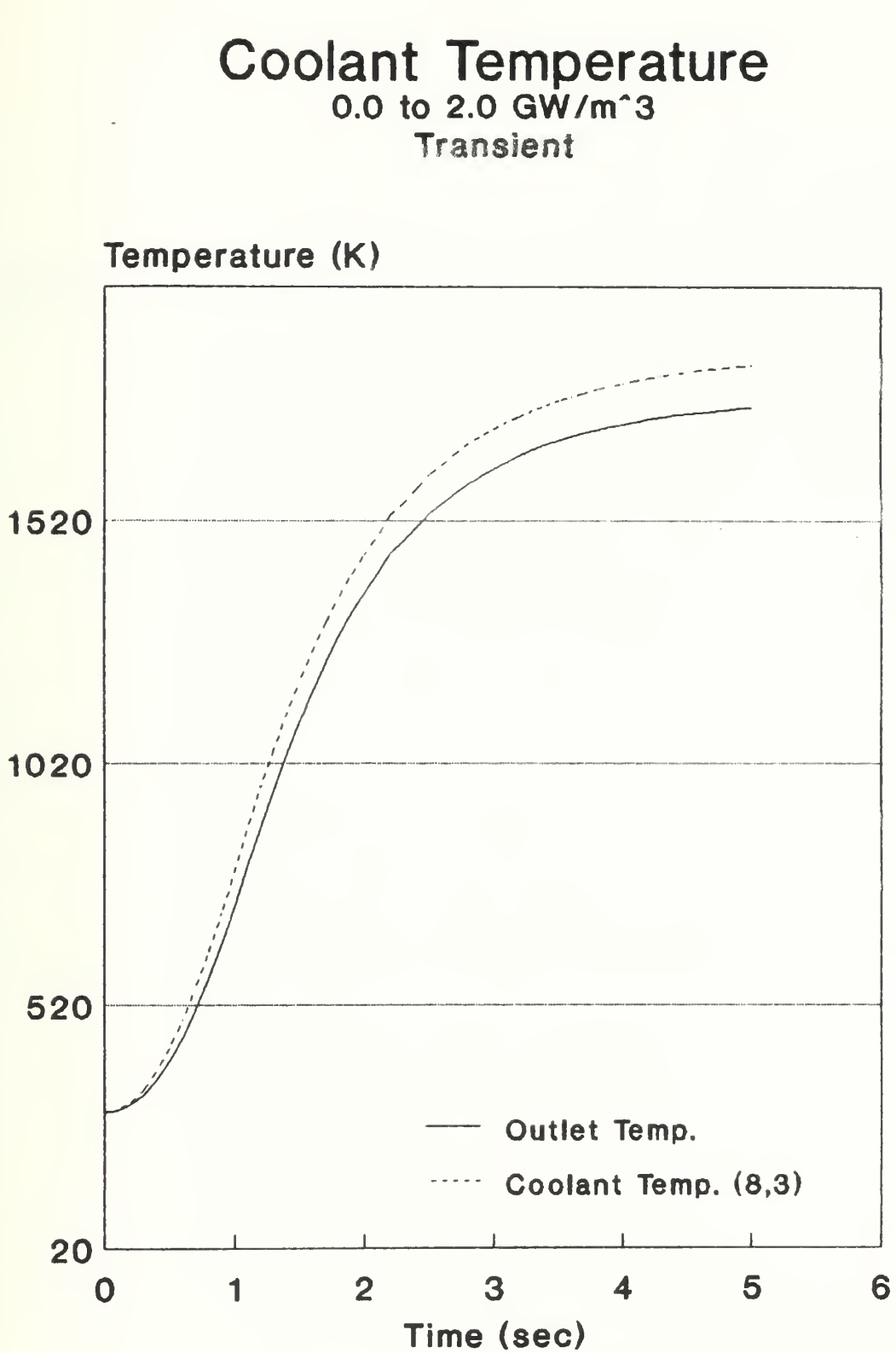
Coolant Temperature
0.0 to 2.0 GW/m^3
Transient
Temperature (K)
1520
1020
520
20
0
1
2
3
4
5
6
Time (sec)
Outlet Temp.
Coolant Temp. (8,3)

Figure 6.14

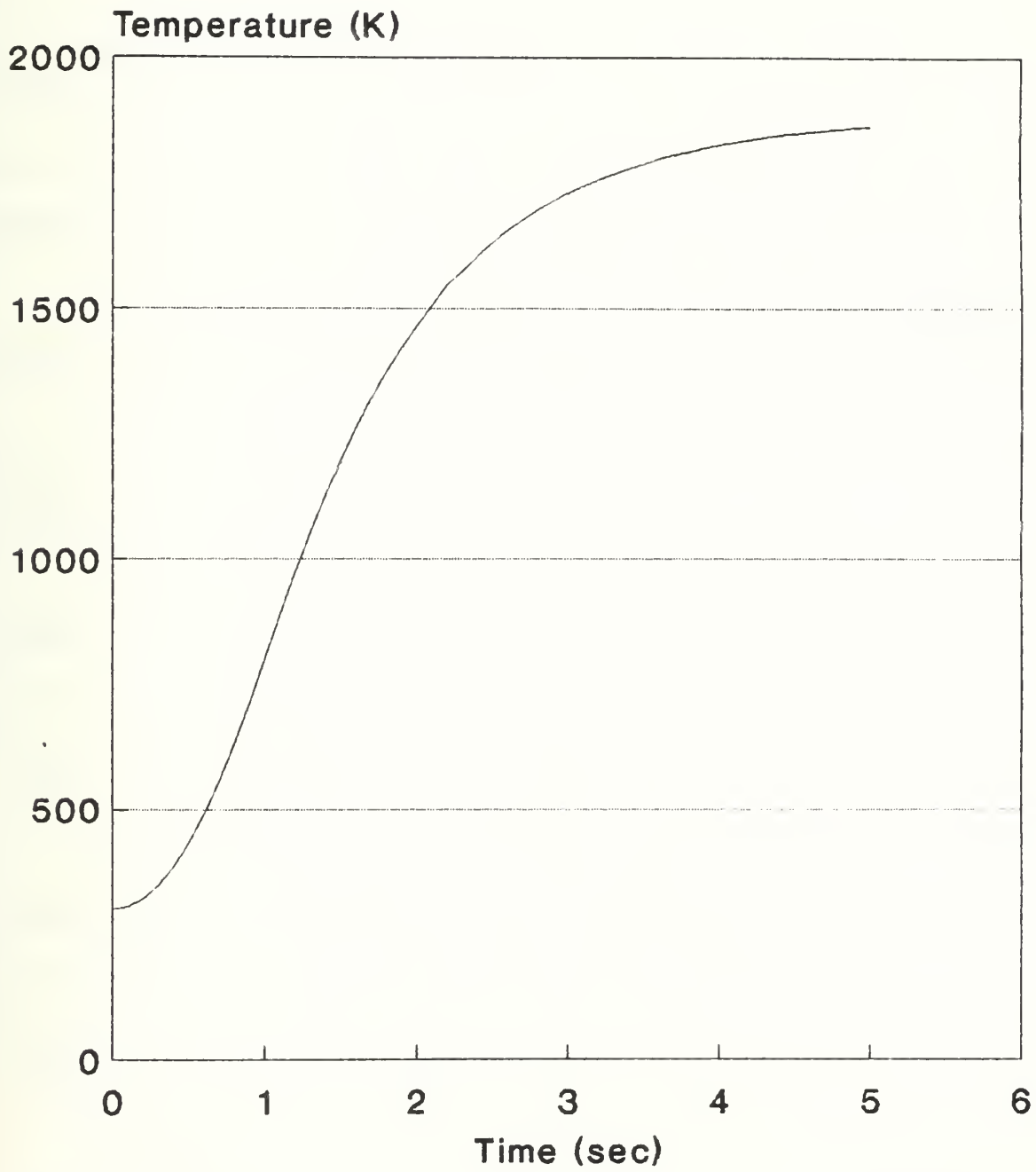

node 8,3

Figure 6.15

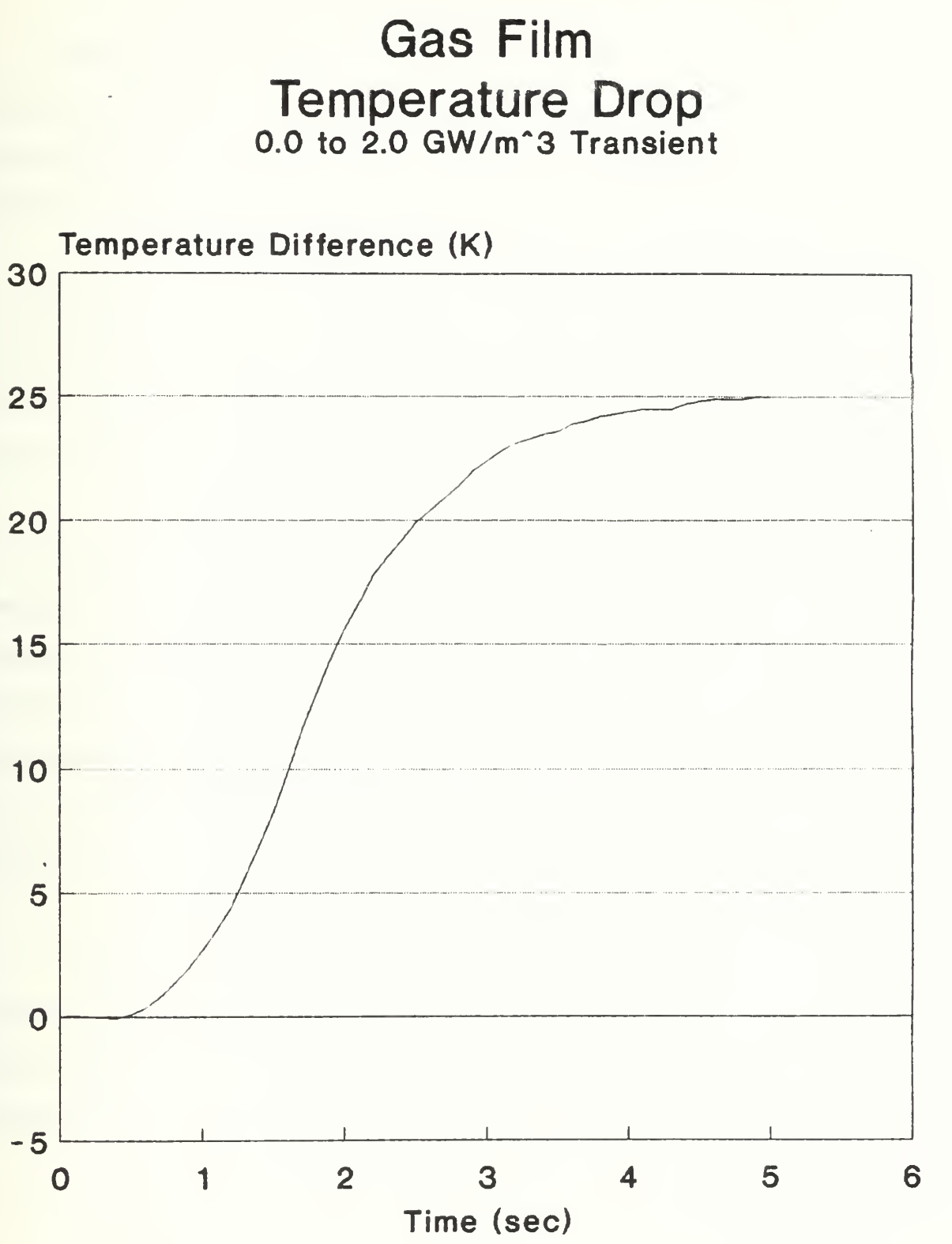

node 8,3

Figure 6.16

6.4 CONCLUSIONS

While the data used in the test problems are representative of the Sandia PIPE experiment fuel element, the numerical results may not be directly applicable due to approximations made where PIPE data are not readily available. However, from a more general perspective several basic ideas are demonstrated in the model results.

Two dimensional modeling is required to reflect accurately the axial flow in the fuel particle bed which is present to some degree in all cases. Mass flow is a function of temperature for a given pressure drop across the fuel element. It decreases as power increases due to the increased flow resistance of the hotter, lower density hydrogen coolant.

As power increases, the pressure losses across the hot frit and in the outlet plenum also increase. Thus, if the total ΔP remains unchanged, then the pressure loss in the cold frit must decrease to compensate. This reduces the total mass flow rate and drives a partial redistribution of the coolant flow to the shorter flow paths which see less of the change in the outlet plenum pressures. The redistribution is manifested in increased axial flow through the fuel bed and an increased percentage of the flow through the thicker sections of the cold frit near the inlet port.

The cold frit flow distribution design is specific to the conditions assumed in the design process. If power pressure or flow rate are changed the cold frit will not provide the desired flow profile. Higher power favors the more direct flow paths from the inlet to the outlet port. This potentially could place the maximum flow in the area of minimum power.

The cold frit does not act in isolation. Therefore, its design should be approached from a system perspective that looks at the total fuel element pressure drop and the contributions from each component in each flow path. Once the cold frit design is fixed, it is the variation of the pressure losses in the other components with changing conditions that determines the final flow distribution.

The thermal model demonstrates the necessity to consider conduction and radiation processes when predicting fuel element behavior.

CHAPTER 7

SUMMARY AND CONCLUSIONS

7.1 OBJECTIVE AND METHODOLOGY

Considerable work is in progress to design and develop new space based reactors. The designs by necessity must be lightweight and small with high power densities. One reactor being studied at the Brookhaven and Sandia National Laboratories uses a hydrogen cooled packed bed fuel element. The MIT interest in this system is the development of a closed loop digital controller for reactor power.

In order to control the reactor properly, the controller must evaluate the reactivity effects of the hydrogen coolant and fuel element temperature distribution. Therefore, in addition to a good neutronic model, a real time thermal hydraulic analysis capability is required. The purpose of this investigation is to perform the initial steps in the building of a thermal hydraulic module for the controller. Specifically, a detailed model of the fuel element thermal hydraulic behavior is presented. It forms the reference case against which simpler real time models can be compared.

The first step in the modeling process is to look at the details of the actual fuel element. This model is based on the element constructed for the Pulsed Irradiation of a Particle-bed Element (PIPE) experiment being conducted at the Sandia National Laboratory. The cross-section is shown in Fig. 7.1. The fuel is installed in the annular space between two cylindrical concentrically mounted porous retention elements (frits). Coolant is directed around the

outside of the outer frit then turns and flows radially through the cold frit, fuel and inner frit to the collection plenum at the center of the element. The fuel consists of 500 μm diameter particles with a UC_2 core and pyrographite and zirconium carbide coatings.

The form of the model is determined by the identifying the features and processes that affect the fuel element behavior. The flow portion must accurately represent the velocity and pressure of the coolant as a function of position. Thus, manifold distribution effects and friction processes are important. Coolant and fuel particle temperature are also required. As a result, intra and interphase heat transfer processes must be considered.

The transport mechanisms can be related by fundamental principles of momentum, energy and mass conservation. Applying these with a lumped parameter approach to an array of control volumes forms the basis of the fuel element model.

The unifying structure is provided by using a staggered grid, Fig 7.2, to link the control volumes. The staggered grid is based on placing points where velocity is defined between the points where pressure is defined. In this arrangement, the control volumes can be matched to the components of the fuel element. The fuel element model assumes cylindrical symmetry, allowing the problem to be reduced to two dimensions (radial and axial).

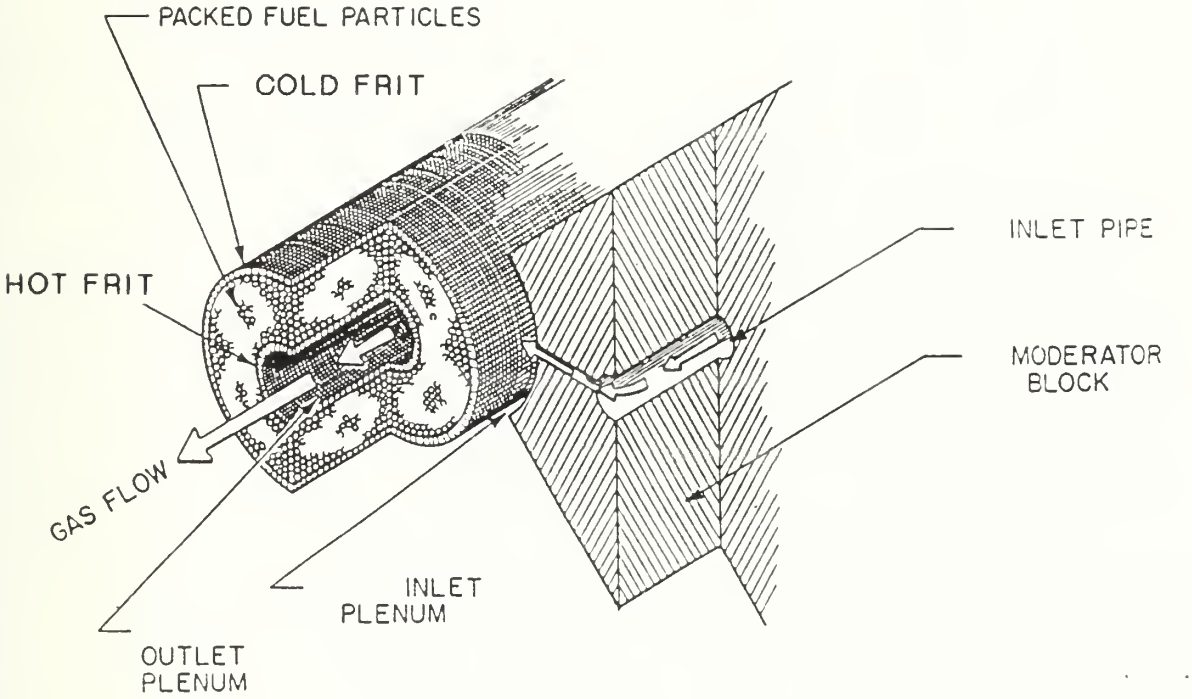

Figure 7.1

Packed Bed Fuel Element

(From L-1)

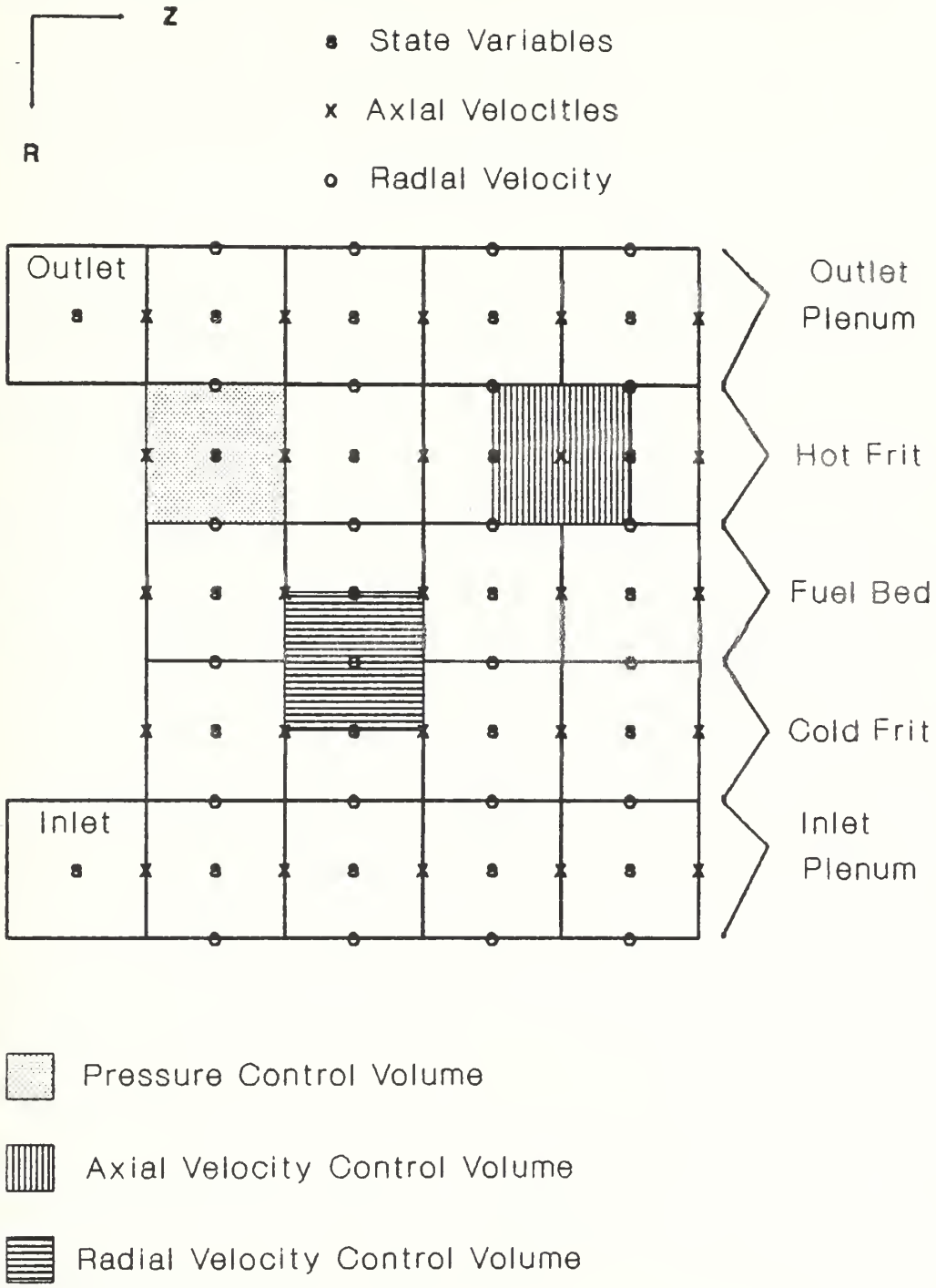

Figure 7.2 **The Staggered Grid**

The final step in constructing the model is the discretization of the control volume conservation equations to make them compatible with digital computer solution techniques.

The gas and solid phases are modeled independently except for the interphase heat transfer term which couples the two models. The coupling is addressed in the solution process.

7.2 THE GAS PHASE

7.2.1 The Model

The gaseous hydrogen coolant is highly compressible. As a result, simultaneous momentum, mass and energy balances are required to define the state of the coolant. The momentum and energy balances are identical in form and can be described using the general variable ϕ .

$$\frac{d}{dt}\phi = \sum \text{sources} + \sum \dot{m}\phi \qquad 7.1$$

ϕ represents the superficial radial and axial velocities in the momentum balances and the specific enthalpy in the energy balance.

The momentum source terms include the pressure drop across the control volume and the frictional losses. The pressure drop is easily evaluated, since the staggered grid defines pressure on the faces of the momentum control volume.

Two models are used for the friction term. The frits and the packed bed are characterized by the Ergun relation which treats flow in the bed as flow through tubes with irregular cross-sections (E-1).

$$\frac{\Delta P}{L} = \frac{150\mu\vec{v}_o(1-\varepsilon)^2}{D_p^2}\frac{}{\varepsilon^3} + \frac{1.75\rho\vec{v}_o|v|}{D_p}\frac{(1-\varepsilon)}{\varepsilon^3} \qquad 7.2$$

From Eq. 7.2 it can be seen that frictional losses are a function of velocity and velocity squared. $\vec{v}_s$ is the component of velocity in the direction of the momentum balance and $|v|$ is the magnitude of the superficial velocity.

Frictional losses in the plenums are described using a pipe flow relation that assumes they are proportional to a friction factor, f.

$$\Delta P = f\left(\frac{L}{D}\right)\frac{\rho v^2}{2} \qquad 7.3a$$

$$f = 0.138\mathrm{Re}^{-0.151} \qquad 7.3b$$

L = length $\qquad$ D = equivalent pipe diameter

Eq. 7.3b is a modified form of the McAdams relation to account for surface roughness.

The cold and hot frits and their associated plenums serve as dividing and combining manifolds respectively. Bajura and other investigators found that direct application of the momentum conservation equations to manifolds did not accurately represent experimental behavior because they failed to account for the axial momentum contained in the portion of the stream which turns in the control volume and leaves it flowing radially (B-4,B-5 and

B-6). They found that adding two constants to the momentum balance equation which characterize the velocity profile of the axial stream and the axial momentum of the turning stream significantly improved the accuracy of his model. A similar analysis was applied to the outlet plenum. The momentum equations are summarized in Table 7.1 where the constants have been combined to form the turning coefficient, θ .

The energy balance contains two source terms. The first is a pressure change term. The second enthalpy source is the heat transferred from the fuel particles to the coolant. It is a function of the temperature difference across the gas film, the overall heat transfer coefficient and the surface area per unit volume ratio. The heat transfer coefficient is evaluated using the Colburn *j* factor empirical correlation and the single node analysis of the fuel particles (B-3). The final form of the enthalpy balance is shown in Table 7.1.

Table 7.1

The Gas Phase Conservation Equations[1]		
Axial Momentum	$\left(\frac{d}{dt} m \vec{v}_{axial}\right)_{cv} = \vec{F}_{press} + \vec{F}_{friction} + \theta \sum_{i=1}^{I} \dot{m}_i \vec{v}_{axial,i}$	note a
Radial Momentum	$\left(\frac{d}{dt} m \vec{v}_{radial}\right)_{cv} = \vec{F}_{press} + \vec{F}_{friction} + \sum_{i=1}^{I} \dot{m}_i \vec{v}_{radial,i}$	
Mass	$\left(\frac{d}{dt} m\right)_{cv} = \sum_{i=1}^{I} \dot{m}_i$	
Energy	$\left(\frac{d}{dt} H\right)_{cv} = hA_v V(T_S - T_G) + V\frac{dP}{dt} + \sum_{i=1}^{I} \dot{m}_i h_i$	
Note a: θ: Inlet Plenum 0.95, Outlet Plenum 2.66, Otherwise 1.0		

1 $\vec{v}_i$ should be the interstitial velocity. Refer to sec. 7.5.

The mass balance, also shown in Table 7.1, uses only the flux term, since there is no source of mass in the control volume.

7.2.2 The Solution

Before the variables can be advanced in time using the balance equations, the continuous form of the equations must be discretized. The fuel element model equations are developed using a semi-implicit five point difference method. A donor cell, upwind, system is used to evaluate the scalar variables at the control volume interfaces. In the discrete form the balances are implicit using the time n+1 value of the balance variable. However, the coefficients (such as the mass flow in the flux term) are evaluated using the time n values. This introduces a semi-implicit nature to the overall equation. The discretization also serves to linearize the relations. In cases where squared terms appear, they are approximated by using the product of the time n+1 and time n values keeping the equation linear in the n+1 variable.

The Pressure Implicit with Splitting of Operators (PISO) method forms the basis of the solution algorithm (I-1, I-2). As used in this model, it is a two stage predictor corrector technique that advances the variables in time by calculating up to three successively more refined estimates of the n+1 value of the variables. Because it is noniterative and has reasonably good stability, it is relatively fast and requires less computing effort than competing methods. Each step of the solution sequence applies the appropriate balance equation to each control volume to generate a system of simultaneous linear equations which are solved using standard matrix techniques.

The first predictor solves the momentum balances for the velocity field. Then taking advantage of the staggered grid, which defines the velocities on the faces of a pressure cen-

tered control volume, the momentum and mass balances are combined to form a pressure equation which yields new velocities and pressures that simultaneously satisfy both balances. The second predictor is the energy balance which contains the coupling to the solid phase solution. The second corrector applies the pressure equation again with the updated temperatures. At the end of the process three estimates of the velocity field, two of the pressure and one of the temperature have been made.

7.3 THE SOLID PHASE

7.3.1 The Model

The solid phase is abstracted to mathematical form by using the energy balance. The balance includes three basic processes, heat generation and storage, energy transfer to the coolant and heat transfer to the surrounding solid material.

The first two processes are initially modeled on a single particle basis. To simplify the model, the single node technique of reference M-1 is used. This assumes a steady state temperature distribution in the multilayer fuel particle and then homogenizes it to calculate effective overall properties which are representative of the original particle. The temperature distribution in the particle can then be described by a single temperature which satisfies the heat balance equation. Since the lumped parameter approach is being used, only one particle needs to be modeled in each control volume. The results can then be rescaled to include all of the particles in the control volume.

Heat transfer to the surrounding particles is modeled on a control volume basis. The driving force is the temperature difference between adjacent control volumes. Two mecha-

nisms contribute to the transfer. The conduction process in a packed bed actually occurs through the gas layer near the points of contact. The Kunii and Smith model is used to evaluate the control volume conductivities (K-3). In addition to thermal conduction, radiative mechanisms are significant when particle temperatures exceed 1000 K. This is evaluated using the relation proposed by Schotte (S-4). The effective conductivity of the packed bed is the sum of the thermal and radiative components. Because of differences between the control volumes the harmonic mean of the conductivities is used to estimate the effective conductivity at the interface.

The solid phase energy balance then becomes:

$$m_a \bar{C}_P V_{cv} A_V \left(\frac{\bar{T}^{n+1} - \bar{T}^n}{\delta t} \right) = \left(k_{total} a \frac{(\bar{T}_E^{n+1} - \bar{T}_O^{n+1})}{\delta z} \right)_e + \left(k_{total} a \frac{(\bar{T}_O^{n+1} - \bar{T}_W^{n+1})}{\delta z} \right)_w$$
$$+ \left(k_{total} a \frac{(\bar{T}_N^{n+1} - \bar{T}_O^{n+1})}{\delta r} \right)_n + \left(k_{total} a \frac{(\bar{T}_O^{n+1} - \bar{T}_S^{n+1})}{\delta r} \right)_s$$
$$+ q'' V_{cv} A_V - \bar{U} V_{cv} A_V \left(\bar{T}^{n+1} - T_G^n \right) \qquad 5.14$$

This is discretized in the same fashion as the gas phase relations.

7.3.2 The Coupling of the Gas and Solid Phase Solutions

The last part of the model is the coupling of the gas and solid phases. The heat transferred between phases is the only term common to both models. The relatively small volume and heat capacity of the hydrogen require that this term be treated implicitly for numerical stability. This is accomplished using the technique developed by Reed and Stewart for the

THERMIT code (R-1). It first estimates the new fuel temperature assuming the old value of the gas temperature. The method then solves the coolant energy balance using the estimated solid temperature plus a correction for the original assumption, based on $\partial T_S/\partial T_G$ which is calculated in the solid phase energy balance. Finally, the estimate of the solid phase temperature is corrected.

7.4 MODEL VERIFICATION AND RESULTS

The model was encoded in a micro computer based Fortran program and applied to several steady state and transient problems to test its validity. Required input information includes the physical dimensions of the element, initial values of the variables, the nodalization scheme and boundary conditions. The boundary conditions can be completely specified by the inlet pressure, inlet temperature, outlet pressure and peak power density, all of which are easily measured quantities. Transients can be modeled by varying the outlet pressure and/or the power density.

The steady state cases were identical except for the power density which was varied from zero to 2.1 GW/m^3. The hydraulic results revealed significant axial flow in the fuel particle bed which resulted in a redistribution of the coolant mass flow between the frits as shown in Fig. 7.3. This effect is more pronounced as power increases.

Increasing power also changes the distribution of flow along the inlet plenum and cold frit. This is illustrated in Fig 7.4. This second redistribution effect was also noted when the model was altered to prevent axial flow in the fuel bed. Power also affected the mass flow rate. Flow decreased when power increased for a given pressure drop across the fuel element.

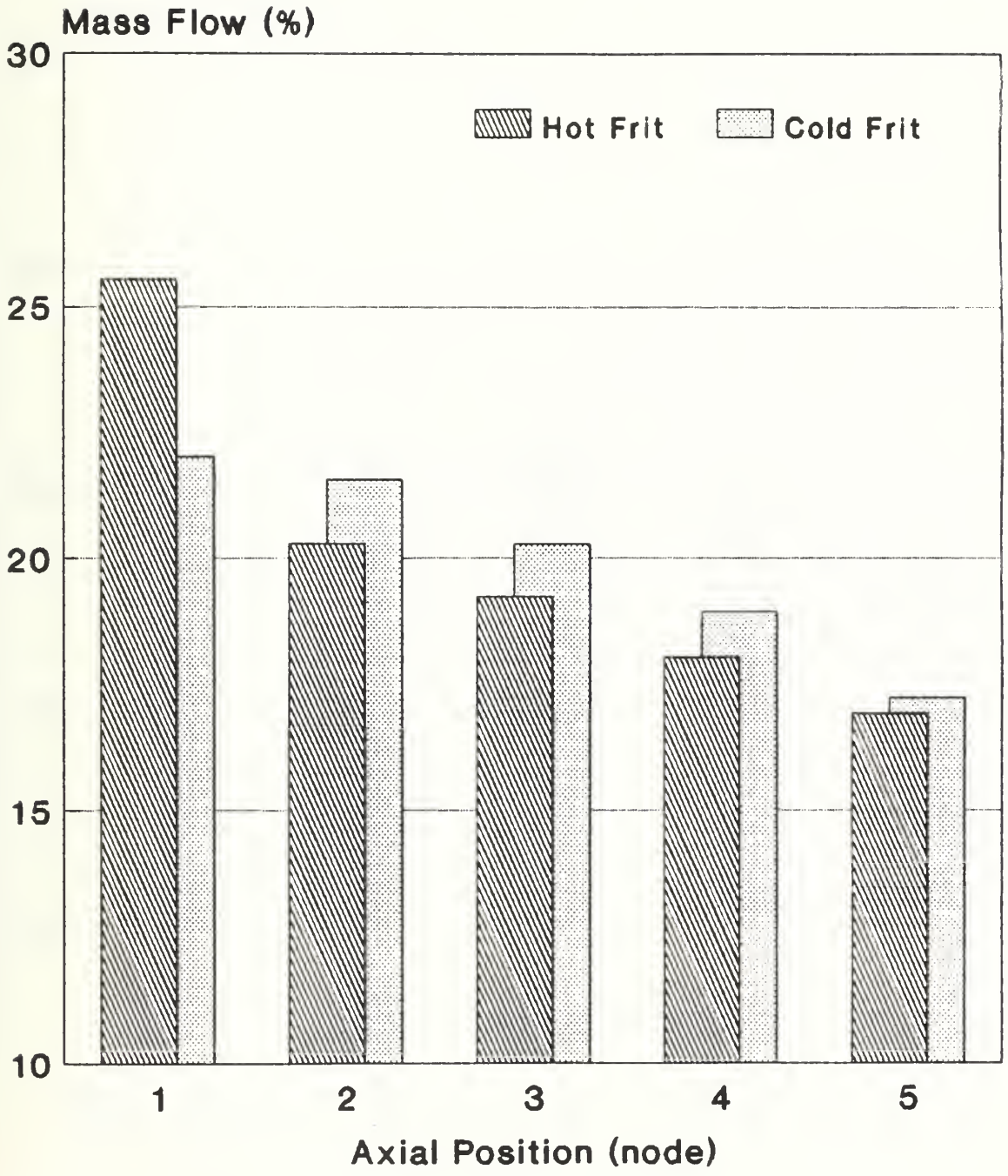
Flow Distribution
2.1 GW/m^3
Mass Flow (%)
30
25
20
15
10
Hot Frit
Cold Frit
1
2
3
4
5
Axial Position (node)

Figure 7.3

Comparative Flow Distribution
Cold Frit

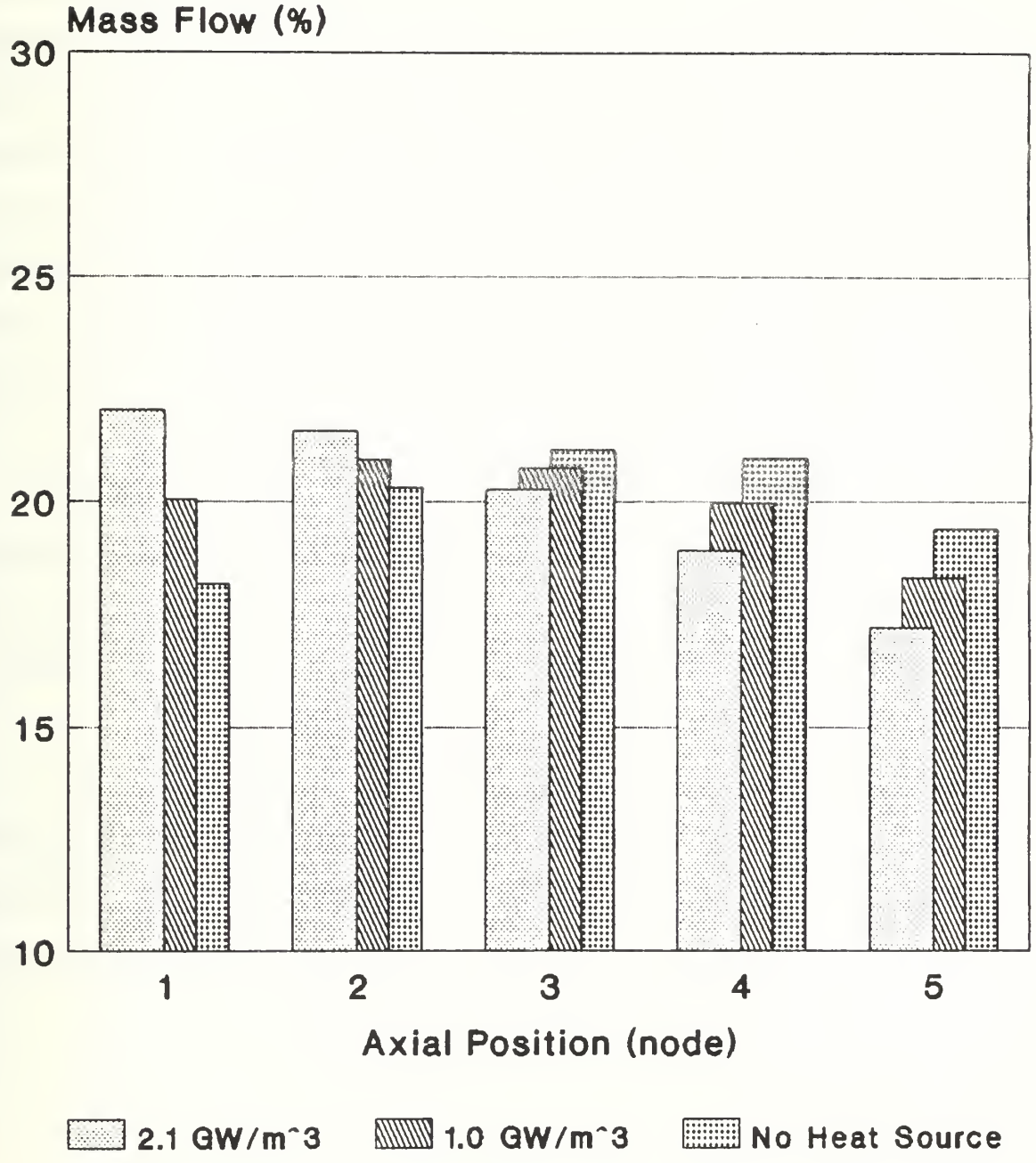

Figure 7.4

These effects are the direct result of heating the coolant, reducing its density, thereby increasing its velocity and causing a realignment of the pressure field. In the zero power case, 85 to 95% of the pressure drop occurs across the cold frit. When power is raised to 2.1 GW/m^3, only 62% of the pressure drop occurs across the cold frit (at the axial center of the element). The frictional losses increase due to the higher velocities, especially in the hot frit and outlet plenum. Looking at the fuel element as a network of parallel paths between the inlet and outlet ports (the paths must have a common pressure drop), the higher velocities in the bed and outlet plenum increase the pressure drop in the paths through these elements. In order to satisfy the total pressure condition, which remains constant, flow must decrease in the high loss paths. This is reflected by an increase in the flow through the more direct paths between the ports and an increase in the axial flow in the bed that bypasses the outlet plenum. The total redistribution was less than 10% in the cases examined.

Although the thickness of the cold frit is varied to force a particular mass flow distribution, the flow can be significantly altered by the outlet plenum and hot frit. The cold frit does not act in isolation. The thickness must therefore be chosen to obtain a specified flow pattern at power in concert with the design of the other fuel element components.

The thermal results predict significant temperature variation along the hot frit, contrary to the design objective of approximately equal temperatures. This is the direct result of the mass flow redistribution producing a mismatch in the power and flow profiles. The temperature distribution is shown in Fig 7.5.

Coolant Temperature Distribution Along the Hot Frit

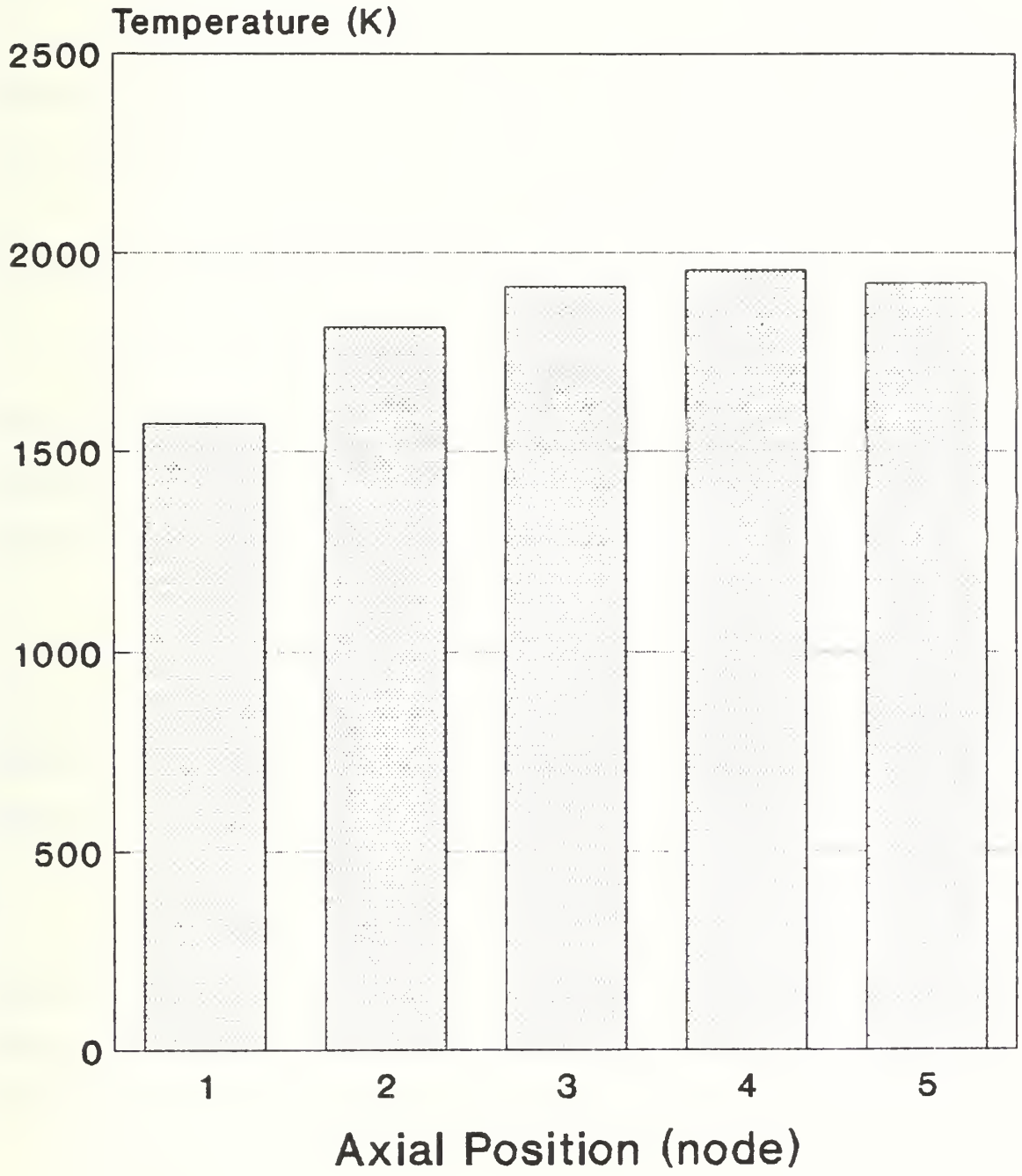

2.1 GW/m^3

Figure 7.5

The test cases also indicate that conduction and radiation are important mechanisms for heat transfer especially at the higher fuel temperatures near the hot frit. In these locations up to 30% of the energy generated in the fuel particles is removed from the control volume by transfer to adjacent solid material in the fuel element.

A transient problem, which raised peak power from zero to 2.0 GW/m^3 in one second, confirmed the trends observed in the comparisons of the steady state results. The system time constant was estimated at .6 to 1.0 seconds.

7.5 RECOMMENDATIONS FOR FURTHER INVESTIGATION

The model developed in this investigation represents a first step in the design and construction of a thermal hydraulic module of a controller for reactor power. It is the reference case against which other simpler and faster versions can be compared. Several refinements would greatly increase its utility.

First, the model predictions should be compared to experimental results. Several model parameters such as the turning coefficients in the momentum equations may require adjustment, since the current values, based on the literature, were obtained under much different conditions.

Second, the reference case should be corrected and expanded. The incorrect use of the superficial velocity instead of the interstitial velocity in the momentum balance time derivative and flux terms should be corrected. Preliminary calculations based on steady state results show that the error in the momentum flux term is approximately 3% of the pressure

source term in the momentum equations shown in Table 7.1. The effect of the error on transient calculations has not been evaluated. Within the fuel element the effects of conduction to the moderator block and component expansion due to heating have not been addressed. The latter could have a significant effect on the hot frit and fuel bed pressure losses. Once the fuel element analysis is complete, it should be broadened to include the entire core and reactor system.

The third area for investigation starts the process of designing a real time controller module. A series of model simplifications should be developed and tested against the reference case to determine which provide the required prediction accuracy. Areas that should be looked at are:

1. The numerical scheme. Is the PISO algorithm really the most efficient numerical technique or would the technique of one of the commercial codes be better?

2. The nodalization. Is a fine node analysis really required or can the fuel element be adequately represented with just a few control volumes? Can one fuel element be modeled in detail and the results generalized to the other elements in the core?

3. Model basis. Can the model be simplified by using another approach to the solution of the basic conservation equations? For example, could the momentum integral method used in the MINET code be applied (M-3,V-2,V-3)?

Packed bed reactors have tremendous potential because of their high power density and inherently safe design. It is hoped that the thermal hydraulic model presented here will contribute to their development.

APPENDIX A

FUEL ELEMENT MODEL

PROGRAM DESIGN AND OPERATION

A.1 OBJECTIVE

HTWOCOOL is a PC compatible program that performs the calculations associated with the model developed in chapters 3, 4 and 5. This appendix presents the operational details required to use the code for further analysis.

A.2 PROGRAM DESCRIPTION

The HTWOCOOL code advances the fuel element pressure, velocity and temperature fields in time using initial values of the variables and a set of boundary conditions. The code is capable of tracking transients or calculating steady state solutions.

The code is written in Fortran 77 using the Microsoft 4.10 compiler. As such, it is intended for use on a personal computer. However, the test problems conducted to date indicate that the time step must be restricted to values between .25 and .5 ms. This small time step requires exceedingly long computing times for PCs (48 hrs or more on an AT compatible to get to steady state). Therefore, conversion to a mini computer may be more practical than using a PC

The program's design is modular with a shell program to assemble data and sequence the subroutines. The following modules comprise HTWOCOOL:

Shell Program

MAIN: Assembles data, sequences the subroutines, keeps track of the time step, calculates transient parameters.

Solid Phase Subroutines

ONCNST: Calculates constants for the single node fuel particle model.

SOLID: Performs the solid phase heat balance.

PISO Subroutines

AXLMOM: Performs the axial momentum balance.

RADMOM: Performs the radial momentum balance.

PRESUR: Solves the first stage pressure equation.

ENTHLP: Calculates the coolant energy balance and corrects the initial estimate of solid phase temperature.

PRESII: Solves the second stage pressure equation.

Support Subroutines

H2EOS: Evaluates the parahydrogen physical constants.

LUDCMP and LUBKSB: Matrix equation solution routines.

To advance the variables one time step MAIN establishes matrices for each variable with its time n value in each control volume. It then passes the appropriate data to each of the subroutines which calculate the successive approximations to the time n+1 values. Each of these approximations is maintained in its own array. When the calculation for the time step is complete and the results recorded, MAIN substitutes the n+1 values into the time n matrices to set up the calculation of the next time step and advances the time counters.

The PISO and Solid phase subroutines function in a similar manner. They take the appropriate conservation equation for each of the control volumes and evaluate the coefficients of the balance variable using the time n values received from the shell program. This creates a set of simultaneous linear equations in the following form.

[Coefficient Matrix][Variable Vector]=[Constant Vector]

The subroutine then calls LUDCMP and LUBKSB including the matrix and constant vector as arguments. These routines perform an L-U decomposition and back substitution respectively to solve for the new value of the variable. This result is passed back to the calling subroutine in the form of a modified constant vector. The PISO or Solid subroutine then converts the vector to a two dimensional matrix of the updated values and updates other variables as appropriate. For example, PRESUR calculates the new pressure field then advances the velocity and density fields. Finally, the results and control are passed back to the shell program.

The updated variables are identified by the number of Ts in the name. For example VZ and VZO are the original axial velocity field. VZST, VZSTT and VZSTTT are the first, second and third updates of the velocity. The third estimate is the one carried forward to the next time step. Similar naming schemes have been set up for the other variables.

The nodalization scheme is defined by the user in the input data. The code does require that one radial node be assigned to the each plenum and frit. Any deviation from this will not work. However, there is no restriction on the dimensions of these preassigned nodes.

The sign convention used in the development of the code is positive radially moving from the outside toward the center-line of the fuel element. Axially velocity is positive moving away from the inlet end of the element. The north side of a control volume is the side facing the center-line. The other faces line up according to the compass.

The H2EOS module was developed by the National Bureau of Standards and modified by the Sandia National Laboratory (R-2). The LUDCMP and LUBKSB routines were taken from reference P-5.

A.3 PROGRAM OPERATION

The program is simple to run. It is not interactive. The only operator action required is the assembly of the data set. All operational choices are entered via the data set.

Power and outlet pressure transients can be run as well as steady state calculations. Transients are either in the form of a step change or ramp and are initiated immediately or after a time delay. In the case of ramped change the final value is specified and the time over which the transient is to occur (TOPT or TOQT). The applicable equations are

$$\text{Power} \quad \text{Density} = A + B\,\frac{QTime}{TOQT}$$

$$\text{Outlet} \quad \text{Pressure} = -\frac{PTime}{TOPT}\,(P_{initial} - P_{final}) + P_{initial}$$

where:

$$QTime = Time - Delay \quad time$$

$$B = \text{Final} \quad \text{Power} \quad \text{Density}$$

Note that the overall power density is the actual variable used in the transient simulation. Once MAIN determines the power density for the time step, it applies a chopped cosine function to represent the axial power distribution. Power density is assumed to be constant radially. Changes to the power distribution function would require program modifications and recompiling.

Once the data file is prepared, the program is executed by entering the word MAIN. A MAKE file is also included should program modifications be required. This file is a Microsoft utility that contains the compile and link commands. After modifying the source code of the any of the routines, simply enter "make main" (quotes omitted) and the utility will recompile the updated modules and relink the program giving a new executable file.

A.4 INPUT-OUTPUT

The input is list directed and the majority of the output is formatted. The list directed input leaves the operator some freedom to place decimal points and vary the size of the entries. The values are entered sequentially, in the order the program reads them. Each entry is separated by a comma. There is no restriction on the number of values per line except that the program automatically skips to the next line of data when a new READ statement is executed.

The SI system of units is used exclusively. All lengths are entered in meters, masses in kilograms, pressures in Pascals and temperature in Kelvin.

The Program looks for the input data in a file called PBR.DAT. This file contains the following information:

a. Physical dimension of the cell, fuel and control volumes.

b. User defined boundary conditions.

c. Time step size, number of time steps to be executed.

d. Initial conditions, TGO, TSO, PO, VRO, VZO matrices.

e. Transient control parameters.

To define the control volumes the program requires the axial length (DZ) and the a vector of radii. The axial dimension is assumed to be the same for all nodes. The grid is variable in the radial dimension. While considerable latitude in the fuel element and node configuration is allowed, some of the geometry has been built into the program. The nodes for the coolant state variables align with the components of the fuel element. The velocity nodes, however, may lie across component boundaries (see Fig. 2.6 The Staggered Grid). Up to ten nodes radially and 10 nodes axially can be defined for a total of 100 control volumes.

The fuel element is pictured to be lying horizontally so that in an I, J array of control volumes the values of I and J represent the radial and axial positions respectively. I follows flow, increasing as the position moves inward. J starts at the end of the fuel element with the inlet and outlet ports and follows flow in the inlet plenum.

The values of the radius vector define the centers and surfaces of the control volumes. R(1) is the outside surface of the inlet plenum and R(2*M+1) is the center-line of the fuel element, where M is the number of radial nodes. The radial position of the center of the Ith node is designated R(2*I) and the north and south faces are R(2*I+1) and R(2*I-1) respectively.

The program assumes a minimum of 4 nodes radially. Any additional nodes are added to the fuel region of the element. The fixed control volume assignment assignments are:

I	Location
1	Inlet Plenum
2	Cold Frit
M-1	Hot Frit
M	Outlet Plenum

Table A.1 gives the order of data entry and a line breakdown.

Output of the velocity, pressure, density, enthalpy and temperature variables is formatted and prints as an array. The staggered grid shows the relationship of the variables. Note that the program as written inverts the order of the points showing the coolant entering at the top of the fuel element rather than at the bottom as shown in chapters 4, 5 and 6. The indexes printed next to the array are correct.

Also included in the output are list directed records of the time step, power level, overall heat balance and overall mass balance which facilitate following a transient. Refer to the MAIN program listing to determine exactly which ones are used. Some of the output is directed to the screen.

The formatted output is accomplished by the RESULT subroutine. This may be called at any time during the program, after every time step or at the end of the transient. Program modifications and recompiling are required to change it.

The current program is configured to direct the results to an output file and the screen. However, Fortran does allow the option of going directly to the printer. The required OPEN statement is included in the program but not activated.

Table A.1

Input Data Format

Line	Data Elements (in required sequence)
1	Number of radial nodes (M), number of axial nodes (N), inlet coolant temperature, inlet pressure, fuel particle diameter, cold frit particle diameter, axial node length, time step size, number of time steps to advance variables
2	Void fraction (M values starting with I=1)
3	Cold frit thickness (N values starting with J=1)
4	Radii to control volume centers and interfaces (Starting with outside of inlet plenum and working inward to 2*I+1; this may take several lines)
5	Initial value of the radial velocity (The order should be all the J=1 values from I=1 to M+1, then all the values for J=2 etc to J=N. This may be more than one line.)
6	Initial value of the axial velocities (The same order as the radial velocities except I=1 to M and J=1 to N+1)
7	Initial value of pressure (The same order as the radial velocities except that I=1 to M and J=1 to M)
8	Initial solid temperature (Use the same entry scheme as pressure)
9	Initial coolant temperature field (Use the same sequence as the pressure)
10	Pressure transient parameters: initial outlet pressure, final outlet pressure, transient duration, time delay for initiation of the transient
11	Power transient parameters: initial power density, final power density, transient duration, time delay for initiation of the transient

APPENDIX B

PROGRAM LISTING

The following program listing contains the source code for the original segments of the program. The code for the H2EOS, LUDCMP, LUBKSB modules is contained in references R-2 and P-5.

```
C   PROGRAM TO EVALUATE THE HYDROGEN COOLANT TEMPERATURE PRESSURE AND
C   DENSITY IN A PACKED BED REACTOR
C
C   INITIALIZATION AND DATA INPUT
C
      COMMON/GEOTRY/R(45),EP(20),DZ,THKCF(30),DV(20),DP,DPCF,M,N,DT
      COMMON/BOUCON/PBI,PBO,TBI,RHOBI,HBI
      REAL DT, DZ, VR(11,10),VZ(10,11),P(10,10),TG(10,10),TS(10,10),
     + RHO(10,10),RHST(10,10),VZST(10,11),VRST(11,10),VRSTT(11,10),
     + VZSTT(10,11),BRAF(11,10),BZAF(10,11)
      REAL VRSTTT(11,10),VZSTTT(10,11),TIME,A,B,C,TAU,PWRDEN
      REAL PST(10,10),Q(10,10),PIO(10,10)
      REAL BVR(11,10),ARF(11,10),AWR(11,10),AER(11,10),ASR(11,10)
      REAL ANR(11,10)
      REAL BVZ(10,11),AZF(10,11),AWZ(10,11),AEZ(10,11),ASZ(10,11)
      REAL ANZ(10,11)
      REAL H(10,10),R,EP,PBI,PBO,RHOBI,TBI,PI
      REAL AOZ(10,11),BZ(10,11),AOR(11,10),BR(11,10),THKCF
      REAL HST(10,10),TGST(10,10),PSTT(10,10),RHSTT(10,10)
      REAL VRO(11,10),VZO(10,11),PO(10,10),TSO(10,10),TGO(10,10)
      REAL RHOO(10,10),HO(10,10),HTI,HTO,NN,KK
      REAL PBOI,PBOF,TOPT,PDLAY,PTIME,MAVE
      REAL QTIME,TOQT,QDLAY
      REAL MA(10),CPBAR(10),UT(10,10),FBAR(10,10),TSST(10,10)
      REAL UBAR(10,10),AV(10)
      REAL QIN(10,10),TSSTT(10,10),ANN(10,10),KZC(10,10)
      INTEGER M, N, UNITS, I, J, IT, TSTOP, CT
      PARAMETER (PI=3.14159, UNITS=1)
C   NOTE: TO CHANGE THE GRID SIZE THE TYPE STATEMENTS MUST BE MODIFIED
C   IN ADDITION TO THE DATA FILE.
C
C   ASSIGN PRINTER, INPUT DATA FILE AND OUTPUT DATA FILE
C   OPEN(3,FILE='LPT1')
C     OPEN(4,FILE='C:\LANG\FORBIN\PROG\PBR.DAT')
      OPEN(4,FILE='PBR.DAT')
      OPEN(3,FILE='PBRRES.DAT')
C   IMPORT GEOMETRY DATA AND CONSTANTS
      READ (4,*)M, N, TBI,PBI,DP,DPCF,DZ,DT,TSTOP
      READ (4,*) (EP(I), I=1,M)
      READ (4,*) (THKCF(I),I=1,N)
      READ (4,*) (R(I), I=1,2*M+1)
C   IMPORT INITIAL GUESS VALUES FOR VARIABLES
      READ (4,*) ((VRO(I,J), I=1,M+1), J=1,N)
      READ (4,*) ((VZO(I,J), I=1,M), J=1,N+1)
      READ (4,*) ((PO(I,J), I=1,M), J=1,N)
      READ (4,*) ((TSO(I,J), I=1,M), J=1,N)
      READ (4,*) ((TGO(I,J), I=1,M), J=1,N)
C   IMPORT TRANSIENT PARAMETERS
      READ (4,*) PBOI,PBOF,TOPT,PDLAY
      READ (4,*) A,B,TOQT,QDLAY
C   INITIZLIZE TIME
      TIME=0.
```

```
      RHOBI=PTDENS(PBI,TBI,UNITS)
      HBI=PTENTH(PBI,TBI,UNITS)
      NN=REAL(N)
      CT=0
      DO 565 TT=1,TSTOP
C     CONSTRUCT THE INITIAL MATRICIES FOR RHOO, HO AND CONTROL VOLUME DV.
C     INITIALIZE MATRICES USED FOR CALCULATING COEFFICIENTS
      DO 200 I=1,M
      DO 100 J=1,N
         IF (I .EQ. 1) TGO(1,J)=TBI
         IF (TT .GT. 1) GOTO 10
         RHOO(I,J)=PTDENS(PO(I,J),TGO(I,J),UNITS)
         HO(I,J)=PTENTH(PO(I,J),TGO(I,J),UNITS)
10       P(I,J)=PO(I,J)
         TS(I,J)=TSO(I,J)
         TG(I,J)=TGO(I,J)
         RHO(I,J)=RHOO(I,J)
         H(I,J)=HO(I,J)
100   CONTINUE
      DV(I)=PI*(R(2*I-1)**2-R(2*I+1)**2)*DZ*EP(I)
200   CONTINUE
      DO 202 I=1,M+1
      DO 201 J=1,N
         VR(I,J)=VRO(I,J)
201   CONTINUE
202   CONTINUE
      DO 204 I=1,M
      DO 203 J=1,N+1
         VZ(I,J)=VZO(I,J)
203   CONTINUE
204   CONTINUE
C     CALCULATE TRANSIENT PARAMETERS
      IF (TIME .GE. PDLAY) THEN
         PTIME=TIME-PDLAY
         ELSE
         PTIME=0.
      ENDIF
      IF (TIME .GE. QDLAY) THEN
         QTIME=TIME-QDLAY
         ELSE
         QTIME=0.
      ENDIF
      WRITE(6,*)'TIME',TIME
      WRITE(6,*)'PTIME',PTIME,'QTIME',QTIME
      IF (PTIME .GT. TOPT) GOTO 206
      IF (TOPT .EQ. 0.) THEN
         PBO=PBOF
         GOTO 206
      ENDIF
      PBO=-(PTIME/TOPT)*(PBOI-PBOF)+PBOI
206   WRITE(6,*)'PBO',PBO
      IF (QTIME .GT. TOQT) GOTO 207
      PWRDEN=A+B*QTIME
```

```
207     WRITE(6,*)'PWR DENSITY',PWRDEN
        DO 220 L=3,M-2
           DO 210 K=1,N
              KK=REAL(K)
              Q(L,K)=PWRDEN*(DV(L)/EP(L))*(COS(2*PI-(1-((2*KK-1)/NN))
     +         *.5886))
210        CONTINUE
220     CONTINUE
C    PERFORM FIRST UPDATE OF SOLID PHASE TEMPERATURE
        CALL ONCNST(TSO,MA,CPBAR,UT,FBAR,KZC)
        CALL SOLID(MA,CPBAR,UT,FBAR,TSO,TGO,PO,RHO,Q,VRO,VZO,KZC,
     +     TSST,UBAR,AV,ANN)
C        CALL RESULT(VR,VZ,PO,RHO,TG,H,TSST)
C    PERFORM GAS PHASE UPDATE
        CALL RADMOM(VR,VRO,VZ,RHO,RHOO,P,TG,BRAF,VRST,BVR,ARF,AWR,
     +     AER,ASR,ANR)
300     CALL AXLMOM(VR,VZ,VZO,RHO,RHOO,P,TG,BZAF,VZST,BVZ,AZF,AWZ,
     +     AEZ,ASZ,ANZ)
C       CALL RESULT(VRST,VZST,P,RHO,TG,H,TS)
500     CALL PRESUR(VRST,VZST,RHO,RHOO,RHST,P,PO,PST,PIO,TG,BZAF,
     +     BRAF,VRSTT,VZSTT)
C        CALL RESULT(VRSTT,VZSTT,PST,RHST,TG,H,TS)
        CALL ENTHLP(VZSTT,VRSTT,RHO,RHOO,RHST,PST,PIO,H,HO,UBAR,TSST,
     +    TGO,ANN,HST,TGST,AV,QIN,TSSTT)
C        CALL RESULT(VRSTT,VZSTT,PST,RHST,TGST,HST,TSSTT)
        CALL PRESII(VRST,VZST,VRSTT,VZSTT,P,PST,PO,TGST,RHOO,
     +     RHST,VRSTTT,VZSTTT,PSTT,RHSTT,BVZ,BVR,ARF,AZF,AWR,
     +     AER,ASR,ANR,AWZ,AEZ,ASZ,ANZ,RHO)
C    HEAT BALANCE CHECK
        QCONV=0.
        HTI=0.
        DO 542 K=3,M-2
        DO 541 L=1,N
           HTI=Q(K,L)+HTI
           QCONV=QCONV+QIN(K,L)
541     CONTINUE
542     CONTINUE
        MAVE=(ABS(VZSTTT(M,1))*RHSTT(M,1)*PI*(R(2*M-1)**2)
     +     +ABS(VZSTTT(1,1))*RHOBI*PI*(R(1)**2-R(3)**2))/2
        HTO=MAVE*(HO(M,1)-HBI)
C     WRITE(3,*)'HEAT BALANCE',HTI,HTO,QCONV
        WRITE(6,*)'HEAT BALANCE',HTI,HTO,QCONV
        WRITE(6,*)QIN(M-2,1),QIN(M-2,3),QIN(M-2,5)
        WRITE(6,*)Q(M-2,1),Q(M-2,3),Q(M-2,5)
        IF (CT .EQ. 20) THEN
        WRITE(3,*)TIME,HTO,QCONV,VZSTTT(M,1)*RHSTT(M,1)*PI*(R(2*M-1)**2
     +     ),TGST(M,1),HTI,TSSTT(M-2,3),TGST(M-2,3)
        CT=1
        ELSE
        CT=CT+1
        ENDIF
        WRITE(6,*)HST(1,3),PST(5,3),PSTT(5,3)
560     CONTINUE
```

```
      TIME=TIME+DT
      DO 563 L=1,M
      DO 561 K=1,N
         VRO(L,K)=VRSTTT(L,K)
         VZO(L,K)=VZSTTT(L,K)
         RHOO(L,K)=RHSTT(L,K)
         PO(L,K)=PSTT(L,K)
         HO(L,K)=HST(L,K)
         TGO(L,K)=TGST(L,K)
         TSO(L,K)=TSSTT(L,K)
561   CONTINUE
563   CONTINUE
565   CONTINUE
600   WRITE(3,9001)
9001  FORMAT('0',6X,'RADIAL VELOCITY')
      WRITE(3,9002)
9002  FORMAT('0',10X,'  1',TR6,'  2',TR6,'  3',TR6,'  4',TR6,'  5',TR6,
     + '  6')
      DO 9004 I=1,M+1
      WRITE(3,9003)I,(VRSTTT(I,J),J=1,N)
9003  FORMAT('0',6X,I2,3X,5(F8.4,3X))
9004  CONTINUE
      WRITE(3,9005)
9005  FORMAT('0',6X,'AXIAL VELOCITY')
      WRITE(3,9002)
      DO 9007 I=1,M
      WRITE(3,9006) I,(VZSTTT(I,J),J=1,N+1)
9006  FORMAT('0',6X,I2,3X,6(F10.4,1X))
9007  CONTINUE
      WRITE(3,9008)
9008  FORMAT('0',6X,'PRESSURE')
      WRITE(3,9020)
9020  FORMAT('0',10X,'   1',TR6,'   2',TR6,'   3',TR6,'   4',TR6,
     + '   5')
      DO 9010 I=1,M
      WRITE(3,9009) I,(PSTT(I,J),J=1,N)
9009  FORMAT('0',6X,I2,3X,1P,6(E11.5,1X))
9010  CONTINUE
      WRITE(3,9011)
9011  FORMAT('0',6X,'DENSITY')
      WRITE(3,9002)
      DO 9013 I=1,M
      WRITE(3,9012) I,(RHSTT(I,J),J=1,N)
9012  FORMAT('0',6X,I2,3X,5(F6.4,3X))
9013  CONTINUE
      WRITE(3,9014)
9014  FORMAT('0',6X,'COOLANT TEMPERATURE')
      WRITE(3,9002)
      DO 9016 I=1,M
      WRITE(3,9015) I,(TGST(I,J),J=1,N)
9015  FORMAT('0',6X,I2,3X,5(F6.1,4X))
9016  CONTINUE
      WRITE(3,9017)
```

```
9017   FORMAT('0',6X,'ENTHALPY')
       WRITE(3,9020)
       DO 9019 I=1,M
       WRITE(3,9018) I,(HST(I,J),J=1,N)
9018   FORMAT('0',6X,I2,3X,1P,5E10.4)
9019   CONTINUE
       WRITE(3,9021)
9021   FORMAT('0',6X,'SOLID TEMPERATURE')
       WRITE(3,9002)
       DO 9022 I=1,M
       WRITE(3,9015)I,(TSSTT(I,J),J=1,N)
9022   CONTINUE
570    STOP
       END
590    SUBROUTINE RESULT(VR,VZ,P,RHO,TG,H,TSST)
       COMMON/GEOTRY/R(45),EP(20),DZ,THKCF(30),DV(20),DP,DPCF,M,N,DT
       COMMON/BOUCON/PBI,PBO,TBI,RHOBI,HBI
       REAL VR(11,10),VZ(10,11),P(10,10),RHO(10,10),TG(10,10),H(10,10)
       REAL R,EP,DZ,THKCF,DV,DP,DPCF,DT,TSST(10,10)
       REAL PBI,PBO,TBI,RHOBI,HBI
       INTEGER I,J,K,L,M,N
600    WRITE(3,9001)
9001   FORMAT('0',6X,'RADIAL VELOCITY')
       WRITE(3,9002)
9002   FORMAT('0',10X,'  1',TR6,'  2',TR6,'  3',TR6,'  4',TR6,'  5',TR6,
     + '  6')
       DO 9004 I=1,M+1
       WRITE(3,9003)I,(VR(I,J),J=1,N)
9003   FORMAT('0',6X,I2,3X,5(F8.4,3X))
9004   CONTINUE
       WRITE(3,9005)
9005   FORMAT('0',6X,'AXIAL VELOCITY')
       WRITE(3,9002)
       DO 9007 I=1,M
       WRITE(3,9006) I,(VZ(I,J),J=1,N+1)
9006   FORMAT('0',6X,I2,3X,6(F10.4,1X))
9007   CONTINUE
       WRITE(3,9008)
9008   FORMAT('0',6X,'PRESSURE')
       WRITE(3,9020)
9020   FORMAT('0',10X,'    1',TR6,'    2',TR6,'    3',TR6,'    4',TR6,
     + '    5')
       DO 9010 I=1,M
       WRITE(3,9009) I,(P(I,J),J=1,N)
9009   FORMAT('0',6X,I2,3X,1P,6(E11.5,1X))
9010   CONTINUE
       WRITE(3,9011)
9011   FORMAT('0',6X,'DENSITY')
       WRITE(3,9002)
       DO 9013 I=1,M
       WRITE(3,9012) I,(RHO(I,J),J=1,N)
9012   FORMAT('0',6X,I2,3X,5(F6.4,3X))
9013   CONTINUE
```

```
      WRITE(3,9014)
9014  FORMAT('0',6X,'COOLANT TEMPERATURE')
      WRITE(3,9002)
      DO 9016 I=1,M
      WRITE(3,9015) I,(TG(I,J),J=1,N)
9015  FORMAT('0',6X,I2,3X,5(F6.1,4X))
9016  CONTINUE
      WRITE(3,9017)
9017  FORMAT('0',6X,'ENTHALPY')
      WRITE(3,9020)
      DO 9019 I=1,M
      WRITE(3,9018) I,(H(I,J),J=1,N)
9018  FORMAT('0',6X,I2,3X,1P,5E10.4)
9019  CONTINUE
      WRITE(3,9021)
9021  FORMAT('0',6X,'SOLID TEMPERATURE')
      WRITE(3,9002)
      DO 9022 I=1,M
      WRITE(3,9015)I,(TSST(I,J),J=1,N)
9022  CONTINUE
      RETURN
      END
C
C   SUBROUTINE TO CALCULATE CONSTANTS USED IN EVALUATION OF SOLID PHASE
C   TEMPERATURES
C
      SUBROUTINE ONCNST(TSO,MA,CPBAR,UT,FBAR,KZC)
C
      COMMON/GEOTRY/R(45),EP(20),DZ,THKCF(30),DV(20),DP,DPCF,M,N,DT
      REAL MAZ,RHZC,MACI,RHCI,MACII,RHCII,MAF,RHF,MA(10),CPZ,CPCI
      REAL CPCII,CPF,UZC(10,10),UCI(10,10),UCII(10,10),UF(10,10)
      REAL KZC(10,10),KCI(10,10),KF(10,10),PI
      REAL CPBAR(10),UT(10,10),FONE(10,10),FTWO(10,10),FTHR(10,10)
      REAL FBAR(10,10),TSO(10,10)
      REAL PR1,PR2,PR3,PR4
      PARAMETER (PI=3.14159,PR1=.000250,PR2=.0002,PR3=.00015)
      PARAMETER (PR4=.000117,RHZC=6300.,RHCI=1900.,RHCII=1000.)
      PARAMETER (RHF=10500.,CPZ=200.,CPCI=3000.,CPCII=3000.,CPF=200.)
      PARAMETER (KZC=40.,KCI=3.0,KCII=1.5,KF=30.)
C
      DO 60 I=2,M-1
C   CALCULATE MASS PER UNIT OUTSIDE SURFACE AREA
      MAZ=(PR1**3-PR2**3)*RHZC/(3*(PR1**2))
      MACI=(PR2**3-PR3**3)*RHCI/(3*(PR1**2))
      MACII=(PR3**3-PR4**3)*RHCII/(3*(PR1**2))
      MAF=(PR4**3)*RHF/(3*(PR1**2))
      MA(I)=MAZ+MACI+MACII+MAF
      IF (I .EQ. 2) MA(2)=.0072
      IF (I .EQ. M-1) MA(M-1)=5.73
C
C   CALCULATE AVERAGE SPECIFIC HEAT
      CPBAR(I)=((MAZ*CPZ+MACI*CPCI+MACII*CPCII+MAF*CPF)/MA(I))
      IF (I .EQ. 2) CPBAR(2)=422.
```

```
      IF (I .EQ. M-1) CPBAR(M-1)=155.
C
      DO 50 J=1,N
         KF(I,J)=1.7307*26.0*(AMAX1(TSO(I,J)*1.8-459.67,260.0))
     +       **(-0.1093)
         KZC(I,J)=22.67+.00867*TSO(I,J)
         KCI(I,J)=AMAX1(1.7307*(179.1-19.7*ALOG(1.8*TSO(I,J)
     +       -459.67)),10.0)
         IF (I .EQ. 2) THEN
            UT(2,J)=1.
            FBAR(2,J)=1.
            KZC(2,J)=15.
            GOTO 50
         ENDIF
         IF (I .EQ. M-1) THEN
            UT(M-1,J)=1.
            FBAR(M-1,J)=1.
            KZC(M-1,J)=47.
            GOTO 50
         ENDIF
C    CALCULATE INTERNAL PARTICLE HEAT TRANSFER COEFFICIENTS
         UZC(I,J)=(PR2*PR1/(PR1-PR2))*KZC(I,J)/(PR1**2)
         UCI(I,J)=(PR3*PR2/(PR2-PR3))*KCI(I,J)/(PR1**2)
         UCII(I,J)=(PR4*PR3/(PR3-PR4))*KCI(I,J)/(PR1**2)
         UF(I,J)=(2*KF(I,J))/(3*PR4)
         UT(I,J)=((1/UZC(I,J))+(1/UCI(I,J))+(1/UCII(I,J))
     +       +(1/UF(I,J)))**(-1)
C
C    CALCULATE THE SINGLE NODE FRACTIONS FOR TEMPERATURE DISTRIBUTION
         FONE(I,J)=UT(I,J)/UZC(I,J)
         FTWO(I,J)=FONE(I,J)+(UT(I,J)/UCI(I,J))
         FTHR(I,J)=FTWO(I,J)+(UT(I,J)/UCII(I,J))
         FBAR(I,J)=(1/(2*MA(I)*CPBAR(I)))*((MAZ*CPZ*FONE(I,J))
     +    +(MACI*CPCI*(FONE(I,J)+FTWO(I,J)))
     +    +(MACII*CPCII*(FTHR(I,J)+FTWO(I,J)))+(MAF*CPF
     +    *(FTHR(I,J)+1)))
50       CONTINUE
60    CONTINUE
C    THE FOLLOWING MATERIAL PROPERTIES ARE ASSUMED FOR THE COLD FRIT
C       DENSITY=7.95 E03 kg/m**3
C       SPECIFIC HEAT=422 J/kg K
C       CONDUCTIVITY=15 W/m K
C    THE FOLLOWING MATERIAL PROPERTIES ARE ASSUMED FOR THE HOT FRIT
C       DENSITY=2.10 E04 kg/m**3
C       SPECIFIC HEAT=155 J/kg K
C       CONDUCTIVITY=47 W/m K
       RETURN
       END
```

```
C
C   SUBROUTINE TO ADVANCE SOLID PHASE TEMPERATURES ONE TIME STEP
C
      SUBROUTINE SOLID(MA,CPBAR,UT,FBAR,TSO,TGO,PO,RHO,Q,VRO,VZO,
     + KZC,TSST,UBAR,AV,ANN)
      COMMON/GEOTRY/R(45),EP(20),DZ,THKCF(30),DV(20),DP,DPCF,M,N,DT
      COMMON/BOUCON/PBI,PBO,TBI,RHOBI,HBI
      COMMON/SOLVER/SOLSLD(100,100)
      INTEGER I,J,K,M,N,UNITS
      REAL KG(10,10),KAP(10,10),PHI,PHII,PH,KEO,KRO,EMM,EDP
      REAL DP,DPCF,KR,RE,THI,THII,CTHI,CTHII,MA(10),CPBAR(10)
      REAL UT(10,10)
      REAL FBAR(10,10),TSO(10,10),TSST(10,10),TGO(10,10),KSOL(10,10)
      REAL AV(10),EP,VIS,GSO,FJH,TFLM,CPB,CPFLM,VISFLM,KFLM
      REAL HLOC(10,10),PO(10,10),Q(10,10),VRO(11,10),VZO(10,11)
      REAL KW(10,10),KE(10,10),KS(10,10),KN(10,10)
      REAL ACW(10,10),ACE(10,10),ACN(10,10),ACS(10,10),ACO(10,10)
      REAL CONVC(100),BC(10,10),UBAR(10,10),KZ,RHO(10,10)
      REAL ANN(10,10),KZC(10,10)
      PARAMETER (PI=3.14159,UNITS=1,EMM=.78)
C   INITIALIZE THE SOLUTION MATRIX
      DO 2 I=1,M*N
         DO 1 J=1,M*N
            SOLSLD(I,J)=0.
1        CONTINUE
2     CONTINUE
C
C   CALCULATE GAS AND SOLID CONDUCTIVITIES
      THI=.68
      CTHI=.565
      THII=.144
      CTHII=.925
      DO 20 I=2,M-1
         DO 10 J=1,N
C   CALCULATE THE GAS PHASE CONDUCTIVITY
           KG(I,J)=PTCOND(PO(I,J),TGO(I,J),UNITS)
C   CALCULATE THE THERMAL CONDUCTIVITY IN THE SOLID
           KZ=KZC(I,J)
           IF (I .EQ. M-1) THEN
              KEO=KZ
              GOTO 5
           ENDIF
           KAP(I,J)=KZ/KG(I,J)
           PHI=.5*((((KAP(I,J)-1)/KAP(I,J))**2)*THI)/(ALOG(KAP(I,J)
     +     -((KAP(I,J)-1)*CTHI))-(KAP(I,J)-1)*(1-CTHI)/KAP(I,J))
     +     -(2/3)*(1/(KAP(I,J)))
           PHII=.5*((((KAP(I,J)-1)/KAP(I,J))**2)*THII)/(ALOG(KAP(I,J)
     +     -((KAP(I,J)-1)*CTHII))-(KAP(I,J)-1)*(1-CTHII)/KAP(I,J))
     +     -(2/3)*(1/(KAP(I,J)))
           PH=PHII+((PHI-PHII)*(EP(I)-.260)/.216)
           KEO=KG(I,J)*(EP(I)+((1-EP(I))/(PH+((2/3)*KAP(I,J)))))
5          IF (I .EQ. 2) THEN
```

```
                EDP=DPCF                ELSE
                EDP=DP
              ENDIF
C     CALCULATE THE RADIATION CONTRIBUTION TO SOLID CONDUCTIVITY
              KRO=0.229*EMM*EP(I)*EDP*(TSO(I,J)**3)/(10**6)
              KR=(1-EP(I))/((1/KZ)+(1/KRO))+EP(I)*KRO
C     COMBINE THERMAL AND RADIATION CONDUCTIVITIES TO GET OVERALL VALUE
              KSOL(I,J)=KEO+KR
C     CALCULATE HEAT TRANSFER COEFFICIENT FOR SOLID TO GAS HEAT TRANSFER
C     CALCULATE THE RE
              AV(I)=3*(1-EP(I))/(EDP/2)
              IF (I .EQ. M-1) AV(M-1)=3659.
              VIS=PTVISC(PO(I,J),TGO(I,J),UNITS)
              GSO=SQRT(AMAX1(ABS(((VRO(I,J)+VRO(I+1,J))/2)**2)+ABS(((
     +        VZO(I,J)+VZO(I,J+1))/2)**2),.00001))*RHO(I,J)
              RE=GSO/(AV(I)*VIS)
C     DETERMINE RELATION FOR THE COULBURN FACTOR ON THE RE
              IF (RE .LT. 50.) THEN
                 FJH=0.91*(RE**(-.51))
                 ELSE
                 FJH=0.61*(RE**(-.41))
              ENDIF
              TFLM=.5*(TSO(I,J)+TGO(I,J))
              CPB=PTCP(PO(I,J),TGO(I,J),UNITS)
              CPFLM=PTCP(PO(I,J),TFLM,UNITS)
              VISFLM=PTVISC(PO(I,J),TFLM,UNITS)
              KFLM=PTCOND(PO(I,J),TFLM,UNITS)
              HLOC(I,J)=FJH*CPB*GSO/(((CPFLM*VISFLM)/KFLM)**(2/3))
C     CALCULATE UBAR
C     UBAR FOR THE FRITS IS ASSUMED TO BE EQUAL TO HLOC
              IF (I .EQ. 2) THEN
                UBAR(2,J)=HLOC(2,J)
                GOTO 9
              ENDIF
              IF (I .EQ. M-1) THEN
                UBAR(M-1,J)=HLOC(M-1,J)
                GOTO 9
              ENDIF
              UBAR(I,J)=UT(I,J)*HLOC(I,J)/(FBAR(I,J)*HLOC(I,J)+UT(I,J))
              IF (I .EQ. 2) UBAR(2,J)=HLOC(I,J)
9       CONTINUE
C        WRITE(3,*)I,KSOL(I,J),KRO,KR,KEO,HLOC(I,J),UBAR(I,J),
C       +  AV(I),RE,PHI,PHII,PH,GSO
10         CONTINUE
20      CONTINUE
C     CALCULATE EAST AND WEST FACE CONDUCTORS AND COEFFICIENTS BASED ON
C     THE HARMONIC MEAN OF THE CONDUCTIVITIES ON EITHER SIDE OF THE
C     INTERFACE
         DO 40 I=2,M-1
            DO 30 J=2,N
              KW(I,J)=2*KSOL(I,J)*KSOL(I,J-1)/(KSOL(I,J)+KSOL(I,J-1))
              KE(I,J-1)=KW(I,J)
              ACW(I,J)=KW(I,J)*(R(2*I-1)**2-R(2*I+1)**2)*PI/DZ
```

```
            ACE(I,J-1)=ACW(I,J)
30          CONTINUE
            KW(I,1)=0.
            ACW(I,1)=0.
            KE(I,N)=0.
            ACE(I,N)=0.
40        CONTINUE
C     CALCULATE NORTH AND SOUTH FACE CONDUCTANCES AND COEFFICIENTS
C     BASED ON THE HARMONIC MEAN CONDUCTIVITY
          DO 60 J=1,N
             DO 50 I=3,M-1
               F=(R(2*I-2)-R(2*I-1))/(R(2*I-2)-R(2*I))
               KS(I,J)=(((1-F)/KSOL(I,J))+(F/KSOL(I-1,J)))**(-1)
               KN(I-1,J)=KS(I,J)
               ACS(I,J)=KS(I,J)*2*PI*R(2*I-1)*DZ/(R(2*I-2)-R(2*I))
               ACN(I-1,J)=ACS(I,J)
50           CONTINUE
             KS(2,J)=0.
             ACS(2,J)=0.
             KN(M-1,J)=0.
             ACN(M-1,J)=0.
60        CONTINUE

C     CALCULATE THE CENTRAL POINT COEFFICIENT
          DO 80 I=2,M-1
             DO 70 J=1,N
               ACO(I,J)=-(ACW(I,J)+ACE(I,J)+ACS(I,J)+ACN(I,J))
C     CALCULATE TIME DERIVATIVE COEFFICIENT
               BC(I,J)=MA(I)*CPBAR(I)*DV(I)*AV(I)/(DT*EP(I))
               ANN(I,J)=(BC(I,J)-ACO(I,J)+UBAR(I,J)*(DV(I)/EP(I))*AV(I))
70           CONTINUE
80        CONTINUE
C     BUILD THE SOLUTION MATRIX AND CONSTANT VECTOR
          DO 100 I=2,M-1
             DO 90 J=1,N
               K=(I-2)*N+J
               SOLSLD(K,K)=-ANN(I,J)
               IF (J .LT. N) SOLSLD(K,K+1)=ACE(I,J)
               IF (K+N .LE. (M-2)*N) SOLSLD(K,K+N)=ACN(I,J)
               IF (J .GT. 1) SOLSLD(K,K-1)=ACW(I,J)
               IF (K-N .GT. 0) SOLSLD(K,K-N)=ACS(I,J)
               CONVC(K)=-Q(I,J)-UBAR(I,J)*(DV(I)/EP(I))*AV(I)*TGO(I,J)
     +           -BC(I,J)*TSO(I,J)
90           CONTINUE
100       CONTINUE
C     CALL SOLUTION ROUTINES
          NP=100
          CALL LUDCMP(SOLSLD,((M-2)*N),NP,INDX,D)
          CALL LUBKSB(SOLSLD,((M-2)*N),NP,INDX,CONVC)
C     UPDATE THE SOLID PHASE TEMPERATURES
          I=2
          J=1
          DO 110 K=1,((M-2)*N)
```

```
            TSST(I,J)=CONVC(K)
            IF ((K-(I-2)*N) .EQ. N) THEN
               J=1
               I=I+1
               ELSE
               J=J+1
            ENDIF
110      CONTINUE
         TMCON1=MA(3)*CPBAR(3)/UBAR(3,1)
         TMCON2=MA(3)*CPBAR(3)/UBAR(M-2,3)
         WRITE(6,*)'TMCON1',TMCON1,'TMCON2',TMCON2
         RETURN
         END


C    SUBROUTINE TO PERFORM THE AXIAL MOMENTUM BALANCE
C
         SUBROUTINE AXLMOM(VR,VZ,VZO,RHO,RHOO,P,TG,BZAF,VZST,BVZ,AZF,
     + AWZ,AEZ,ASZ,ANZ)
         COMMON/GEOTRY/R(45),EP(20),DZ,THKCF(30),DV(20),DP,DPCF,M,N,DT
         COMMON/BOUCON/PBI,PBO,TBI,RHOBI,HBI
         COMMON/SOLVER/SOLZ(100,100)
         INTEGER M,N,I,J,K,UNITS
         REAL VR(11,10),VZ(10,11),R,EP,RHO(10,10),P(10,10),TG(10,10)
         REAL MEZ(10,11),MWZ(10,11),MNZ(10,11),MSZ(10,11),VZST(10,11)
         REAL AEZ(10,11),AWZ(10,11),ANZ(10,11),ASZ(10,11),AOZ(10,11)
         REAL BZ(10,11),ALF,ALFB,ALFC,ALFD,GAM,GAMB,GAMC,SZ(10,11)
         REAL DT,DZ,VSR,THKCF,DVZ,SOLZ,CONVZ(100),BZAF(10,11),ARI,ARO
         REAL FRIC(10,11),REI,REO,VISI,VISO,HDI,HDO,BVZ(10,11),AZF(10,11)
         REAL VZO(10,11),RHOO(10,10),BZO(10,11),RHOOS
         PARAMETER (PI=3.14159, UNITS=1)
C    INITIALIZE THE COEFFICIENT MATRIX
         DO 8 I=1,M*N
            DO 4 J=1,N*M
              SOLZ(I,J)=0.
4           CONTINUE
8        CONTINUE
C    GENERAL FORM OF THE EQUATION:
C    -(BZ-AOZ)*VZ0 + AEZ*VZE + AWZ*VZW + ANZ*VNZ + ASZ*VZS = -SZ - BZ*VR
C
C    CALCULATE CONTROL VOLUME FACE MASS FLUXES AND VELOCITY COEFFICIENTS
C
C    SOUTH AND NORTH
         DO 16 J=2,N
            DO 12 I=2,M
C    UPWIND FACTORS FOR DENSITY
              IF (VR(I,J-1) .GE. 0.) THEN
                ALFB=0.5
                ELSE
                ALFB=-0.5
              ENDIF
              IF (VR(I,J) .GE. 0.) THEN
                ALFC=0.5
```

```
              ELSE
              ALFC=-0.5
            ENDIF
C   FACE FLUX
            MSZ(I,J)=(((0.5+ALFB)*RHO(I-1,J-1)+(0.5-ALFB)*RHO(I,J-1))
     +        *VR(I,J-1)+((0.5+ALFC)*RHO(I-1,J)+(0.5-ALFC)*RHO(I,J))
     +        *VR(I,J))*PI*R(2*I-1)*(DZ)
            MNZ(I-1,J)= MSZ(I,J)
C   UPWIND FACTOR FOR MOMENTUM
            IF ((VR(I,J-1)+VR(I,J)) .GE. 0.) THEN
              ALFD=0.5
              ELSE
              ALFD=-0.5
            ENDIF
C   VELOCITY COEFFICIENT
            ASZ(I,J)=MSZ(I,J)*(0.5+ALFD)
            ANZ(I-1,J)=-MNZ(I-1,J)*(0.5-ALFD)
12      CONTINUE
C   BOUNDARY CONDITIONS
        MSZ(1,J)=0.
        ASZ(1,J)=0.
        MNZ(M,J)=0.
        ANZ(M,J)=0.
16      CONTINUE
        MSZ(1,1)=0
        ASZ(1,1)=0
        IF (VR(2,1) .GE. 0.) THEN
          ALFC=0.5
          ELSE
          ALFC=-0.5
        ENDIF
        MNZ(1,1)=((0.5+ALFC)*RHO(1,1)+(0.5-ALFC)*RHO(2,1))*VR(2,1)*PI
     + *(DZ)*R(3)
        ANZ(1,1)=-MNZ(1,1)*(0.5-ALFC)
        IF (VR(M,1) .GE. 0.) THEN
          ALFC=0.5
        ELSE
          ALFC=-0.5
        ENDIF
        MSZ(M,1)=((0.5+ALFC)*RHO(M-1,1)+(0.5-ALFC)*RHO(M,1))*VR(M,1)
     +     *PI*R(2*M-1)*(DZ)
C   EAST AND WEST FACE FLUXES AND COEFFICIENTS
        DO 28 I=1,M
            DO 24 J=2,N
              MWZ(I,J)=RHO(I,J-1)*((VZ(I,J-1)+VZ(I,J))/2)*(R(2*I-1)**2
     +         -R(2*I+1)**2)*PI
              MEZ(I,J-1)=MWZ(I,J)
C   UPWIND FACTOR FOR MOMENTUM
              IF ((VZ(I,J)+VZ(I-1,J)) .GE. 0.) THEN
                GAMB=0.5
                ELSE
                GAMB=-0.5
              ENDIF
```

```
C   VELOCITY COEFFICIENT
              AWZ(I,J)=MWZ(I,J)*(0.5+GAMB)
              AEZ(I,J-1)=-MEZ(I,J-1)*(0.5-GAMB)
24          CONTINUE
28        CONTINUE
C   BOUNDARY CONDITIONS
          DO 29 I=2,M-1
             IF (VR(I,1) .GE. 0.) THEN
               ALFC=0.5
               ELSE
               ALFC=-0.5
             ENDIF
             MSZ(I,1)=((0.5+ALFC)*RHO(I-1,1)+(0.5-ALFC)*RHO(I,1))
     +        *VR(I,1)*PI*R(2*I-1)*DZ
             MNZ(I-1,1)=MSZ(I,1)
             ASZ(I,1)=MSZ(I,1)*(0.5+ALFC)
             ANZ(I-1,1)=-MNZ(I-1,1)*(0.5-ALFC)
             MWZ(I,1)=0.
             AWZ(I,1)=0.
29        CONTINUE
C   BOUNDARY FLUXES AND COEFFICIENTS
C   EAST FACES NOT CO-LOCATED WITH WEST FACES
          DO 32 I=1,M
             MEZ(I,N)=RHO(I,N)*(VZ(I,N)/2)*PI*(R(2*I-1)**2-R(2*I+1)
     +        **2)
             IF (VZ(I,N) .GE. 0.) THEN
               AEZ(I,N)=0.
               ELSE
               AEZ(I,N)=-MEZ(I,N)
             ENDIF
32        CONTINUE
C   INLET AND OUTLET TO PLENUMS
          MWZ(1,1)=RHOBI*VZ(1,1)*(R(1)**2-R(3)**2)*PI
          MWZ(M,1)=RHO(M,1)*VZ(M,1)*(R(2*M-1)**2)*PI
          AWZ(1,1)=0.
          AWZ(M,1)=0.
C   CALCULATE NODE CENTRAL POINT COEFFICIENT
          DO 44 I=1,M
             DO 40 J=1,N
               AOZ(I,J)=-(AEZ(I,J)+AWZ(I,J)+ANZ(I,J)+ASZ(I,J)+MEZ(I,J)
     +          -MWZ(I,J)+MNZ(I,J)-MSZ(I,J))
40           CONTINUE
44        CONTINUE
C   CALCULATE CONSTANT TERMS
          DO 52 J=2,N
             DO 48 I=1,M
C   UPWIND FACTOR FOR DENSITY
               IF (VZ(I,J) .GE. 0.) THEN
                 GAM=0.5
                 ELSE
                 GAM=-0.5
               ENDIF
               RHOS=(0.5+GAM)*RHO(I,J-1)+(0.5-GAM)*RHO(I,J)
```

```
            RHOOS=(0.5+GAM)*RHOO(I,J-1)+(0.5-GAM)*RHOO(I,J)
            DVZ=PI*(R(2*I-1)**2-R(2*I+1)**2)*DZ
            BZ(I,J)=RHOS*DVZ*EP(I)/DT
            BZO(I,J)=RHOOS*DVZ*EP(I)/DT
            BVZ(I,J)=DVZ*EP(I)/DT
C   SUPERFICIAL VELOCITY
            VZS=(((.25*(VR(I+1,J)+VR(I+1,J-1)+VR(I,J)+VR(I,J-1)))**2
     +       +VZ(I,J)**2)**0.5)
C   CORRECTION FOR COLD FRIT VARIABLE THICKNESS
            IF (I .EQ. 2) DVZ=(THKCF(J)+THKCF(J-1))*PI*R(2*I)*DZ
C   SOURCE TERM
            SORC=(P(I,J-1)-P(I,J))*(DVZ/DZ)*EP(I)
C   FRICTION TERM
            PS=(0.5+GAM)*P(I,J-1)+(0.5-GAM)*P(I,J)
            TS=(0.5+GAM)*TG(I,J-1)+(0.5-GAM)*TG(I,J)
            VIS=PTVISC(PS,TS,UNITS)
            IF (I .EQ. 2 .OR. I .EQ. (M-1)) THEN
              DPA=DPCF
              ELSE
              DPA=DP
            ENDIF
            FRIC(I,J)=DVZ*((150*VIS*((1-EP(I))**2)/((DPA**2)*
     +        (EP(I)**3)))+(1.75*RHOS*ABS(VZS)*(1-EP(I))/(DPA*
     +       (EP(I)**3))))*EP(I)
            SZ(I,J)=SORC
C            WRITE(3,*)I,J,DPA,EP(I),DVZ
C            WRITE(3,*)SORC,VZS,VZSUP,VIS
48          CONTINUE
52       CONTINUE
C   INLET AND OUTLET PLENUMS
C   SOURCE TERMS
      ARI=PI*(R(1)**2-R(3)**2)
      ARO=PI*(R(2*M-1)**2)
      SZ(1,1)=(PBI-P(1,1))*ARI
      SZ(M,1)=(PBO-P(M,1))*ARO
      BZ(1,1)=RHOBI*ARI*DZ/DT
      BZO(1,1)=BZ(1,1)
      BZ(M,1)=RHO(M,1)*ARO*DZ/DT
      BZO(M,1)=RHOO(M,1)*ARO*DZ/DT
      BVZ(1,1)=BZ(1,1)/RHOBI
      BVZ(M,1)=BZ(M,1)/RHO(M,1)
C   FRICTIONAL LOSSES IN THE PLENUMS
C   CALCULATE HDI, HDO, THE HYDRAULIC DIAMETERS
      HDI=2*(R(1)-R(3))
      HDO=2*R(2*M-1)
C   CALCULATE REYNOLDS NUMBERS, UPWINDING OF DENSITIES CONSIDERED
C   UNNECESSARY
      DO 53 J=1,N
         VISI=PTVISC(P(1,J),TG(1,J),UNITS)
         REI=RHO(1,J)*ABS(VZ(1,J))*HDI/VISI
         VISO=PTVISC(P(M,J),TG(M,J),UNITS)
         REO=RHO(M,J)*ABS(VZ(M,J))*HDO/VISO
C   CALCULATE FRICTION FORCE USING ACURVE FITTED TO THE MOODY DIAGRAM
```

```
C   FOR FRICTION FACTOR CALCULATIONS
          IF (REI .LT. 1000.) THEN
            FRIC(1,J)=.0482*RHO(1,J)*DZ*ARI/(2*HDI)
            GOTO 531
          ENDIF
          FRIC(1,J)=.138*(REI**(-.151))*RHO(1,J)*DZ*ARI*ABS(VZ(1,J))
     +       /(2*HDI)
531       IF (REO .LT. 1000.) THEN
            FRIC(M,J)=.0482*RHO(M,J)*DZ*ARO/(2*HDO)
            GOTO 53
          ENDIF
          FRIC(M,J)=.138*(REO**(-.151))*RHO(M,J)*DZ*ARO*ABS(VZ(M,J))
     +      /(2*HDO)
53      CONTINUE
        DO 55 I=1,M
           DO 54 J=2,N
             BZAF(I,J)=BZ(I,J)-AOZ(I,J)+FRIC(I,J)
             AZF(I,J)=-(BZAF(I,J)-BZ(I,J))
C            WRITE(3,*) BZ(I,J),FRIC(I,J),BZAF(I,J)
54         CONTINUE
55      CONTINUE
        BZAF(1,1)=BZ(1,1)-AOZ(1,1)+FRIC(1,1)
        BZAF(M,1)=BZ(M,1)-AOZ(M,1)+FRIC(M,1)
        AZF(1,1)=-(BZAF(1,1)-BZ(1,1))
        AZF(M,1)=-(BZAF(M,1)-BZ(M,1))
C        WRITE(3,*)BZAF(1,1),BZ(1,1),SZ(1,1),FRIC(1,1)
C        WRITE(3,*)BZAF(M,1),BZ(M,1),SZ(M,1),FRIC(M,1)
C   FORCE WALL VZ TO ZERO
        DO 56 I=2,M-1
           SZ(I,1)=0.
           RHOS=RHO(I,1)
           RHOOS=RHOO(I,1)
           DVZ=PI*(R(2*I-1)**2-R(2*I+1)**2)*DZ
           BZ(I,1)=RHOS*(DVZ/2)*EP(I)/DT
           BZO(I,1)=RHOOS*(DVZ/2)*EP(I)/DT
           BVZ(I,1)=DVZ*EP(I)/(2*DT)
           VZS=.5*(VR(I,1)+VR(I+1,1))
           DPA=DPCF
           FRIC(I,1)=DVZ*((150*VIS*((1-EP(I))**2)/((DPA**2)*
     +        (EP(I)**3)))+(1.75*RHOS*ABS(VZS)*(1-EP(I))/(DPA*
     +        (EP(I)**3))))*EP(I)
           BZAF(I,1)=(BZ(I,1)-AOZ(I,1)+FRIC(I,1))
           AZF(I,1)=AOZ(I,1)-FRIC(I,1)
56      CONTINUE
C   CONSTRUCT THE SOLUTION MATRIX AND CONSTANT VECTOR
C   ENTERING THE MANIFOLD TURNING COEFFICIENT FOR THE INLET AND
C   OUTLET PLENUMS
        CTD=1.05
        CTC=2.66
        DO 64 J=1,N
           SOLZ(J,J)=-(BZ(1,J)-(CTD*AOZ(1,J))+FRIC(1,J))
           IF (J .LT. N) SOLZ(J,J+1)=CTD*AEZ(1,J)
```

```
            IF (J .GT. 1) SOLZ(J,J-1)=CTD*AWZ(1,J)
            SOLZ(J,J+N)=ANZ(1,J)
            CONVZ(J)=-SZ(1,J)-(BZO(1,J)*VZO(1,J))
            DO 60 I=2,M-1
              K=(I-1)*N+J
              SOLZ(K,K)=-BZAF(I,J)
              IF (J .LT. N) SOLZ(K,K+1)=AEZ(I,J)
              IF (K+N .LE. ((M-2)*N)) SOLZ(K,K+N)=ANZ(I,J)
              IF (J .GT. 1) SOLZ(K,K-1)=AWZ(I,J)
              IF (K-N .GT. 0) SOLZ(K,K-N)=ASZ(I,J)
              CONVZ(K)=-SZ(I,J)-(BZO(I,J)*VZO(I,J))
60          CONTINUE
64        CONTINUE
C     SKIP OVER HOT FRIT SINCE THERE IS NO AXIAL MOTION AND THIS WOULD
C     RESULT IN A SOLUTION MATRIX WITH A ROW OF ZEROS WHICH IS
C     INCOMPATIBLE WITH THE SOLUTION METHOD USED.
          DO 65 J=1,N
             K=(M-1)*N+J
             SOLZ(K,K)=-(BZ(M,J)-(CTC*AOZ(M,J))+FRIC(M,J))
             IF (J .LT. N) SOLZ(K,K+1)=AEZ(M,J)*CTC
             IF (J .GT. 1) SOLZ(K,K-1)=AWZ(M,J)*CTC
             CONVZ(K)=-SZ(M,J)-(BZO(M,J)*VZO(M,J))
65        CONTINUE
          NP=100
          DO 66 K=1,45
C              WRITE(3,*) K,SOLZ(K,K)
66        CONTINUE
C     CALL SOLUTION SUBROUTINES
C     NOTE THET THE UPDATED VELOCITIES ARE RETURNED AS A MODIFIED CONVZ
C     VECTOR
          CALL LUDCMP(SOLZ,(M*N),NP,INDX,D)
          CALL LUBKSB(SOLZ,(M*N),NP,INDX,CONVZ)
C     CONVERT CONVZ TO I,J FORM
          I=1
          J=1
          DO 68 K=1,(M*N)
          '    VZST(I,J)=CONVZ(K)
             IF((K-(I-1)*N) .EQ. N) THEN
                J=1
                I=I+1
                ELSE
                J=J+1
              ENDIF
68         CONTINUE
C     CORRECTIONS TO CONSTANTS USED IN LATER PARTS OF THE PROGRAM TO
C     REFLECT THE TURNING COEFFICIENTS
         DO 69 J=1,N
            AZF(1,J)=AOZ(1,J)*CTD-FRIC(1,J)
            AZF(M,J)=AOZ(M,J)*CTC-FRIC(M,J)
            BZAF(1,J)=(BZ(1,J)-(AOZ(1,J)*CTD)+FRIC(1,J))
            BZAF(M,J)=(BZ(M,J)-(AOZ(M,J)*CTC)+FRIC(M,J))
            AEZ(1,J)=AEZ(1,J)*CTD
            AWZ(1,J)=AWZ(1,J)*CTD
```

```
        AEZ(M,J)=AEZ(M,J)*CTC
        AWZ(M,J)=AWZ(M,J)*CTC
69    CONTINUE
      RETURN
      END


C     SUBROUTINE TO PERFORM THE RADIAL MOMENTUM BALANCE
C
C     MODIFIED TO WORK IN SUPERFICIAL VELOCITIES
C
        SUBROUTINE RADMOM(VR,VRO,VZ,RHO,RHOO,P,TG,BRAF,VRST,BVR,
     + ARF,AWR,AER,ASR,ANR)
        COMMON/GEOTRY/R(45),EP(20),DZ,THKCF(30),DV(20),DP,DPCF,M,N,DT
        COMMON/BOUCON/PBI,PBO,TBI,RHOBI,HBI
        COMMON/SOLVER/SOLR(100,100)
        INTEGER M,N,I,J,K,UNITS
        REAL VR(11,10),VZ(10,11),R,EP,RHO(10,10),P(10,10),TG(10,10)
        REAL MER(11,10),MWR(11,10),MNR(11,10),MSR(11,10),VRST(11,10)
        REAL AER(11,10),AWR(11,10),ANR(11,10),ASR(11,10)
        REAL AOR(11,10),BR(11,10),ALF,ALFB,ALFC,ALFD,GAM,GAMB,GAMC
        REAL SR(11,10),FRIC,BRAF(11,10),BVR(11,10),ARF(11,10)
        REAL DT,DZ,VSR,THKCF,DV,SOLR,CONVR(100)
        REAL VRO(11,10),RHOO(10,10),BRO(11,10),RHOOS
        PARAMETER (PI=3.14159, UNITS=1)
C
C     GENERAL FORM OF THE EQUATION:
C     -(BR-AOR)*VRO + AER*VRE + AWR*VRW + ANR*VRN + ASR*VRS = -S - BR*VR
C
C     CALCULATE CONTROL VOLUME FACE MASS FLUXES AND VELOCITY COEFFICIENTS
C
C     INITIALIZE SOLR
        DO 2 I=1,M
          DO 1 J=1,N
            SOLR(I,J)=0
1         CONTINUE
2     ' CONTINUE
C     SOUTH AND NORTH
        DO 10 I=2,M
          DO 8 J=1,N
C     SOUTH
C     ESTIMATE VELOCITY AT THE INTERFACE USING:
C     VRi*AREAi=VR*(R(2I-1)/R(2I-2))*R(2I-2)*2*PI*DZ
            MSR(I,J)=RHO(I-1,J)*VR(I,J)*R(2*I-1)*2*PI*
     +      DZ
C     NORTH
7           MNR(I-1,J)=MSR(I,J)
            IF ((VR(I,J)+VR(I-1,J)) .GE. 0.) THEN
              ALFB=0.5
              ELSE
              ALFB=-0.5
            ENDIF
C COEFFICIENTS
```

```
            ASR(I,J)=MSR(I,J)*(.5+ALFB)
            ANR(I-1,J)=-MNR(I-1,J)*(.5-ALFB)
8         CONTINUE
10      CONTINUE
C    BOUNDARIES
        DO 12 J=1,N
           MNR(M,J)=RHO(M,J)*VR(M,J)*2*PI*R(2*M)*DZ
           ANR(M,J)=0.0
12      CONTINUE
C    EAST AND WEST
        DO 20 I=2,M
           DO 18 J=2,N
C    FLUX UPWIND FACTORS
             IF (VZ(I,J) .GE. 0.) THEN
               GAMB=0.5
               ELSE
                  GAMB=-0.5
             ENDIF
             IF (VZ(I-1,J) .GE. 0.) THEN
               GAMC=0.5
               ELSE
               GAMC=-0.5
             ENDIF
C    WEST FACE FLUX
             MWR(I,J)=((.5+GAMB)*RHO(I,J-1)+(.5-GAMB)*RHO(I,J))*VZ(I,J)
     +       *PI*(R(2*I-1)**2-R(2*I)**2)+((.5+GAMC)*RHO(I-1,J-1)+
     +       (0.5-GAMC)*RHO(I-1,J))*VZ(I-1,J)*PI*(R(2*I-2)**2-R(2*I-1)
     +       **2)
C    EAST FACE FLUX
             MER(I,J-1)=MWR(I,J)
C    MOMENTUM UPWIND
             IF ((VZ(I-1,J)+VZ(I,J)) .GE. 0.) THEN
               GAMBC=0.5
               ELSE
               GAMBC=-0.5
             ENDIF
C    WEST VELOCITY COEFFICIENT
             AWR(I,J)=MWR(I,J)*(0.5+GAMBC)
C    EAST VELOCITY COEFFICIENT
             AER(I,J-1)=-MER(I,J-1)*(0.5-GAMBC)
18         CONTINUE
20      CONTINUE
C    BOUNDARY CONTROL VOLUMES
C    VZ(1,1) ASSUMED GE 0 AND VZ(M,1) LT 0
        MWR(2,1)=RHOBI*(R(2)**2-R(3)**2)*PI*VZ(1,1)
        AWR(2,1)=MWR(2,1)
        MWR(M,1)=RHO(M,1)*PI*(R(2*M-1)**2-R(2*M)**2)*VZ(M,1)
        AWR(M,1)=0.
        MER(2,N)=0.
        AER(2,N)=0.
        MER(M,N)=0.
        AER(M,N)=0.
        DO 24 I=3,M-1
```

```
          MWR(I,1)=.0
          AWR(I,1)=0.
          MER(I,N)=0.
          AER(I,N)=0.
24      CONTINUE
C     CALCULATE THE CENTRAL POINT COEFFICIENT
        DO 32 I=2,M
          DO 28 J=1,N
            AOR(I,J)=-(AER(I,J)+AWR(I,J)+ASR(I,J)+ANR(I,J)+MER(I,J)
     +       -MWR(I,J)+MNR(I,J)-MSR(I,J))
28        CONTINUE
32      CONTINUE
C     CALCULATE THE CONSTANT TERMS
        DO 40 J=1,N
          DO 36 I=2,M
            IF (VR(I,J) .GE. 0.) THEN
              ALF=0.5
              ELSE
              ALF=-0.5
            ENDIF
C     CALCULATE GAS VOLUMES USED TO CALCULATE BR(I,J)
            DVA=(R(2*I-2)**2-R(2*I-1)**2)*PI*DZ*EP(I-1)
            DVB=(R(2*I-1)**2-R(2*I)**2)*PI*DZ*EP(I)
            RHOS=((0.5+ALF)*RHO(I-1,J)+(0.5-ALF)*RHO(I,J))
            RHOOS=((0.5+ALF)*RHOO(I-1,J)+(0.5-ALF)*RHOO(I,J))
C     FIND SMALLER VOID FRACTION IN THE CONTROL VOLUME
            EPS=MIN(EP(I-1),EP(I))
            BR(I,J)=RHOS*(DVA+DVB)/DT
            BRO(I,J)=RHOOS*(DVA+DVB)/DT
            BVR(I,J)=BR(I,J)/RHOS
C     SUPERFICIAL VELOCITY WEIGHTED BY VOLUMES
            VRSB=((0.5*(VZ(I,J)+VZ(I,J+1))**2)+VRSC**2)**0.5
            VRSA=((0.5*(VZ(I-1,J)+VZ(I-1,J+1))**2)+VRSC**2)
     +        **0.5
            PS=(0.5+ALF)*P(I-1,J)+(0.5-ALF)*P(I,J)
            TIS=(0.5+ALF)*TG(I-1,J)+(0.5-ALF)*TG(I,J)
            VIS=PTVISC(PS,TIS,UNITS)
C     CALCULATION OF THE SOURCE TERM
            AREAA=PI*DZ*(R(2*I-2)+R(2*I))
C     PRESSURE DIFFERENCE ACTS ON SMALLEST GAS AREA OF THE CONTROL VOLUME
            SORC=AREAA*(P(I-1,J)-P(I,J))*EPS
C     FRICTION TERM
            THKA=R(2*I-2)-R(2*I-1)
            THKB=R(2*I-1)-R(2*I)
C     CORRECTION FOR THE VARIABLE THICKNESS OF THE COLD FRIT
            IF (I .EQ. 2) THEN
              THKB=THKCF(J)/2
              DPB=DPCF
              DPA=DP
              ELSE
              DPA=DP
              DPB=DP
            ENDIF
```

```
            IF (I .EQ. 3) THEN
               THKA=THKCF(J)/2
               DPA=DPCF
               DPB=DP
            ENDIF
            FRICA=THKA*((150*VIS*((1-EP(I-1))**2)/((DPA**2)*
     +        (EP(I-1)**3)))+(1.75*RHOS*VRSA*(1-EP(I-1))/(DPA*
     +        (EP(I-1)**3))))
            FRICB=THKB*((150*VIS*((1-EP(I))**2)/((DPB**2)*
     +        (EP(I)**3)))+(1.75*RHOS*VRSB*(1-EP(I))/(DPB*
     +        (EP(I)**3))))
            FRIC=(FRICA+FRICB)*AREAA*EPS
            SR(I,J)=SORC
            BRAF(I,J)=(BR(I,J)-AOR(I,J)+FRIC)
            ARF(I,J)=-(BRAF(I,J)-BR(I,J))
C             WRITE(3,*)I,J,DPA,DPB,EP(I)
C             WRITE(3,*)THKA,THKB
C             WRITE(3,*)SORC,FRICA,FRICB,FRIC
C             WRITE(3,*)VRSA,VRSB,VRSC,SR(I,J)
36       CONTINUE
40    CONTINUE
C   CONSTRUCT THE SOLUTION MATRIX AND CONSTANT VECTOR
      DO 48 I=2,M
         DO 44 J=1,N
           K=(I-2)*N+J
           SOLR(K,K)=-BRAF(I,J)
           IF (J .LT. N) SOLR(K,K+1)=AER(I,J)
           IF ((K+N) .LE. (M-1)*N) SOLR(K,K+N)=ANR(I,J)
           IF (J .GT. 1) SOLR(K,K-1)=AWR(I,J)
           IF (K-N .GT. 0) SOLR(K,K-N)=ASR(I,J)
           CONVR(K)=-SR(I,J)-(BRO(I,J)*VRO(I,J))
44       CONTINUE
48    CONTINUE
      NP=100
C   CALL SOLUTION SUBROUTINES
C   NOTE THAT THE UPDATED VELOCITIES ARE RETURNED AS A MODIFIED CONVR
C   VECTOR
      CALL LUDCMP(SOLR,((M-1)*N),NP,INDX,D)
      CALL LUBKSB(SOLR,((M-1)*N),NP,INDX,CONVR)
C   CONVERT UPDATED VELOCITIES TO I,J FORM
      I=2
      J=1
      DO 52 K=1,(M-1)*N
         VRST(I,J)=CONVR(K)
         IF ((K-(I-2)*N) .EQ. N) THEN
            J=1
            I=I+1
            ELSE
            J=J+1
         ENDIF
52    CONTINUE
      RETURN
      END
```

```
C   THE FIRST MOMENTUM CORRECTOR - THE PRESSURE EQUATION
C
      SUBROUTINE PRESUR(VR,VZ,RHO,RHOO,RHST,P,PO,PST,PIO,TG,
     + BZAF,BRAF,VRSTT,VZSTT)
      COMMON/GEOTRY/R(45),EP(20),DZ,THKCF(30),DV(20),DP,DPCF,M,N,DT
      COMMON/BOUCON/PBI,PBO,TBI,RHOBI,HBI
      COMMON/SOLVER/SOLP(100,100)
C   GENERAL FORM OF THE EQUATION
C   NOTE THAT THIS SUBROUTINE SOLVES FOR THE PRESSURE INCREMENT
C   -(RHO*DV/(DT*P)+DO)*PIO + DE*PIE + DW*PIW + DS*PIS + DN*PIN =DIVFLUX
C
      INTEGER M,N,I,J,K,UNITS,IPVT(100)
      REAL VR(11,10),VZ(10,11),RHO(10,10),RHST(10,10),P(10,10),
     + TG(10,10),AOZ(10,11),BZ(10,11),AOR(11,10),BR(11,10),SOLP,
     + CONVP(100),VRSTT(11,10),VZSTT(10,11),BRAF(11,10),BZAF(10,11)
      REAL R,EP,DZ,DV
      REAL GAM,PST(10,10)
      REAL DC(10,10),DE(10,10),DW(10,10),DS(10,10),DN(10,10),
     + FLUXE(10,10),FLUXW(10,10),FLUXS(10,10),FLUXN(10,10),PIO(10,10),
     + DIVFLX(10,10)
      REAL RHOO(10,10),PO(10,10)
      PARAMETER(PI=3.14159,UNITS=1)
C   INITIALIZE THE COEFFICIENT MATRIX
      DO 4 I=1,M*N
        DO 2 J=1,M*N
          SOLP(I,J)=0.
2       CONTINUE
4     CONTINUE
C   CALCULATION OF THE FLUXES AND PRESSURE INCREMENT COEFFICIENTS
C
C   EAST AND WEST FACES
C   WEST BOUNDARY
      DO 8 I=2,M-1
        DW(I,1)=0.
        FLUXW(I,1)=0.
8     CONTINUE
C   INLET, ASSUMING THE VELOCITY IS POSITIVE
      DW(1,1)=RHOBI*(((R(1)**2-R(3)**2)*PI)**2)/BZAF(1,1)
      FLUXW(1,1)=RHOBI*VZ(1,1)*PI*(R(1)**2-R(3)**2)
C   OUTLET, ASSUMING VELOCITY IS NEGATIVE
      DW(M,1)=RHO(M,1)*(((R(2*M-1)**2)*PI)**2)/BZAF(M,1)
      FLUXW(M,1)=RHO(M,1)*VZ(M,1)*PI*(R(2*M-1)**2)
C   EAST BOUNDARY
      DO 16 I=1,M
        DE(I,N)=0.
        FLUXE(I,N)=0.
C   CO-LOCATED EAST AND WEST FACES
        DO 12 J=2,N
C   UPWIND FACTOR FOR DENSITY
          IF (VZ(I,J) .GE. 0.) THEN
            GAM=0.5
            ELSE
            GAM=-0.5
```

```
            ENDIF
C   WEST - EAST PRESSURE INCREMENT COEFFICIENTS
            DW(I,J)=((0.5+GAM)*RHO(I,J-1)+(0.5-GAM)*RHO(I,J))
     +          *((PI*(R(2*I-1)**2-R(2*I+1)**2))**2)*EP(I)/BZAF(I,J)
            DE(I,J-1)=DW(I,J)
            FLUXW(I,J)=((0.5+GAM)*RHO(I,J-1)+(0.5-GAM)*RHO(I,J))
     +          *VZ(I,J)*PI*(R(2*I-1)**2-R(2*I+1)**2)
            FLUXE(I,J-1)=FLUXW(I,J)
12        CONTINUE
16      CONTINUE
C   SOUTH AND NORTH FACES
C   BOUNDARY CONDITIONS
        DO 28 J=1,N
            DN(M,J)=0.
            FLUXN(M,J)=0.0
            DS(1,J)=0.
            FLUXS(1,J)=0.0
C   CO-LOCATED NORTH AND SOUTH FACES
            DO 24 I=2,M
C   UPWIND DENSITY
               IF ((VR(I,J)) .GE. 0.) THEN
                  ALF=0.5
                  ELSE
                  ALF=-.5
               ENDIF
               EPS=MIN(EP(I),EP(I-1))
C   NORTH SOUTH PRESSURE INCREMENT COEFFICIENTS
               DS(I,J)=((0.5+ALF)*RHO(I-1,J)+(0.5-ALF)*RHO(I,J))
     +            *((2*PI*R(2*I-1)*DZ)**2)*EPS/(BRAF(I,J))
               DN(I-1,J)=DS(I,J)
               FLUXS(I,J)=((0.5+ALF)*RHO(I-1,J)+(0.5-ALF)*RHO(I,J))
     +            *VR(I,J)*2*PI*R(2*I-1)*DZ
               FLUXN(I-1,J)=FLUXS(I,J)
24          CONTINUE
28      CONTINUE
C   CENTRAL POINT COEFFICIENTS AND FLUX DIVERGENCE
        DO 36 I=1,M
            DO 32 J=1,N
              DC(I,J)=DE(I,J)+DW(I,J)+DS(I,J)+DN(I,J)
              DIVFLX(I,J)=FLUXE(I,J)-FLUXW(I,J)+FLUXN(I,J)-FLUXS(I,J)
C   CONSTRUCT SOLUTION MATRIX AND CONSTANT VECTOR
               K=(I-1)*N+J
               SOLP(K,K)=-((DV(I)/DT)*(RHOO(I,J)/PO(I,J))+DC(I,J))
               IF (J .LT. N) SOLP(K,K+1)=DE(I,J)
               IF ((K+N) .LE. (M*N)) SOLP(K,K+N)=DN(I,J)
               IF (J .GT. 1) SOLP(K,K-1)=DW(I,J)
               IF ((K-N) .GT. 0) SOLP(K,K-N)=DS(I,J)
               CONVP(K)=DIVFLX(I,J)
C           WRITE(3,*)I,FLUXS(I,J),FLUXN(I,J),FLUXW(I,J),FLUXE(I,J)
C           WRITE(3,*)DS(I,J),DN(I,J),DW(I,J),DE(I,J),DC(I,J)
C           WRITE(3,*)DV(I),RHOO(I,J),PO(I,J),BZAF(I,J),BRAF(I,J)
32          CONTINUE
36      CONTINUE
```

```
      NP=100
      MP=1
      MPP=1
      NR=M*N
C     CALL SOLUTION SUBROUTINES
      CALL LUDCMP(SOLP,NR,NP,INDX,D)
      CALL LUBKSB(SOLP,NR,NP,INDX,CONVP)
C     SOLUTION RETURNED AS MODIFIED CONVP VECTOR
C     UPDATE PRESSURES
      I=1
      J=1
      DO 40 K=1,M*N
          PST(I,J)=PO(I,J)+CONVP(K)
          PIO(I,J)=CONVP(K)
C       WRITE(3,*)P(I,J),PIO(I,J)
          IF ((K-(I-1)*N) .EQ. N) THEN
            J=1
            I=I+1
            ELSE
            J=J+1
          ENDIF
40    CONTINUE
C     UPDATE DENSITIES BASED ON NEW PRESSURES
      DO 52 I=1,M
          DO 44 J=1,N
            RHST(I,J)=PTDENS(PST(I,J),TG(I,J),UNITS)
44        CONTINUE
C     UPDATE VELOCITIES
C     AXIAL VELOCITIES
C     GENERAL FORM OF THE EQUATIONS
C     VZSTT(I,J)=(DW(I,J)*(PIO(I,J-1)-PIO(I,J))+VZ(I,J)*RHZOLD*AREA)
C          /(RHZ*AREA)
C       IF (I .EQ. M-1) GOTO 52
          DO 48 J=2,N
C     UPWIND TO COMPUTE DENSITY AT VZ
            IF (VZ(I,J) .GT. 0.) THEN
              RHZOLD=RHO(I,J-1)
              RHZ=RHST(I,J-1)
              ELSE
              RHZOLD=RHO(I,J)
              RHZ=RHST(I,J)
            ENDIF
C     COMPUTE AXIAL VELOCITY, SECOND ESTIMATE
            VZSTT(I,J)=(DW(I,J)*(PIO(I,J-1)-PIO(I,J))/(RHZ*PI
     +          *(R(2*I-1)**2-R(2*I+1)**2)))+VZ(I,J)*RHZOLD/RHZ
48        CONTINUE
52    CONTINUE
C     VELOCITY AT THE BOUNDARY, J=1
      VZSTT(1,1)=DW(1,1)*(-PIO(1,1))/(RHOBI*PI*(R(1)**2-R(3)**2))
     +    +VZ(1,1)
      VZSTT(M,1)=DW(M,1)*(-PIO(M,1))/(RHO(M,1)*PI*(R(2*M-1)**2))
     +    +VZ(M,1)*(RHO(M,1)/RHST(M,1))
      DO 56 I=2,M-1
```

```
            VZ(I,1)=0
56        CONTINUE
C     RADIAL VELOCITY
C     GENERAL FORM OF THE EQUATION
C     VRSTT(I,J)=(DS(I,J)*(PIO(I-1,J)-PIO(I,J)+R(I,J)*RHZOLD*AREA)/
C           (RHZ*AREA)
          DO 64 I=2,M
             DO 60 J=1,N
C     UPWIND TO DETERMINE DENSITY AT VR
             IF (VR(I,J) .GT. 0.) THEN
                RHZOLD=RHO(I-1,J)
                RHZ=RHST(I-1,J)
                ELSE
                RHZOLD=RHO(I,J)
                RHZ=RHST(I,J)
             ENDIF
C     COMPUTE RADIAL VELOCITY, SECOND ESTIMATE
             VRSTT(I,J)=(DS(I,J)*(PIO(I-1,J)-PIO(I,J))/(RHZ*2*PI*
     +           R(2*I-1)*DZ))+VR(I,J)*RHZOLD/RHZ
60            CONTINUE
64        CONTINUE
C     CHECK OVERALL SYSTEM MASS BALANCE
          GI=RHOBI*VZSTT(1,1)*PI*(R(1)**2-R(3)**2)
          GD=RHST(M,1)*VZSTT(M,1)*PI*(R(2*M-1)**2)
C      WRITE(3,*) GI,GD
          WRITE(6,*) GI,GD
          RETURN
          END

C
C     SUBROUTINE TO PERFORM THE ENTHALPY BALANCE
C
          SUBROUTINE ENTHLP(VZSTT,VRSTT,RHO,RHOO,RHST,PST,PIO,H,HO,
     +     UBAR,TSST,TGO,ANN,HST,TGST,AV,QIN,TSSTT)
          COMMON/GEOTRY/R(45),EP(20),DZ,THKCF(30),DV(20),DP,DPCF,M,N,DT
          COMMON/BOUCON/PBI,PBO,TBI,RHOBI,HBI
          COMMON/SOLVER/SOLH(100,100)
          INTEGER M,N,I,J,K,L,UNITS,NP
          REAL VZSTT(10,11),VRSTT(11,10),RHST(10,10),RHO(10,10)
          REAL PST(10,10),MWH(10,10),MEH(10,10),MSH(10,10),MNH(10,10)
          REAL AWH(10,10),AEH(10,10),ASH(10,10),ANH(10,10),AOH(10,10)
          REAL Q(10,10),PIO(10,10),H(10,10),HST(10,10),TGST(10,10)
          REAL CONVH(100),GAM,HSP,QUAL(10,10)
          REAL RHOO(10,10),HO(10,10)
          REAL UBAR(10,10),TSST(10,10),AV(10),QIN(10,10),TGO(10,10)
          REAL ANN(10,10),MIKE(10,10),CONST(10,10),TSSTT(10,10)
          PARAMETER (PI=3.14159, UNITS=1)
C     INITIALIZE THE COEFFICIENT MATRIX
          DO 10 I=1,M*N
              DO 5 J=1,N*M
                SOLH(I,J)=0.
5             CONTINUE
10        CONTINUE
```

```
C
C   CALCULATE ENTHALPY FLUX AND ENTHALPY COEFFICIENTS
C   EAST AND WEST FACES
      DO 30 J=2,N
           DO 20 I=1,M
C   UPWIND DENSITY
             IF (VZSTT(I,J) .GT. 0.) THEN
               GAM=0.5
               ELSE
               GAM=-0.5
             ENDIF
C   WEST FACE MASS FLUX
             MWH(I,J)=((0.5+GAM)*RHST(I,J-1)+(0.5-GAM)*RHST(I,J))*PI
     +            *(R(2*I-1)**2-R(2*I+1)**2)*VZSTT(I,J)
             IF (I .EQ. (M-1)) MWH(I,J)=0.
C   WEST FACE COEFFICIENT
             AWH(I,J)=MWH(I,J)*(0.5+GAM)
C   EAST FACE MASS FLUX
             MEH(I,J-1)=MWH(I,J)
C   EAST FACE COEFFICIENT
             AEH(I,J-1)=-MEH(I,J-1)*(0.5-GAM)
20         CONTINUE
30    CONTINUE
C   BOUNDARIES, EAST AND WEST FACES NOT CO-LOCATED
C   INLET PORT ASSUMING VELOCITY IS POEITIVE
      MWH(1,1)=RHOBI*VZSTT(1,1)*PI*(R(1)**2-R(3)**2)
      AWH(1,1)=MWH(1,1)
C   OUTLET PORT ASSUMING VELOCITY IS NEGATIVE
      MWH(M,1)=RHST(M,1)*VZSTT(M,1)*PI*(R(2*M-1)**2)
      AWH(M,1)=0.
      DO 40 I=2,M-1
           MWH(I,1)=0.
           AWH(I,1)=0.
           MEH(I,N)=0.
           AEH(I,N)=0.
40    CONTINUE
      MEH(1,N)=0.
      AEH(1,N)=0.
      MEH(M,N)=0.
      AEH(M,N)=0.
C   NORTH AND SOUTH FACES
      DO 60 J=1,N
C   BOUNDARY FACES
         MNH(M,J)=0.
         ANH(M,J)=0.
         MSH(1,J)=0.
         ASH(1,J)=0.
         DO 50 I=2,M
```

```
C   UPWINDING DENSITY
            IF (VRSTT(I,J) .GE. 0.) THEN
              ALF=0.5
              ELSE
              ALF=-0.5
            ENDIF
C   SOUTH FACE MASS FLUX
            MSH(I,J)=((0.5+ALF)*RHST(I-1,J)+(0.5-ALF)*RHST(I,J))
     +          *VRSTT(I,J)*2*PI*R(2*I-1)*DZ
C   SOUTH COEFFICIENT
            ASH(I,J)=MSH(I,J)*(0.5+ALF)
C   NORTH FACE MASS FLUX
            MNH(I-1,J)=MSH(I,J)
C   NORTH COEFFICIENT
            ANH(I-1,J)=-MNH(I-1,J)*(0.5-ALF)
50        CONTINUE
60      CONTINUE
C   CALCULATE CENTRAL COEFFICIENT AND HEAT INPUT FROM THE SOLID PHASE
        DO 80 J=1,N
            AOH(1,J)= -(AEH(1,J)+AWH(1,J)+ANH(1,J)+ASH(1,J)+MEH(1,J)
     +          -MWH(1,J)+MNH(1,J)-MSH(1,J))
            MIKE(1,J)=(DV(1)*RHST(1,J)/DT-AOH(1,J))
            CONST(1,J)=(DV(1)/DT)*(PIO(1,J)+RHO(1,J)*HO(1,J))
            AOH(M,J)= -(AEH(M,J)+AWH(M,J)+ANH(M,J)+ASH(M,J)+MEH(M,J)
     +          -MWH(M,J)+MNH(M,J)-MSH(M,J))
            MIKE(M,J)=(DV(M)*RHST(M,J)/DT-AOH(M,J))
            CONST(M,J)=(DV(M)/DT)*(PIO(M,J)+RHO(M,J)*HO(M,J))
            DO 70 I=2,M-1
              CPEE=PTCP(PST(I,J),TGO(I,J),UNITS)
              AOH(I,J)= -(AEH(I,J)+AWH(I,J)+ANH(I,J)+ASH(I,J)+MEH(I,J)
     +            -MWH(I,J)+MNH(I,J)-MSH(I,J))
              MIKE(I,J)=(DV(I)*RHST(I,J)/DT-AOH(I,J)+UBAR(I,J)*DV(I)
     +            *AV(I)/(CPEE*EP(I))-((UBAR(I,J)*DV(I)*AV(I)/EP(I))**2)
     +            /(ANN(I,J)*CPEE))
              CONST(I,J)=UBAR(I,J)*(DV(I)/EP(I))*AV(I)*(TSST(I,J)
     +            -TGO(I,J)+(HO(I,J)/CPEE))-(((UBAR(I,J)*DV(I)/EP(I))*
     +            AV(I))**2)*((HO(I,J)/CPEE))/ANN(I,J)+(DV(I)/DT)
     +            *(PIO(I,J)+RHO(I,J)*HO(I,J))
70          CONTINUE
80      CONTINUE
C   CONSTRUCT SOLUTION MATRIX AND CONSTANT VECTOR
        DO 100 I=1,M
            DO 90 J=1,N
              K=(I-1)*N+J
              SOLH(K,K)=-MIKE(I,J)
              IF (J .LT. N) SOLH(K,K+1)=AEH(I,J)
              IF (K+N .LE. M*N) SOLH(K,K+N)=ANH(I,J)
              IF (J .GT. 1) SOLH(K,K-1)=AWH(I,J)
              IF (K-N .GT. 0) SOLH(K,K-N)=ASH(I,J)
              CONVH(K)=-CONST(I,J)
90          CONTINUE
100     CONTINUE
```

```
      CONVH(1)=CONVH(1)-(AWH(1,1)*HBI)
C     CALL SOLUTION SUBROUTINES
C     NOTE THAT THE UPDATED ENTHALPIES ARE RETURNED AS A MODIFIED
C     CONVH VECTOR
      NP=100
      CALL LUDCMP(SOLH,(M*N),NP,INDX,D)
      CALL LUBKSB(SOLH,(M*N),NP,INDX,CONVH)
C   CONVERT UPDATED ENTHALPIES TO I,J SUBSCRIPTED FORM
      I=1
      J=1
      DO 101 K=1,M*N
          HST(I,J)=CONVH(K)
          IF ((K-(I-1)*N) .EQ. N) THEN
            J=1
            I=I+1
            ELSE
            J=J+1
          ENDIF
101     CONTINUE
C     UPDATE GAS PHASE TEMPERATURE MATRIX
      DO 103 I=1,M
          DO 102 J=1,N
            TGST(I,J)=PHTEMP(PST(I,J),HST(I,J),QUAL(I,J),UNITS)
102       CONTINUE
103     CONTINUE
C     UPDATE TSST TO TSSTT AND CALCULATE HEAT TRANSFERRED FROM THE SOLID
C     TO THE GAS PHASE
      DO 105 I=2,M-1
          DO 104 J=1,N
            TSSTT(I,J)=TSST(I,J)+UBAR(I,J)*DV(I)*AV(I)*(TGST(I,J)
     +       -TGO(I,J))/(EP(I)*ANN(I,J))
            QIN(I,J)=UBAR(I,J)*(DV(I)/EP(I))*AV(I)*(TSSTT(I,J)
     +       -TGST(I,J))
104       CONTINUE
105     CONTINUE
      RETURN
      END

C
C     THE SECOND MOMENTUM CORRECTOR - THE PRESSURE EQUATION
C
      SUBROUTINE PRESII(VRST,VZST,VRSTT,VZSTT,P,PST,PO,TGST,RHOO,RHST,
     +   VRSTTT,VZSTTT,PSTT,RHSTT,BVZ,BVR,ARF,AZF,AWR,AER,ASR,ANR,AWZ,
     +   AEZ,ASZ,ANZ,RHO)
      COMMON/GEOTRY/R(45),EP(20),DZ,THKCF(30),DV(20),DP,DPCF,M,N,DT
      COMMON/BOUCON/PBI,PBO,TBI,RHOBI,HBI
      COMMON/SOLVER/SOLC(100,100)
      INTEGER M,N,I,J,K,UNITS,NP
      REAL VRST(11,10),VRSTT(11,10),VZST(10,11),VZSTT(10,11)
      REAL RHOO(10,10),RHST(10,10),P(10,10),PO(10,10),TGST(10,10)
      REAL HPRI(10,10),HPRIZE(10,10),HPRIZW(10,10),HPRIRN(10,10)
      REAL HPRIRS(10,10),RHO(10,10)
      REAL BVR(11,10),BVZ(10,11),ARF(11,10),AZF(10,11)
```

```
      REAL DTC(10,10),DTW(10,10),DTE(10,10),DTS(10,10),DTN(10,10)
      REAL VRSTTT(11,10),VZSTTT(10,11),PIST(10,10),RHSTT(10,10)
      REAL PSTT(10,10),EPS,RHIN,FAEW(10),FAS(10),FAN(10)
      REAL AVEL(10,10),AVELW(10,10),AVELE(10,10),AVELS(10,10)
      REAL AVELN(10,10),CONVC(100),PST(10,10)
      REAL ANR(11,10),ASR(11,10),AER(11,10),AWR(11,10)
      REAL ANZ(10,11),ASZ(10,11),AEZ(10,11),AWZ(10,11)
      PARAMETER (PI=3.14159, UNITS=1)
C   INITIALIZE THE COEFFICIENT MATRIX
      DO 4 I=1,M*N
          DO 2 J=1,M*N
          SOLC(I,J)=0.
2         CONTINUE
4     CONTINUE
C   GENERAL FORM OF THE EQUATION
C   -(DTO-RHST*DV/(PST*DT))*PIST + DTW*PISTW + DTE*PISTE + DTS*PISTS
C    + DTN*PISTN = ((DV/DT-AO/RHST)**(-1))*(DEL(H'(VXSTT-VXST))*A
C    + DEL(AO((RHST-RHO)/RHST)*VXSTT*A))-DV/DT*(RHST/PST-RHO/P)
C
C   CALCULATE THE PRESSURE INCREMENT COEFFICIENTS
C   EAST AND WEST FACES
C   BOUNDARIES
      DO 10 I=2,M-1
          FAEW(I)=PI*(R(2*I-1)**2-R(2*I+1)**2)
          DTW(I,1)=0.
C         DTW(I,1)=(FAEW(I)**2)*EP(I)/(BVZ(I,1)-(AZF(I,1)/RHST(I,1)))
10    CONTINUE
C   INLET, ASSUMING THE VELOCITY IS POSITIVE
      FAEW(1)=((R(1)**2-R(3)**2)*PI)
      DTW(1,1)=(FAEW(1)**2)/(BVZ(1,1)-(AZF(1,1)/RHOBI))
C   OUTLET, ASSUMING THE VELOCITY IS NEGATIVE
      FAEW(M)=((R(2*M-1)**2)*PI)
      DTW(M,1)=(FAEW(M)**2)/(BVZ(M,1)-(AZF(M,1)/RHST(M,1)))
C   EAST BOUNDARY
      DO 30 I=1,M
          DTE(I,N)=0.
C   CO-LOCATED EAST AND WEST FACES
          DO 20 J=2,N
C   UPWIND FOR DENSITY
            IF (VZSTT(I,J) .GE. 0.) THEN
              GAM=0.5
              ELSE
              GAM=-0.5
            ENDIF
C   WEST AND EAST PRESSURE INCREMENT COEFFICIENT
            RHIN=(0.5+GAM)*RHST(I,J-1)+(0.5-GAM)*RHST(I,J)
            DTW(I,J)=(FAEW(I)**2)*EP(I)/(BVZ(I,J)-(AZF(I,J)/RHIN))
            DTE(I,J-1)=DTW(I,J)
20        CONTINUE
30    CONTINUE
C   NORTH AND SOUTH FACE COEFFICIENTS
C   BOUNDARY CONDITIONS
C   CALCULATE THE FACE AREAS
```

```
      DO 50 I=2,M
         FAS(I)=(2*PI*R(2*I-1)*DZ)
         FAN(I-1)=FAS(I)
50    CONTINUE
        FAN(M)=0.
      DO 70 J=1,N
         DTN(M,J)=0.
         DTS(1,J)=0.
C   CO-LOCATED NORTH AND SOUTH FACE COEFFICIENTS
         DO 60 I=2,M
C   UPWIND DENSITY
            IF (VRSTT(I,J) .GE. 0.) THEN
               ALF=0.5
               ELSE
               ALF=-0.5
            ENDIF
            EPS=MIN(EP(I),EP(I-1))
C   NORTH AND SOUTH COEFFICIENTS
            RHIN=(0.5+ALF)*RHST(I-1,J)+(0.5-ALF)*RHST(I,J)
            DTS(I,J)=(FAS(I)**2)*EPS/(BVR(I,J)-(ARF(I,J)/RHIN))
            DTN(I-1,J)=DTS(I,J)
60       CONTINUE
70    CONTINUE
C   CENTRAL POINT COEFFICIENT
      DO 90 I=1,M
         DO 80 J=1,N
            DTC(I,J)=DTE(I,J)+DTW(I,J)+DTS(I,J)+DTN(I,J)
     +         +((RHST(I,J)*DV(I))/(PST(I,J)*DT))
C   CONSTRUCT THE COEFFICIENT MATRIX
            K=(I-1)*N+J
            SOLC(K,K)=-DTC(I,J)
            IF (J .LT. N) SOLC(K,K+1)=DTE(I,J)
            IF ((K+N) .LE. (M*N)) SOLC(K,K+N)=DTN(I,J)
            IF (J .GT. 1) SOLC(K,K-1)=DTW(I,J)
            IF ((K-N) .GT. 0) SOLC(K,K-N)=DTS(I,J)
80       CONTINUE
90    CONTINUE
C   THE CONSTANT TERMS
      DO 110 I=2,M-1
         DO 100 J=2,N-1
C   UPWIND FOR DENSITY
            IF (VZSTT(I,J+1) .GE. 0.) THEN
               RHE=RHST(I,J)
               RHEE=(RHST(I,J)-RHO(I,J))/RHO(I,J)
               ELSE
               RHE=RHST(I,J+1)
               RHEE=(RHST(I,J+1)-RHO(I,J+1))/RHO(I,J+1)
            ENDIF
            IF (VRSTT(I+1,J) .GE. 0.) THEN
               RHN=RHST(I,J)
               RHNN=(RHST(I,J)-RHO(I,J))/RHO(I,J)
               ELSE
               RHN=RHST(I+1,J)
```

```
                RHNN=(RHST(I+1,J)-RHO(I+1,J))/RHO(I+1,J)
              ENDIF
C   CLACULATION OF THE CONSTANTS ON CO-LOCATED FACES
              HPRIZE(I,J)=(AWZ(I,J+1)*(VZSTT(I,J)-VZST(I,J))
     +            +AEZ(I,J+1)*(VZSTT(I,J+2)-VZST(I,J+2))
     +            +ANZ(I,J+1)*(VZSTT(I+1,J+1)-VZST(I+1,J+1))
     +            +ASZ(I,J+1)*(VZSTT(I-1,J+1)-VZST(I-1,J+1)))
     +            *FAEW(I)/(BVZ(I,J+1)-(AZF(I,J+1)/RHE))
              HPRIZW(I,J+1)=HPRIZE(I,J)
              HPRIRN(I,J)=(AWR(I+1,J)*(VRSTT(I+1,J-1)-VRST(I+1,J-1))
     +            +AER(I+1,J)*(VRSTT(I+1,J+1)-VRST(I+1,J+1))
     +            +ASR(I+1,J)*(VRSTT(I,J)-VRST(I,J))
     +            +ANR(I+1,J)*(VRSTT(I+2,J)-VRST(I+2,J)))
     +            *FAN(I)/(BVR(I+1,J)-(ARF(I+1,J)/RHN))
              HPRIRS(I+1,J)=HPRIRN(I,J)
              AVELE(I,J)=AZF(I,J+1)*RHEE*VZSTT(I,J+1)
     +            *FAEW(I)/(BVZ(I,J+1)-(AZF(I,J+1)/RHE))
              AVELW(I,J+1)=AVELE(I,J)
              AVELN(I,J)=ARF(I+1,J)*RHNN*VRSTT(I+1,J)
     +            *FAN(I)/(BVR(I+1,J)-(ARF(I+1,J)/RHN))
              AVELS(I+1,J)=AVELN(I,J)
100         CONTINUE
110       CONTINUE
C   CALCULATION OF THE CONSTANTS ALONG THE BOUNDARIES
C   THE INLET PORT
          IF (VZSTT(1,2) .GE. 0.) THEN
              RHE=RHST(1,1)
              RHEE=(RHST(1,1)-RHO(1,1))/RHO(1,1)
              ELSE
              RHE=RHST(1,2)
              RHEE=(RHST(1,2)-RHO(1,2))/RHO(1,2)
          ENDIF
          HPRIZE(1,1)=(AWZ(1,2)*(VZSTT(1,1)-VZST(1,1))
     +            +AEZ(1,2)*(VZSTT(1,3)-VZST(1,3))
     +            +ANZ(1,2)*(VZSTT(2,2)-VZST(2,2)))
     +            *FAEW(1)/(BVZ(1,2)-(AZF(1,2)/RHE))
          HPRIZW(1,1)=(AEZ(1,1)*(VZSTT(1,2)-VZST(1,2)))
     +            *FAEW(1)/(BVZ(1,1)-(AZF(1,1)/RHOBI))
          IF (VRSTT(2,1) .GE. 0.) THEN
              RHN=RHST(1,1)
              RHNN=(RHST(1,1)-RHO(1,1))/RHO(1,1)
              ELSE
              RHN=RHST(2,1)
              RHNN=(RHST(2,1)-RHO(2,1))/RHO(2,1)
          ENDIF
          HPRIRN(1,1)=(AER(2,1)*(VRSTT(2,2)-VRST(2,2))
     +            +ANR(2,1)*(VRSTT(3,1)-VRST(3,1)))
     +            *FAN(1)/(BVR(2,1)-(ARF(2,1)/RHN))
          HPRIRS(1,1)=0.
          AVELE(1,1)=AZF(1,2)*RHEE*VZSTT(1,2)
     +            *FAEW(1)/(BVZ(1,2)-(AZF(1,2)/RHE))
          AVELW(1,1)=0.
          AVELN(1,1)=ARF(2,1)*RHNN*VRSTT(2,1)
```

```
     +          *FAN(1)/(BVR(2,1)-(ARF(2,1)/RHN))
        AVELS(1,1)=0.
C    THE OUTLET PORT
        IF (VZSTT(M,2) .GE. 0.) THEN
            RHE=RHST(M,1)
            RHEE=(RHST(M,1)-RHO(M,1))/RHO(M,1)
            ELSE
            RHE=RHST(M,2)
            RHEE=(RHST(M,2)-RHO(M,2))/RHO(M,2)
        ENDIF
        IF (VRSTT(M,1) .GE. 0.) THEN
            RHS=RHST(M-1,1)
            RHSS=(RHST(M-1,1)-RHO(M-1,1))/RHO(M-1,1)
            ELSE
            RHS=RHST(M,1)
            RHSS=(RHST(M,1)-RHO(M,1))/RHO(M,1)
        ENDIF
        HPRIZE(M,1)=(AWZ(M,2)*(VZSTT(M,1)-VZST(M,1))
     +           +AEZ(M,2)*(VZSTT(M,3)-VZST(M,3))
     +           +ASZ(M,2)*(VZSTT(M-1,2)-VZST(M-1,2)))
     +           *FAEW(M)/(BVZ(M,2)-(AZF(M,2)/RHE))
        HPRIZW(M,1)=(AEZ(M,1)*(VZSTT(M,2)-VZST(M,2)))
     +           *FAEW(M)/(BVZ(M,1)-(AZF(M,1)/RHST(M,1)))
        HPRIRN(M,1)=0.
        HPRIRS(M,1)=(AER(M,1)*(VRSTT(M,2)-VRST(M,2))
     +           +ASR(M,1)*(VRSTT(M-1,1)-VRST(M-1,1)))
     +           *FAS(M)/(BVR(M,1)-(ARF(M,1)/RHS))
        AVELE(M,1)=AZF(M,2)*RHEE*VZSTT(M,2)
     +           *FAEW(M)/(BVZ(M,2)-(AZF(M,2)/RHE))
        AVELW(M,1)=AZF(M,1)*((RHST(M,1)-RHO(M,1))/RHO(M,1))*VZSTT(M,1)
     +           *FAEW(M)/(BVZ(M,1)-(AZF(M,1)/RHST(M,1)))
        AVELN(M,1)=0.
        AVELS(M,1)=ARF(M,1)*RHSS*VRSTT(M,1)
     +           *FAS(M)/(BVR(M,1)-(ARF(M,1)/RHS))
C    THE CORNER CONTROL VOLUMES
        IF (VZSTT(1,N) .GE. 0.) THEN
             RHW=RHST(1,N-1)
             RHWW=(RHST(1,N-1)-RHO(1,N-1))/RHO(1,N-1)
             ELSE
             RHW=RHST(1,N)
             RHWW=(RHST(1,N)-RHO(1,N))/RHO(1,N)
        ENDIF
        IF (VRSTT(2,N) .GE. 0.) THEN
             RHN=RHST(1,N)
             RHNN=(RHST(1,N)-RHO(1,N))/RHO(1,N)
             ELSE
             RHN=RHST(2,N)
             RHNN=(RHST(2,N)-RHO(2,N))/RHO(2,N)
        ENDIF
        HPRIZE(1,N)=0.
        HPRIZW(1,N)=(AWZ(1,N)*(VZSTT(1,N-1)-VZST(1,N-1))
     +           +ANZ(1,N)*(VZSTT(2,N)-VZST(2,N)))
     +           *FAEW(1)/(BVZ(1,N)-(AZF(1,N)/RHW))
```

```
      HPRIRN(1,N)=(AWR(2,N)*(VRSTT(2,N-1)-VRST(2,N-1))
     +           +ANR(2,N)*(VRSTT(3,N)-VRST(3,N)))
     +           *FAN(1)/(BVR(2,N)-(ARF(2,N)/RHN))
      HPRIRS(1,N)=0.
      AVELE(1,N)=0.
      AVELW(1,N)=AZF(1,N)*RHWW*VZSTT(1,N)
     +           *FAEW(1)/(BVZ(1,N)-(AZF(1,N)/RHW))
      AVELN(1,N)=ARF(2,N)*RHNN*VRSTT(2,N)
     +           *FAN(1)/(BVR(2,N)-(ARF(2,N)/RHN))
      AVELS(1,N)=0.
      IF (VZSTT(M,N) .GE. 0.) THEN
            RHW=RHST(M,N-1)
            RHWW=(RHST(M,N-1)-RHO(M,N-1))/RHO(M,N-1)
            ELSE
            RHW=RHST(M,N)
            RHWW=(RHST(M,N)-RHO(M,N))/RHO(M,N)
      ENDIF
      IF (VRSTT(M,N) .GE. 0.) THEN
            RHS=RHST(M-1,N)
            RHSS=(RHST(M-1,N)-RHO(M-1,N))/RHO(M-1,N)
            ELSE
            RHS=RHST(M,N)
            RHSS=(RHST(M,N)-RHO(M,N))/RHO(M,N)
      ENDIF
      HPRIZE(M,N)=0.
      HPRIZW(M,N)=(AWZ(M,N)*(VZSTT(M,N-1)-VZST(M,N-1))
     +           +ASZ(M,N)*(VZSTT(M-1,N)-VZST(M-1,N)))
     +           *FAEW(M)/(BVZ(M,N)-(AZF(M,N)/RHW))
      HPRIRN(M,N)=0.
      HPRIRS(M,N)=(AWR(M,N)*(VRSTT(M,N-1)-VRST(M,N-1))
     +           +ASR(M,N)*(VRSTT(M-1,N)-VRST(M-1,N)))
     +           *FAS(M)/(BVR(M,N)-(ARF(M,N)/RHS))
      AVELE(M,N)=0.
      AVELW(M,N)=AZF(M,N)*RHWW*VZSTT(M,N)
     +           *FAEW(M)/(BVZ(M,N)-(AZF(M,N)/RHW))
      AVELN(M,N)=0.
      AVELS(M,N)=ARF(M,N)*RHSS*VRSTT(M,N)
     +           *FAS(M)/(BVR(M,N)-(ARF(M,N)/RHS))
C     THE EAST AND WEST BOUNDARY CONTROL VOLUMES
      DO 120 I=2,M-1
           IF (VZSTT(I,2) .GE. 0.) THEN
              RHE=RHST(I,1)
              RHEE=(RHST(I,1)-RHO(I,1))/RHO(I,1)
              ELSE
              RHE=RHST(I,2)
              RHEE=(RHST(I,2)-RHO(I,2))/RHO(I,2)
           ENDIF
           IF (VRSTT(I+1,1) .GE. 0.) THEN
              RHN=RHST(I,1)
              RHNN=(RHST(I,1)-RHO(I,1))/RHO(I,1)
              ELSE
              RHN=RHST(I+1,1)
              RHNN=(RHST(I+1,1)-RHO(I+1,1))/RHO(I+1,1)
```

```
      ENDIF
      IF (VRSTT(I,1) .GE. 0.) THEN
         RHS=RHST(I-1,1)
         RHSS=(RHST(I-1,1)-RHO(I-1,1))/RHO(I-1,1)
         ELSE
         RHS=RHST(I,1)
         RHSS=(RHST(I,1)-RHO(I,1))/RHO(I,1)
      ENDIF
      HPRIZE(I,1)=(AEZ(I,2)*(VZSTT(I,3)-VZST(I,3))
+              +ANZ(I,2)*(VZSTT(I+1,2)-VZST(I+1,2))
+              +ASZ(I,2)*(VZSTT(I-1,2)-VZST(I-1,2)))
+              *FAEW(I)/(BVZ(I,2)-(AZF(I,2)/RHE))
      HPRIZW(I,1)=0.
      HPRIRN(I,1)=(AER(I+1,1)*(VRSTT(I+1,2)-VRST(I+1,2))
+              +ANR(I+1,1)*(VRSTT(I+2,1)-VRST(I+2,1))
+              +ASR(I+1,1)*(VRSTT(I,1)-VRST(I,1)))
+              *FAN(I)/(BVR(I+1,1)-(ARF(I+1,1)/RHN))
      HPRIRS(I,1)=(AER(I,1)*(VRSTT(I,2)-VRST(I,2))
+              +ANR(I,1)*(VRSTT(I+1,1)-VRST(I+1,1))
+              +ASR(I,1)*(VRSTT(I-1,1)-VRST(I-1,1)))
+              *FAS(I)/(BVR(I,1)-(ARF(I,1)/RHS))
      AVELE(I,1)=AZF(I,2)*RHEE*VZSTT(I,2)
+              *FAEW(I)/(BVZ(I,2)-(AZF(I,2)/RHE))
      AVELW(I,1)=0.
      AVELN(I,1)=ARF(I+1,1)*RHNN*VRSTT(I+1,1)
+          *FAN(I)/(BVR(I+1,1)-(ARF(I+1,1)/RHN))
      AVELS(I,1)=ARF(I,1)*RHSS*VRSTT(I,1)
+          *FAS(I)/(BVR(I,1)-(ARF(I,1)/RHS))
      IF (VZSTT(I,N) .GE. 0.) THEN
         RHW=RHST(I,N-1)
         RHWW=(RHST(I,N-1)-RHO(I,N-1))/RHO(I,N-1)
         ELSE
         RHW=RHST(I,N)
         RHWW=(RHST(I,N)-RHO(I,N))/RHO(I,N)
      ENDIF
      IF (VRSTT(I,N) .GE. 0.) THEN
         RHS=RHST(I-1,N)
         RHSS=(RHST(I-1,N)-RHO(I-1,N))/RHO(I-1,N)
         ELSE
         RHS=RHST(I,N)
         RHSS=(RHST(I,N)-RHO(I,N))/RHO(I,N)
      ENDIF
      IF (VRSTT(I+1,N) .GE. 0.) THEN
         RHN=RHST(I,N)
         RHNN=(RHST(I,N)-RHO(I,N))
         ELSE
         RHN=RHST(I+1,N)
         RHNN=(RHST(I+1,N)-RHO(I+1,N))
      ENDIF
```

```
            HPRIZE(I,N)=0.
          HPRIZW(I,N)=(AWZ(I,N)*(VZSTT(I,N-1)-VZST(I,N-1))
     +               +ANZ(I,N)*(VZSTT(I+1,N)-VZST(I+1,N))
     +               +ASZ(I,N)*(VZSTT(I-1,N)-VZST(I-1,N)))
     +               *FAEW(I)/(BVZ(I,N)-(AZF(I,N)/RHW))
          HPRIRN(I,N)=(AWR(I+1,N)*(VRSTT(I+1,N-1)-VRST(I+1,N-1))
     +               +ANR(I+1,N)*(VRSTT(I+2,N)-VRST(I+2,N))
     +               +ASR(I+1,N)*(VRSTT(I,N)-VRST(I,N)))
     +               *FAN(I)/(BVR(I+1,N)-(ARF(I+1,N)/RHN))
          HPRIRS(I,N)=(AWR(I,N)*(VRSTT(I,N-1)-VRST(I,N-1))
     +               +ANR(I,N)*(VRSTT(I+1,N)-VRST(I+1,N))
     +               +ASR(I,N)*(VRSTT(I-1,N)-VRST(I-1,N)))
     +               *FAS(I)/(BVR(I,N)-(ARF(I,N)/RHS))
          AVELE(I,N)=0.
          AVELW(I,N)=AZF(I,N)*RHWW*VZSTT(I,N)
     +               *FAEW(I)/(BVZ(I,N)-(AZF(I,N)/RHW))
          AVELN(I,N)=ARF(I+1,N)*RHNN*VRSTT(I+1,N)
     +               *FAN(I)/(BVR(I+1,N)-(ARF(I+1,1)/RHN))
          AVELS(I,N)=ARF(I,N)*RHSS*VRSTT(I,N)
     +               *FAS(I)/(BVR(I,N)-(ARF(I,N)/RHS))
120     CONTINUE
C    NORTH AND SOUTH BOUNDARY CONTROL VOLUMES
        DO 130 J=2,N-1
          IF (VZSTT(M,J) .GE. 0.) THEN
            RHW=RHST(M,J-1)
            RHWW=(RHST(M,J-1)-RHO(M,J-1))/RHO(M,J-1)
            ELSE
            RHW=RHST(M,J)
            RHWW=(RHST(M,J)-RHO(M,J))/RHO(M,J)
          ENDIF
          IF (VZSTT(M,J+1) .GE. 0.) THEN
            RHE=RHST(M,J)
            RHEE=(RHST(M,J)-RHO(M,J))/RHO(M,J)
            ELSE
            RHE=RHST(M,J+1)
            RHEE=(RHST(M,J+1)-RHO(M,J+1))/RHO(M,J+1)
          ENDIF
          IF (VRSTT(M,J) .GE. 0.) THEN
            RHS=RHST(M-1,J)
            RHSS=(RHST(M-1,J)-RHO(M-1,J))/RHO(M-1,J)
            ELSE
            RHS=RHST(M,J)
            RHSS=(RHST(M,J)-RHO(M,J))/RHO(M,J)
          ENDIF
          HPRIZE(M,J)=(AWZ(M,J+1)*(VZSTT(M,J)-VZST(M,J))
     +               +AEZ(M,J+1)*(VZSTT(M,J+2)-VZST(M,J+2))
     +               +ASZ(M,J+1)*(VZSTT(M-1,J+1)-VZST(M-1,J+1)))
     +               *FAEW(M)/(BVZ(M,J+1)-(AZF(M,J+1)/RHE))
          HPRIZW(M,J)=(AWZ(M,J)*(VZSTT(M,J-1)-VZST(M,J-1))
     +               +AEZ(M,J)*(VZSTT(M,J+1)-VZST(M,J+1))
     +               +ASZ(M,J)*(VZSTT(M-1,J)-VZST(M-1,J)))
     +               *FAEW(M)/(BVZ(M,J)-(AZF(M,J)/RHW))
          HPRIRN(M,J)=0.
```

```
      AVELE(M,J)=AZF(M,J+1)*RHEE*VZSTT(M,J+1)
     +          *FAEW(M)/(BVZ(M,J+1)-(AZF(M,J+1)/RHE))
      AVELW(M,J)=AZF(M,J)*RHWW*VZSTT(M,J)
     +          *FAEW(M)/(BVZ(M,J)-(AZF(M,J)/RHW))
      AVELN(M,J)=0.
      IF (VZSTT(1,J) .GE. 0.) THEN
         RHW=RHST(1,J-1)
         RHWW=(RHST(1,J-1)-RHO(1,J-1))/RHO(1,J-1)
         ELSE
         RHW=RHST(1,J)
         RHWW=(RHST(1,J)-RHO(1,J))/RHO(1,J)
      ENDIF
      IF (VZSTT(1,J+1) .GE. 0.) THEN
         RHE=RHST(1,J)
         RHEE=(RHST(1,J)-RHO(1,J))/RHO(1,J)
         ELSE
         RHE=RHST(1,J+1)
         RHEE=(RHST(1,J+1)-RHO(1,J+1))/RHO(1,J+1)
      ENDIF
      IF (VRSTT(2,J) .GE. 0.) THEN
         RHN=RHST(1,J)
         RHNN=(RHST(1,J)-RHO(1,J))/RHO(1,J)
         ELSE
         RHN=RHST(2,J)
         RHNN=(RHST(2,J)-RHO(2,J))/RHO(2,J)
      ENDIF
      HPRIZE(1,J)=(AWZ(1,J+1)*(VZSTT(1,J)-VZST(1,J))
     +          +AEZ(1,J+1)*(VZSTT(1,J+2)-VZST(1,J+2))
     +          +ANZ(1,J+1)*(VZSTT(2,J+1)-VZST(2,J+1)))
     +          *FAEW(1)/(BVZ(1,J+1)-(AZF(1,J+1)/RHE))
      HPRIZW(1,J)=(AWZ(1,J)*(VZSTT(1,J-1)-VZST(1,J-1))
     +          +AEZ(1,J)*(VZSTT(1,J+1)-VZST(1,J+1))
     +          +ANZ(1,J)*(VZSTT(2,J)-VZST(2,J)))
     +          *FAEW(1)/(BVZ(1,J)-(AZF(1,J)/RHW))
      HPRIRN(1,J)=(AWR(2,J)*(VRSTT(2,J-1)-VRST(2,J-1))
     +          +AER(2,J)*(VRSTT(2,J+1)-VRST(2,J+1))
     +          +ANR(2,J)*(VRSTT(3,J)-VRST(3,J)))
     +          *FAN(1)/(BVR(2,J)-(ARF(2,J)/RHN))
      HPRIRS(1,J)=0.
      AVELE(1,J)=AZF(1,J+1)*RHEE*VZSTT(1,J+1)
     +          *FAEW(1)/(BVZ(1,J+1)-(AZF(1,J+1)/RHE))
      AVELW(1,J)=AZF(1,J)*RHWW*VZSTT(1,J)
     +          *FAEW(1)/(BVZ(1,J)-(AZF(1,J)/RHW))
      AVELN(1,J)=ARF(2,J)*RHNN*VRSTT(2,J)
     +          *FAN(1)/(BVR(2,J)-(ARF(2,J)/RHN))
      AVELS(1,J)=0.
130   CONTINUE
C   CALCULATE THE GRADIENT OF THE CONSTANT TERMS ACROSS THE CONTROL
C   VOLUME
      DO 150 I=1,M
         DO 140 J=1,N
            HPRI(I,J)=HPRIZE(I,J)-HPRIZW(I,J)+HPRIRN(I,J)-HPRIRS(I,J)
            AVEL(I,J)=AVELE(I,J)-AVELW(I,J)+AVELN(I,J)-AVELS(I,J)
```

```
140         CONTINUE
150      CONTINUE
C    CONSTRUCT THE CONSTANT VECTOR
         DO 170 I=1,M
              DO 160 J=1,N
                 K=(I-1)*N+J
                 CONVC(K)=HPRI(I,J)-AVEL(I,J)+(DV(I)/DT)*
     +            ((RHST(I,J)/PST(I,J))-(RHOO(I,J)/PO(I,J)))
160           CONTINUE
170      CONTINUE
C    CALL SOLUTION ROUTINES
         NP=100
         NR=M*N
         CALL LUDCMP(SOLC,NR,NP,INDX,D)
         CALL LUBKSB(SOLC,NR,NP,INDX,CONVC)
C    SOLUTION RETURNED AS A MODIFIED CONVC VECTOR
         I=1
         J=1
         DO 180 K=1,NR
              PSTT(I,J)=PST(I,J)+CONVC(K)
              PIST(I,J)=CONVC(K)
              IF ((K-(I-1)*N) .EQ. N)THEN
                 J=1
                 I=I+1
                 ELSE
                 J=J+1
              ENDIF
180      CONTINUE
C  UPDATE DENSITIES
         DO 200 I=1,M
              DO 190 J=1,N
                 RHSTT(I,J)=PTDENS(PSTT(I,J),TGST(I,J),UNITS)
190           CONTINUE
200      CONTINUE
C    UPDATE VELOCITIES
C    AXIAL VELOCITY FIELD
C    GENERAL FORM OF THE EQUATION
C    VZSTTT = (HPRIZW-DTW*(PIST(I,J)-PIST(I,J-1))-AVELW*VZSTT)
C         *(1/(RHSTT*FAEW))+(RHOLD*VZSTT)/RHZ
C
C    UPWIND FOR DENSITY
         DO 220 I=1,M
C             IF (I .EQ. M-1) GOTO 220
              DO 210 J=2,N
                 IF (VZSTT(I,J) .GE. 0.) THEN
                    RHZ=RHSTT(I,J-1)
                    RHOLD=RHST(I,J-1)
                    ELSE
                    RHZ=RHSTT(I,J)
                    RHOLD=RHST(I,J)
                 ENDIF
C    COMPUTE AXIAL VELOCITY FIELD
                 VZSTTT(I,J)=(HPRIZW(I,J)-(DTW(I,J)*(PIST(I,J)-PIST(I,J-1)
```

```
     +             ))-(AVELW(I,J)*VZSTT(I,J)))*(1/(RHZ*FAEW(I)))+(RHOLD*
     +             VZSTT(I,J))/RHZ
210         CONTINUE
220      CONTINUE
C    COMPUTE INLET VELOCITY ASSUMING IT IS POSITIVE
        VZSTTT(1,1)=(HPRIZW(1,1)-(DTW(1,1)*PIST(1,1))-(AVELW(1,1)
     +    *VZSTT(1,1)))*(1/(RHOBI*FAEW(1)))+VZSTT(1,1)
C    COMPUTE OUTLET VELOCITY ASSUMING IT IS NEGATIVE
        VZSTTT(M,1)=(HPRIZW(M,1)-(DTW(M,1)*PIST(M,1))-(AVELW(M,1)
     +    *VZSTT(M,1)))*(1/(RHSTT(M,1)*FAEW(M)))+(RHST(M,1)*VZSTT(M,1)
     +    /RHSTT(M,1))
C    COMPUTE RADIAL VELOCITY FIELD
C    GENERAL FORM OF THE EQUATION
C    VRSTTT = (HPRIRS-DTS*(PIST(I,J)-PIST(I-1,J))-AVELS*VRSTT)
C          *(1/(RHSTT*FAS))+RHOLD*VRSTT/RHZ
C
C    UPWIND FOR DENSITY
        DO 240 I=2,M
            DO 230 J=1,N
               IF (VRSTT(I,J) .GT. 0.) THEN
                  RHOLD=RHST(I-1,J)
                  RHZ=RHSTT(I-1,J)
                  ELSE
                  RHOLD=RHST(I,J)
                  RHZ=RHSTT(I,J)
               ENDIF
C    COMPUTE THE RADIAL VELOCITY FIELD
               VRSTTT(I,J)=(HPRIRS(I,J)-(DTS(I,J)*(PIST(I,J)-PIST(I-1,J)
     +          ))-(AVELS(I,J)*VRSTT(I,J)))*(1/(RHZ*FAS(I)))
     +          +(RHOLD*VRSTT(I,J)/RHZ)
230         CONTINUE
240      CONTINUE
C    CHECK OVERALL SYSTEM MASS BALANCE
        GI=RHOBI*VZSTTT(1,1)*FAEW(1)
        GD=RHSTT(M,1)*VZSTTT(M,1)*FAEW(M)
C     WRITE (3,*) GI,GD
        WRITE (6,*) GI,GD
        RETURN
        END
```

NOMENCLATURE

a	Area of control volume face
A_e, A_n, A_s, A_w, A_O	Finite difference coefficients for momentum balance
A	Area variable for surface integrals
A_V	Particle surface area per unit volume of the bed
C_{Pb}, C_P	Specific heat of the gas at bulk temperature
C_{Pf}	Specific heat of the gas at the film temperature
$\overline{C}_P$	Average fuel particle specific heat
D_e, D_n, D_s, D_w, D_c	Finite difference coefficient for pressure equation
D	Equivalent pipe diameter
D_P	Fuel particle diameter
EM	Emissivity
$f(\vec{r},t)$	General transport function
f	Friction factor
$\overrightarrow{F}$	Force
G_O	Superficial mass velocity
h	Specific enthalpy
h	Heat transfer coefficient
H	Total enthalpy of a control volume
$H'(\ )$	Finite difference operator, The sum of the E, N, S, W control volume variables multiplied by their respective coefficients
j_H	Colburn j factor

k	Conductivity
k_r^o	Radiation conductivity across a void space to an adjacent particle
k^o	Effective bed thermal conductivity
L	Length of control volume
m	Mass
$\dot{m}$	Mass flow rate
m_a	Fuel particle mass per unit particle surface area
M	Mass flow through a control volume face
$\vec{n}$	Unit normal vector
P	Pressure
q''	Heat generation per unit particle outside surface area
Q	Heat input per unit time
Re	Reynolds number
S	Surface area
State Variable	Temperature, Pressure, Density or Enthalpy
t	Time
T	Temperature
$\overline{T}$	Effective fuel particle temperature
$\overline{U}$	Effective overall heat transfer coefficient for solid to gas heat transfer
$\vec{v}_o$	Superficial velocity component in the direction of the momentum balance
v_o	Component of the superficial velocity perpendicular to the face of the control volume
$\|v\|$	Superficial velocity magnitude

V	Volume
$\vec{v}_a$, v_z	Axial velocity
$\vec{v}_r$, v_r	Radial velocity
x	Length variable

Greek Letters

α	Upwinding factor
β	Axial momentum correction factor
γ	Axial momentum correction factor
ε	Void fraction
θ	Overall momentum correction factor
κ	Ratio of solid phase conductivity to gas phase conductivity
μ	Viscosity
μ_f	Viscosity of the coolant at film temperature
ρ	Density
τ	Heat transfer time constant
ϕ	Dummy variable used when equation applies to more than one variable; in heat effective thickness of gas film between particles
ψ	Particle shape factor

Subscripts

a	Axial
cv	Control volume
e, n, s, w	Identifiers for the faces of a control volume, align in accordance with the compass
E, N, S, W	Identifiers for the balance variable in the adjacent control volumes, align in accordance with the compass

O	Identifier for balance variable in the central control volume
G	Gas Phase
r	Radial. In heat transfer, radiation
S	Solid Phase
x	Dummy variable for operations that apply to several different subscripts such as the directional face identifiers (e, w, n, s)
z	Axial direction

Superscripts

n, $n+1$	Time step identifiers
*	Estimate of time n+1 value of a variable, number of * defines which estimate

REFERENCES

A-1 K. J. Araj, H. P. Nourbaksh, "Thermal-Hydraulic Modeling of Porous Bed Reactors," Trans. Am. Nucl. Soc., No. 55, 728-739, (Nov 1987).

A-2 A. H. Arastu, F. P. Berger, "Flow Data for the Thermal Design of Gas Cooled Porous Fuel Elements," Heat Transfer, Vol. 6, 125-130, 1978.

B-1 R. Benenati, K. J. Araj, F. L. Horn, "Thermal-Hydraulic Considerations for Particle Bed Reactors," Space Nuclear Power Systems 1987, M. S. El-Genk and M. D. Hoover eds., Orbit Book Co., Malabar, FL. 1988.

B-2 F. P. Berger, J. P. H. Blake, "Air Flow through Concentric Ducts Separated by a Porous Pipe," Jnl. Br. Nucl. Energy Soc., Vol 10, 217-228, 1971.

B-3 R. B. Bird, W. E. Stewart, E. N. Lightfoot, Transport Phenomena, John Wiley and Sons, New York, 1960.

B-4 R. A. Bajura, "A Model for Distribution in Manifolds," J. of Engineering for Power, Trans. ASME, Vol. 93, No. 1 (January) 1971.

B-5 R. A. Bajura, V. F. LeRose, L. E. Williams, "Fluid Distribution in Combining, Dividing and Reverse Flow Manifolds," ASME paper 73-Pwr-1, 1972.

B-6 R. A. Bajura, E. H. Jones, "Flow Distribution Manifolds," J. of Fluids Engineering, Trans. ASME, Vol 98, (December) 1976.

C-1 C. F. Colebrook, "Turbulent Flow in Pipes, with particular reference to the Transition Region between Smooth and Rough Pipe Laws," J. Inst. of Civil Engrs., Paper No. 5204, Vol 11, 1938.

D-1 A. B. Datta, A. K. Mujumdar, "Flow Distribution in Parallel and Reverse Flow Manifolds," Int. J. Of Heat & Fluid Flow, Vol. 2, No. 4, 1980.

D-2 D. Dobranich, "A Computer Program to Determine the Specific Power of Prismatic Core Reactors," Sandia National Laboratory Report SAND87-0735.UC-80, May 1987.

E-1 S. Ergun, "Fluid Flow Through Packed Columns," Chem. Eng. Prog., Vol. 48, pg. 89-94, 1952.

H-1 F. L. Horn, J. R. Powell, O. W. Lazareth, "Particle Bed Reactor Propulsion Vehicle Performance and Characteristics as an Orbital Transfer Rocket," Space Nuclear Power Systems 1986, M. S. El-Genk and M. D. Hoover eds., Orbit Book Co., Malabar, FL. 1987.

H-2 F. L. Horn, J. R. Powell, J. M. Savino, "Particle Fuel Bed Tests," Space Nuclear Power Systems 1985, M. S. El-Genk and M. D. Hoover eds., Orbit Book Co., Malabar, FL. 1986.

H-3 F. H. Harlow, A. A. Amsden, "A Numerical Fluid Dynamics Calculation Method for All Flow Speeds," J. of Computational Physics, Vol. 8, 197-213, 1971.

I-1 R. I. Issa, "Solution of the Implicitly Discretised Fluid Flow Equations by Operator-Splitting," J. of Computational Physics, Vol. 62, No. 1, 40-65, 1986.

I-2 R. I. Issa, A. D. Gosman, A. P. Watkins, "The Computation of Compressible and Incompressible Recirculating Flows by a Non-iterative Implicit Scheme," J. of Computational Physics, Vol. 62, No. 1, 66-82, 1986.

K-1 J. E. Kelly, S. P. Kao, M. S. Kazimi, THERMIT-2: A Two-Fluid Model for Light Water Reactor Subchannel Transient Analysis, MIT Energy Laboratory Electric Utility Program Report No. MIT-EL-81-014, April 1981.

L-1 O. W. Lazareth, et al., "Analysis of the Start-up and Control of a Particle Bed Reactor," Space Nuclear Power Systems 1987, M. S. El-Genk and M. D. Hoover eds., Orbit Book Co., Malabar, FL. 1988.

M-1 A. K. Majumdar, "Mathematical Modelling of Flows in Dividing and Combining Manifold," Appl. Math. Modelling, Vol. 4, (December) 1980.

M-2 J. E. Meyer, "Some Physical and Numerical Considerations for the SSC-S Code," Brookhaven National Laboratory Report BNL-NUREG-50913, Sep. 1978.

M-3 J. E. Meyer, "Hydrodynamic Models for the Treatment of Reactor Thermal Transients," Nuclear Science and Engineering, Vol. 10, 269-277, 1961.

P-1 J. R. Powell, F. L. Horn, "High Power Density Reactors Based on Direct Cooled Particle Beds," Space Nuclear Power Systems 1985, M. S. El-Genk and M. D. Hoover eds., Orbit Book Co., Malabar, FL. 1986.

P-2 S. V. Patankar, Numerical Heat Transfer, Hemisphere Publishing Co., Washington 1980.

P-3 S. V. Patankar, D. B. Spalding, "A Calculation Procedure for Heat, Mass and Momentum Transfer in Three Dimensional Flows," Int. J. Heat Mass Transfer, Vol. 15, 1787-1806, 1972.

P-4 S. V. Patankar, "A Calculation Procedure for Two Dimensional Elliptic Situations," Numerical Heat Transfer, Vol. 4, 409-425, 1981.

P-5 W. H. Press, B. P. Flannery, S. A. Teukolsky, W. T. Vetterling, Numerical Recipes the Art of Scientific Computing, Cambridge Univ. Press, Cambridge 1986.

R-1 W. H. Reed, H. B. Stewart, "THERMIT; A Computer Program for Three-Dimensional Thermal-Hydraulic Analysis of Light Water Reactor Cores," M.I.T. Report prepared for EPRI, (1978).

R-2 H. M. Roder, R. D. McCarty, W. J. Hall, "Computer Program for Thermodynamic and Transport Properties of Hydrogen (Tabcode-II)," National Bureau of Standards Technical Note 625, October 1972.

S-1 H. P. Smith, A. H. Stenning, "Open Loop Stability and Response of Nuclear Rocket Engines," Nuclear Science and Engineering, Vol. 11, 76-84, 1961.

S-2 H. P. Smith, "Closed Loop Dynamics of Nuclear Rocket Engines with Bleed Turbine Drive," Nuclear Science and Engineering, Vol. 14, 371-379, 1962.

S-3 H. P. Smith, "Closed-Loop Dynamics of Nuclear Rocket Engines with Topping Drive," Nuclear Science and Engineering, Vol. 18, 508-513, 1964.

S-4 W. Schotte, "Thermal Conductivity of Packed Beds," A.I.Ch.E. Journal, Vol. 6, No. 1 (March) 1960.

T-1 N. E. Todreas, M. S. Kazimi, Nuclear Reactor Thermal Analysis, Textbook Draft, June 1988.

V-1 M. E. Vernon, "PIPE Series Experiment Plan," Sandia National Laboratory, Albequeque, NM, 1988.

V-2 G. J. Van Tuyle, T. C. Nepsee, J. G. Guppy, MINET Code Documentation, Brookhaven National Laboratory Report NUREG/CR-3668, BNL-NUREG-51742, February 1984.

V-3 G. J. Van Tuyle, "A Momentum Integral Network Method for Thermal Hydraulic Systems Analysis," Nuclear Engineering and Design, Vol. 91, 17-28, 1986.

Y-1 S. Yagi and D. Kunii, "Studies on Thermal Conductivities in Packed Beds," A.I.Ch.E. Journal, Vol. 3, No. 3, 1957.

Thesis
T848
c.1

Tuddenham
Thermal hydraulic analysis of a packed bed reactor fuel element.